

DEVELOPMENT OF TETRAPHOSPHORUS LIGANDS AND THEIR  
APPLICATIONS IN OLEFIN HYDROFORMYLATION

by

CHAOXIAN CAI

A Dissertation submitted to the  
Graduate School-New Brunswick  
Rutgers, The State University of New Jersey  
in partial fulfillment of the requirements

for the degree of

Doctor of Philosophy

Graduate Program in Medicinal Chemistry

written under the direction of

Professor Xumu Zhang

and approved by

---

---

---

---

New Brunswick, New Jersey

May, 2012

## ABSTRACT OF THE DISSERTATION

### Development of Tetraphosphorus Ligands and Their Applications in Olefin Hydroformylation

By CHAOXIAN CAI

Dissertation Director:  
Professor Xumu Zhang

In Chapter 1, a general introduction to the reaction of rhodium-catalyzed hydroformylation of olefins is presented with its broad utility in organic synthesis, reaction mechanism, and a brief review of the current advances in ligand development.

In Chapter 2, new tetraphosphoramidite ligands have been designed and synthesized. These ligands have been applied in the rhodium-catalyzed regioselective hydroformylation of various functionalized allyl, vinyl, and styrene derivatives. Remarkable high linear selectivity was obtained. The rhodium/tetraphosphoramidite catalyst system is highly effective to produce linear aldehydes from functionalized allyl derivatives with substituents containing heteroatoms such as O, N, Si and halogens either directly adjacent to or at distance to the allyl group. For vinyl derivatives, the ligand is highly linear selective for acrylic derivatives, styrene, vinyl pyridines and vinyl phthalimide. The catalyst system makes it possible to prepare  $C_n$  ( $n \geq 3$ ) functionalized terminal aldehydes from readily available vinyl and allyl derivatives by hydroformylation with high linear selectivity and

efficiency. The electronic effects on catalyst activity and regioselectivity by both ligands and styrene derivatives have been studied with Hammett plots. For the substituent changes in ligands, with the increase of Hammett constant  $\sigma_p$ , the linear selectivity increases but the catalyst activity decreases. For the substituent changes in styrenes, with the increase of  $\sigma_p$ , the linear selectivity decreases but the catalyst activity increases.

In Chapter 3, new class of tetraphosphine ligands has been developed and applied in the rhodium-catalyzed regioselective hydroformylation of terminal and internal olefins. The steric and electronic effects of substituents on tetraphosphine have also been studied. The high linear selectivity (above 97% for 1-octene and 1-hexene) at high temperature (140 °C) showing by those tetraphosphine ligands is remarkable considering the commonly observed low linear selectivity under similar reaction conditions when bisphosphine analogues were used. The rhodium/tetraphosphine catalyst system is also highly effective for the isomerization and hydroformylation of 2-alkenes to form linear aldehydes. Greater than 95% linear selectivity and up to 94% yield of the total aldehydes were obtained for 2-pentene, 2-hexene and 2-octene.

## Acknowledgement

First, I would like to give my deepest appreciation to my advisor, Dr. Xumu Zhang, for his guidance and support during my graduate studies at Rutgers University. I have greatly benefitted from his contributions in the research field.

Next, I am very grateful to my Ph.D. committee. I want to thank Dr. Longqing Hu and Dr. David Kimball of the Medicinal Chemistry Department and Dr. Kai Hultzsich of the Chemistry Department for their service in my committee and their expertise in the field.

I also would like to thank the current and previous group members of Dr. Zhang's research group. Particularly, I want to thank Drs. Shichao Yu and Yongjun Yan for some of their initial work on the tetrphosphorus ligand system.

Finally, I would like to thank my wife and my children for their unfailing love and support.

## Dedication

To my family.

## Table of Contents

Abstract of the Dissertation .....	ii
Acknowledgements .....	iv
Dedication .....	v
List of Figures .....	ix
List of Schemes .....	xi
List of Tables .....	xii
Chapter 1 Introduction .....	1
1.1 Background .....	1
1.2 Utility of Hydroformylation in Organic Synthesis .....	2
1.3 Mechanism and Kinetic Analysis of Rhodium-Catalyzed Hydroformylation .....	4
1.4 Advances in the Development of Phosphorus Ligands .....	10
1.5 Objectives .....	19
References .....	21
Chapter 2 Tetraphosphoramidite Ligands for Regioselective Hydroformylation of	
Olefins .....	25
2.1 Introduction .....	25
2.2 Design of Tetraphosphoramidite Ligands .....	26
2.3 Synthesis of Tetraphosphoramidite Ligands .....	29
2.4 Hydroformylation of Functionalized Olefins .....	31
2.4.1 Hydroformylation of Allyl Cyanide .....	33
2.4.2. Ligand Structural Effects on the Hydroformylation of Allyl Cyanide .....	35

2.4.3 Hydroformylation of Functionalized Allyl and Vinyl Derivatives .....	39
2.4.4 Summary .....	46
2.5 Hydroformylation of Styrene and Its Derivatives .....	47
2.5.1 Hydroformylation of Styrene .....	49
2.5.2 Ligand Structural Effects on the Hydroformylation of Styrene .....	50
2.5.3 Electronic and Steric Effects of Styrene Substrates .....	54
2.5.4 Summary .....	60
2.6. Hydroformylation of Simple Terminal Olefins .....	61
2.7. Hydroformylation of Internal Olefins .....	62
2.7.1 Hydroformylation of $\beta$ - and $\gamma$ -Olefins .....	62
2.7.2 Ligand Structural Effects on the Hydroformylation of 2-Octene .....	64
2.7.3 Summary .....	69
Experimental Section .....	72
References .....	98
Chapter 3 Tetrphosphine Ligands for Highly Regioselective Hydroformylation of	
Terminal and Internal Olefins .....	100
3.1 Introduction .....	100
3.2 Design of Tetrphosphine Ligands .....	101
3.3 Synthesis of Tetrphosphine Ligands .....	103
3.4 Hydroformylation of Terminal Olefins .....	104
3.4.1 Hydroformylation of 1-Hexene and 1-Octene .....	104
3.4.2 Ligands Effects on the Hydroformylation of 1-Hexene and 1-Octene .....	108
3.4.3 Summary .....	110

3.5 Hydroformylation of Internal Olefins .....	111
3.5.1 Optimization of Hydroformylation Conditions .....	113
3.5.2 Ligand Effects on the Hydroformylation of 2-Hexene and 2-Octene .....	115
3.5.3 Hydroformylation of Other C <sub>5</sub> to C <sub>8</sub> Internal Olefins .....	118
3.5.4 Summary .....	122
Experimental Section .....	123
References .....	136
Curriculum Vita .....	138



## List of Figures

Figure 1.1. Bidentate phosphine ligands Bisbi and Naphos .....	12
Figure 1.2. Xantphos based bidentate phosphorus ligands .....	14
Figure 1.3. Bulky diphosphite ligands .....	15
Figure 1.4. Phosphorus ligands containing P-N bonds .....	16
Figure 1.5. Phosphabenzene phosphabarrelene and self-assembled phosphines .....	17
Figure 1.6. Tetraphosphines for bimetallic catalyst system .....	18
Figure 2.1. Tetraphosphoramidite ligands .....	28
Figure 2.2. Biological active compounds can be prepared via hydroformylation of functionalized olefins .....	33
Figure 2.3. Hammett plot of $\log(k_L/k_B)$ versus $\sigma_p$ values of substituents in ligands <b>5-10</b> for the hydroformylation of allyl cyanide .....	39
Figure 2.4. Drugs can be synthesized via hydroformylation of styrene derivatives .....	48
Figure 2.5. Hammett plot of $\log(k_L/k_B)$ versus $\sigma_p$ values of substituents in ligands <b>5-10</b> for the hydroformylation of styrene .....	52
Figure 2.6. Turn over frequency versus $\sigma_p$ values of substituents in ligands <b>5-10</b> for the hydroformylation of allyl cyanide .....	53
Figure 2.7. Hammett plot of $\log(k_L/k_B)$ versus $\sigma_p$ value of substituent on styrene .....	56
Figure 2.8. Turn over frequency versus $\sigma_p$ values of substituents on styrene .....	57
Figure 2.9. Hammett plot of $\log(k_L/k_B)$ versus $\sigma_p$ values of substituents in ligands <b>5-10</b> for the hydroformylation of 2-octene .....	67

Figure 2.10. Turn over frequency versus $\sigma_p$ values of substituents in ligands <b>5-10</b> for the hydroformylation of 2-octene .....	68
Figure 2.11. Hammett plot of $\log(k_L/k_B)$ versus $\sigma_p$ values of substituents in ligands <b>5-10</b> for the hydroformylation of styrene, 2-octene, and allyl cyanide .....	70
Figure 2.12. Turn over frequency versus $\sigma_p$ values of substituents in ligands <b>5-10</b> for the hydroformylation of styrene, 2-octene, and allyl cyanide .....	71
Figure 3.1. Tetraphosphine ligands .....	101

## List of Schemes

Scheme 1.1. Hydroformylation reactions .....	1
Scheme 1.2. Typical uses of aldehydes in organic synthesis .....	3
Scheme 1.3. Catalytic cycles of rhodium-catalyzed hydroformylation .....	4
Scheme 1.4. Intermediate rhodium species that determine regioselectivity .....	6
Scheme 1.5. Steps of olefin isomerization .....	7
Scheme 1.6. Step by step reaction mechanisms of rhodium-catalyzed hydroformylation ...	8
Scheme 1.7. Selectivity and side reactions of olefin hydroformylation .....	11
Scheme 2.1. Rhodium/ligand complexes and ligand dissociation under the influence of CO in hydroformylation .....	26
Scheme 2.2. Enhanced chelating ability of tetraphosphorus ligands through dynamic multiple chelating modes and increased local phosphorus concentration .....	27
Scheme 2.3. Synthesis of tetra substituted biphenyls .....	30
Scheme 2.4. Synthesis of Ligands <b>1-10</b> .....	31
Scheme 2.5. The catalytic cycles of styrene and derivatives to form linear and branched aldehydes .....	60
Scheme 3.1. Multiple chelating modes of tetraphosphine ligands due to enhanced local phosphorus concentration .....	102
Scheme 3.2. Synthesis of tetraphosphine ligands <b>1-6</b> .....	104
Scheme 3.3. Isomerization and hydroformylation of an internal olefin .....	112
Scheme 3.4. Isomerization mechanisms of an internal olefin .....	121

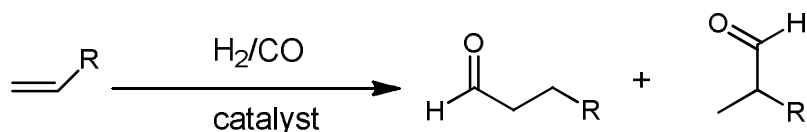
## List of Tables

Table 2.1. Optimization of reaction conditions for the hydroformylation of allyl cyanide using ligand <b>1</b> .....	35
Table 2.2. Hydroformylation of allyl cyanide with ligands <b>1-10</b> .....	36
Table 2.3. Hydroformylation of functionalized allyl derivatives with ligand <b>9</b> .....	40
Table 2.4. Hydroformylation of functionalized vinyl derivates with ligand <b>9</b> .....	43
Table 2.5. Hydroformylation of styrene with ligands <b>1-10</b> .....	50
Table 2.6. Hydroformylation of styrene derivatives with ligands <b>5, 7 and 10</b> .....	55
Table 2.7. Hydroformylation of styrene derivatives with ligand <b>7</b> .....	58
Table 2.8. Hydroformylation of simple terminal using with ligand <b>9</b> .....	62
Table 2.9. Hydroformylation of internal olefins with ligand <b>9</b> .....	63
Table 2.10. Hydroformylation of 2-octene with ligands <b>1-10</b> .....	65
Table 3.1. Optimization of reaction conditions for the hydroformylation of 1-octene ....	105
Table 3.2. Comparison of tetraphosphine and bisphosphine Ligands .....	107
Table 3.3. Hydroformylation of 1-hexene with tetraphosphine ligands <b>2-6</b> .....	109
Table 3.4. Hydroformylation of 1-octene with tetraphosphine ligands <b>2-6</b> .....	110
Table 3.5. Optimization of reaction conditions for the hydroformylation of 2-hexene with Ligand <b>6</b> .....	114
Table 3.6. Hydroformylation of 2-hexene with ligands <b>1-6</b> .....	117
Table 3.7. Hydroformylation of 2-octene with ligands <b>1-6</b> .....	118
Table 3.8. Isomerization-hydroformylation of C <sub>5</sub> to C <sub>8</sub> internal olefins using ligand <b>3</b> ...	120

## Chapter 1 Introduction

### 1.1 Background

Hydroformylation of alkenes is one of the most important homogenous catalytic processes to produce aldehydes (Scheme 1.1). Production of aldehydes via this process is estimated at over 9 million tons per year.<sup>1</sup> The reaction was discovered by Otto Roelen in 1938 as oxygenated products were produced in the cobalt-catalyzed Fischer-Tropsch process.<sup>2</sup> Ever since this discovery, the reaction has been under intensive studies because of its industrial importance. Many catalyst systems have been developed over years.<sup>3</sup> The major arena has been the development of various kinds of auxiliary ligands, which are crucial for catalyst complex stability, catalytic activity and regioselectivity of hydroformylation.



**Scheme 1.1.** Hydroformylation reactions.

The first generation of hydroformylation catalysts was based on cobalt carbonyl without phosphine ligand.<sup>1</sup> The catalyst activity was low and reaction conditions were harsh. Typically, the reaction was operated at temperatures from 110 °C to 180 °C and under H<sub>2</sub>/CO pressure from 200 bar to 300 bar. The cobalt-based hydroformylation process had dominated in industry until the early 1970s. In the 1960s, Wilkinson and coworkers discovered that rhodium complexes modified by phosphine ligands can also catalyze

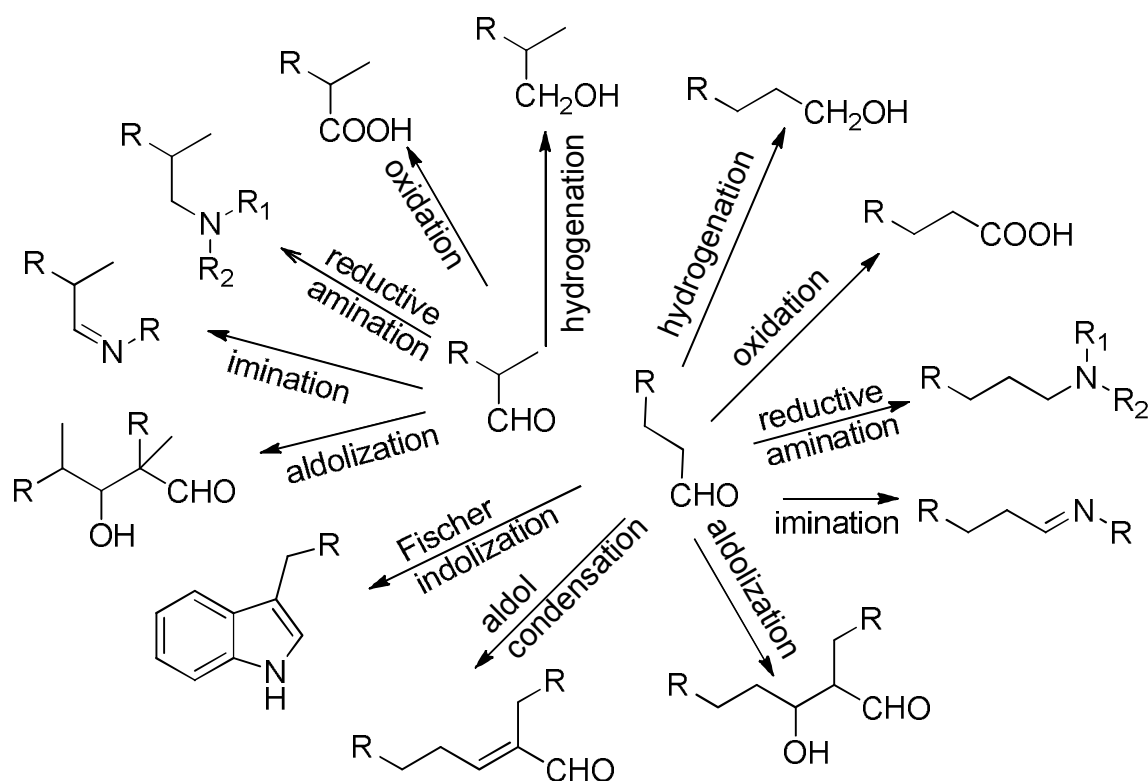
hydroformylation with high catalyst activity and aldehyde selectivity.<sup>4</sup> Moreover, the rhodium catalysts are less toxic and in general much more reactive and selective than cobalt-based catalysts; therefore, they have gradually replaced the cobalt-based catalytical process since the early 1970s. Currently, highly reactive rhodium catalysts modified with monodentate or bidentate ligands are employed in most commercial hydroformylation processes.

## 1.2 Utility of Hydroformylation in Organic Synthesis

Aldehydes are versatile intermediates and building blocks for pharmaceuticals, agrochemicals, and commodity and fine chemicals in organic synthesis.<sup>5</sup> The typical uses of aldehydes are shown in Scheme 1.2. A wide range of compounds can be prepared from aldehydes via hydrogenation, oxidation, reductive amination, and so on. More complex molecules can be prepared via aldolization and aldol condensation. These reaction are the starting points for branched alcohols, carboxylic acids, and amines with doubled carbon numbers. The hydroformylation of olefins allows access to a variety of functional groups including alcohols, amines, imines and enamines from cheap and readily available starting materials. The intermediate aldehydes produced from hydroformylation can be incorporated into the Fischer indole synthesis, which is widely used in the synthesis of heterocyclic pharmaceutical ingredients.

Both branched and terminal aldehydes can be produced via hydroformylation. The discovery of new catalyst systems has enabled the regio- and stereoselectivity of olefin hydroformylation to be controlled, and thus makes the hydroformylation a practicable, useful, and atomically economical reaction in organic synthesis. Traditionally,

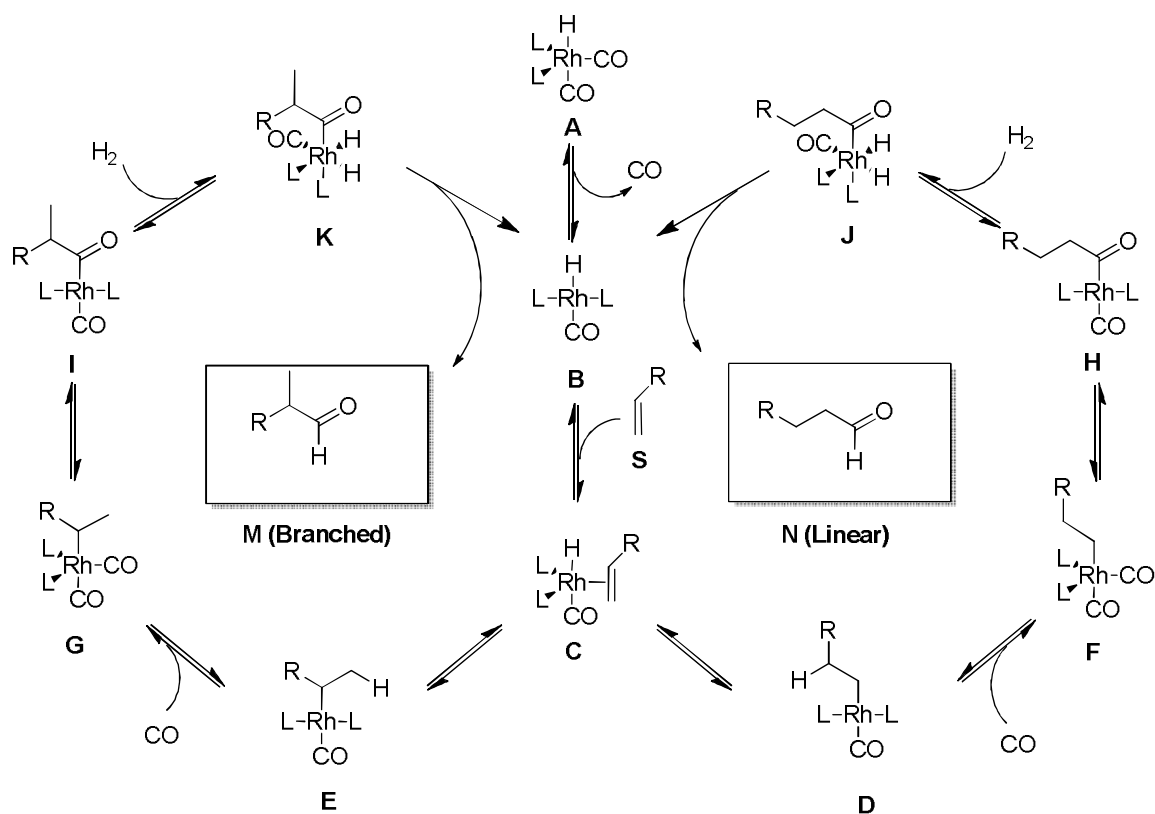
hydroformylation of simple olefins, such as propenes, butenes, hexenes, and octenes, has been the major industrial process towards the synthesis of aliphatic alcohols that have been used to make plasticizers, detergents and surfactants extensively. In the last two decades, the hydroformylation of alkenes as a general organic transformation methodology has gained its usage and importance in other aspects of organic synthesis. These synthetic applications include asymmetric hydroformylation, hydroformylation tandem reactions, hydroaminomethylation, and some other specific applications involving carbon monoxide chemistry. These applications of organic transformations via hydroformylation reaction will allow the syntheses of highly sophisticated molecules, such as pharmaceuticals, which would otherwise require multistep synthesis, from cheap and readily available commodity chemicals. In Chapter 2, we will give several of these examples.



**Scheme 1.2.** Typical uses of aldehydes in organic synthesis.<sup>5</sup>

### 1.3 Mechanism and Kinetic Analysis of Rhodium-Catalyzed Hydroformylation

Currently, Wilkinson's dissociation mechanism is generally accepted for the rhodium-catalyzed hydroformylation of olefins.<sup>4</sup> Using a monodentate ligand **L**, the basic catalytic cycles are depicted in Scheme 1.3. The mechanism is similar to the one originally proposed by Breslow and Heck for cobalt-catalyzed hydroformylation.<sup>6</sup>



**Scheme 1.3.** Catalytic cycles of rhodium-catalyzed hydroformylation.

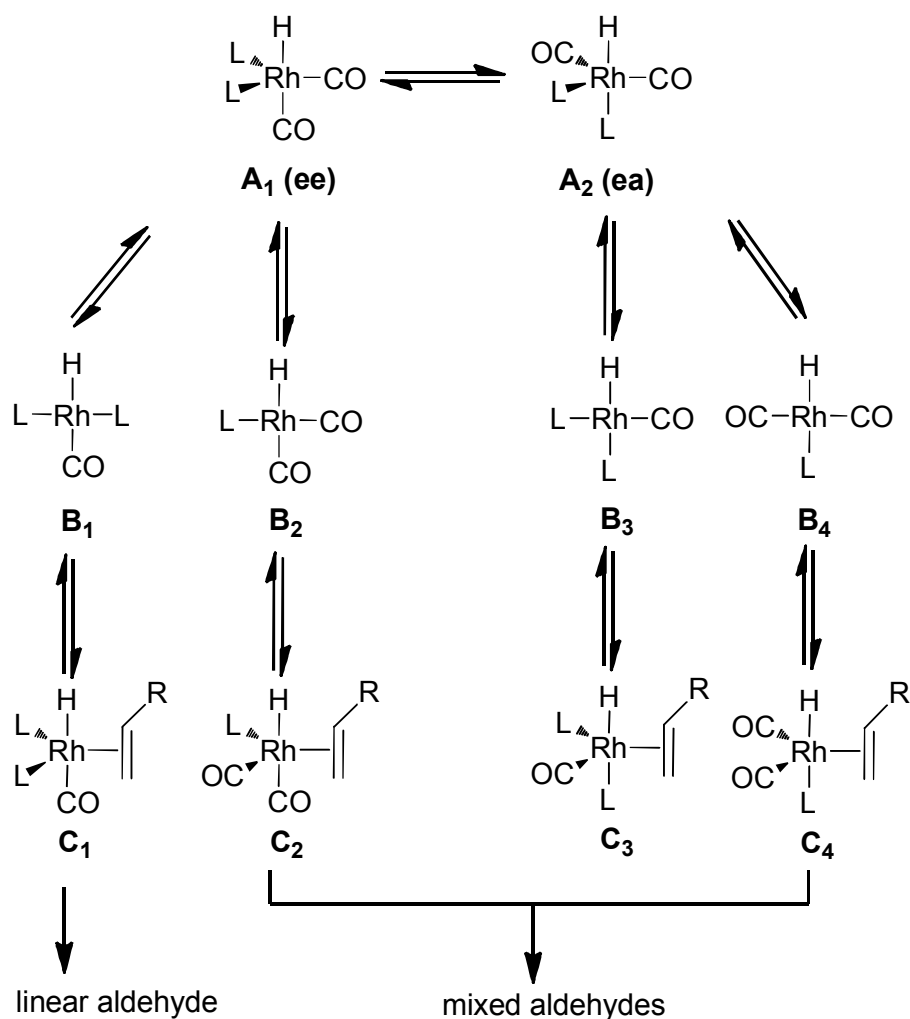
The catalytic cycle starts from an 18e trigonal bipyramidal intermediate **A**, which is formed after the reaction of a rhodium precursor with ligands in the presence of CO and H<sub>2</sub>. The dissociation of one carbon monoxide from this intermediate species generates a 16e coordinatively unsaturated species **B**, which is the catalytic active species. Next, the starting material olefin is coordinating to the rhodium center in the equatorial position,



and a trigonal bipyramidal hydrido olefin complex **C** is formed. The regioselectivity and enantioselectivity of the hydroformylation reaction are determined in the subsequent olefin insertion step that generates square planar rhodium alkyl complexes **D** and **E**, which will lead to the branched aldehyde and the linear aldehyde in subsequent steps, respectively. Next, the coordination of carbon monoxide to the rhodium center generates trigonal bipyramidal complexes **F** and **G**. The subsequent migratory insertion of the alkyl group to one of the coordinated carbon monoxide produces square planar rhodium acyl complexes **H** and **I**. After this step, the oxidative addition of hydrogen to the rhodium center generates tetragonal bipyramidal rhodium complexes **J** and **K**. Finally, the reductive elimination of complexes **J** and **K** produces the linear aldehyde **N** and the branched aldehyde **M**, respectively, and regenerates the catalytically active species **B**.

In general, a complete picture of the full reaction mechanism will be much more complicated than Scheme 1.3, where several important facts are overlooked. In Scheme 1.3, the rhodium species always has 2 monodentate ligands **L** associated, but as shown by experimental evidence,<sup>7</sup> species containing one to four coordinating numbers of ligand **L** will occur, and the numbers of **L** binding to the metal center is depending on the concentrations of ligand **L** and CO, and the nature of ligand **L**. Further, for the trigonal bipyramidal species **A**, the coordinating mode of the ligand can be either equatorial-equatorial (**ee**) or equatorial-axial (**ea**) (Scheme 1.4). There exists an equilibrium between equatorial-equatorial and equatorial-axial coordinating modes of rhodium species **A**. Both coordinating modes were observed by van Leeuwen and coworkers in their mechanistic studies.<sup>8</sup> The coordination mode is found to be a very important factor to determine the regioselectivity in the hydroformylation. Mechanistic

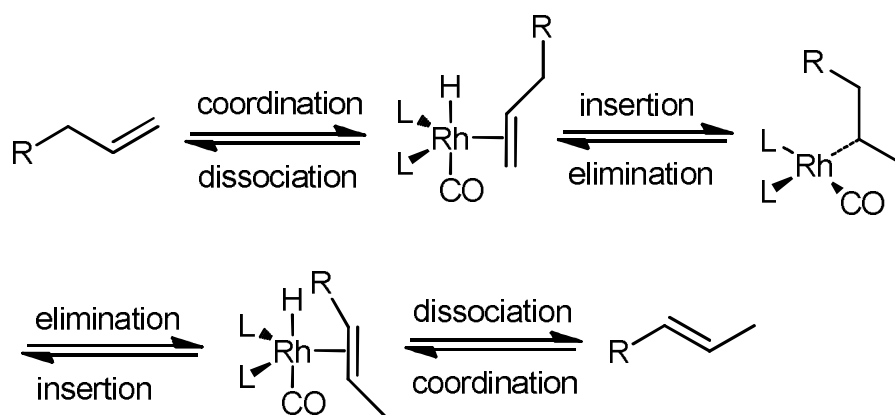
studies by Casey and coworkers suggested that the equatorial-equatorial coordinated intermediate **C**<sub>1</sub> leads to the linear aldehyde while the equatorial-axial coordination intermediate **C**<sub>3</sub> leads to unselective aldehydes.<sup>9</sup>



**Scheme 1.4.** Intermediate rhodium species that determine regioselectivity.<sup>1</sup>

The number of ligands coordinated to rhodium, the stereochemistry at the rhodium center, and the nature of ligand and substrate determine the regioselectivity of hydroformylation. As shown in Scheme 1.4, the dissociation of ligand **L** from the equatorial-equatorial coordinated intermediate **A**<sub>1</sub> forms **B**<sub>1</sub> and **C**<sub>1</sub> in the subsequent steps,

which lead to linear aldehyde. The dissociation of ligand **L** from the equatorial-axial coordinated intermediate **A**<sub>2</sub> forms unselective intermediates **B**<sub>3</sub> and **C**<sub>3</sub>, and **B**<sub>4</sub> and **C**<sub>4</sub>, in the subsequent steps, which lead to mixed aldehydes. In addition, the dissociation of ligand **L** from the equatorial-equatorial coordinated intermediate **A**<sub>1</sub> can form the unselective intermediates **B**<sub>2</sub> and **C**<sub>2</sub>, which also leads to mixed aldehydes.<sup>10</sup>

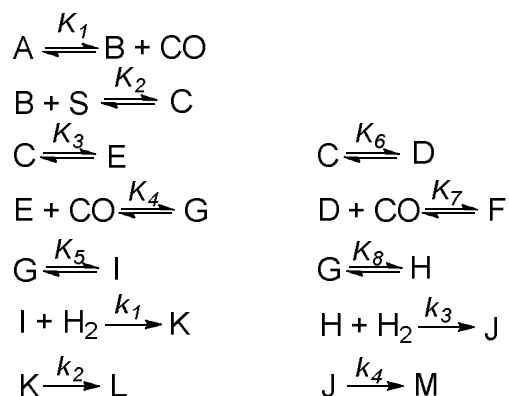


**Scheme 1.5.** Steps of olefin isomerization.

Another issue in the rhodium-catalyzed hydroformylation process is the isomerization of olefins. As shown in Scheme 1.5, the steps of alkene coordination and dissociation are reversible processes, and the same is true for the migratory insertion step and  $\beta$ -elimination step. Therefore, a terminal olefin or an internal olefin will end as a mixture of terminal and internal olefins after a series of reversible steps if the hydroformylation reaction is slow. An internal olefin is usually more sterically hindered for the reaction and hence less reactive. Furthermore, the reaction of an internal olefin will result in branched aldehyde if it is considerably reactive. As a result, the isomerization of a terminal olefin usually leads to decreased regioselectivity and reduced linear aldehyde yield. However, the isomerization step is necessary and desirable if we want to hydroformylate an internal olefin. We will discuss more in detail in Chapter 3.

In the catalytic cycles of Scheme 1.3, Wilkinson and coworkers have proposed that the rate determining step is the oxidative additions of  $H_2$  to the rhodium acyl complexes **H** and **I**. However, recently several research groups have disputed this claim. Moser and coworkers proposed that the rate determining step could be the step of CO dissociation from rhodium species **A**.<sup>11</sup> Mechanism studies by Kastrup and coworkers suggested that the step of alkene coordination to rhodium species **B** could be the rate determining step.<sup>12</sup> Kinetic studies of the Rh/PPh<sub>3</sub> catalyst system by Unruh and coworker reported that several fundamental steps had similar rate constants, which indicated the difficulty to specify one overall rate determining step.<sup>13</sup> The kinetic studies reported in the literature have shown that the rate laws are often differing from or even contrary to each other under varied catalysts, alkenes, and reaction conditions, so it is likely that the rate determining step will vary with the exact reaction conditions.

For our convenience to illustrate the reaction kinetics, we assume that the rate determining step is the oxidative addition of  $H_2$  to the rhodium species **I** (or **H**) in the catalytic cycle. If we apply the fast equilibrium approximation, the step by step reaction mechanisms can be expressed in the following consecutive reactions (Scheme 1.6):



**Scheme 1.6.** Step by step reaction mechanisms of rhodium-catalyzed hydroformylation.

Thus the rate law to produce the linear aldehyde can be expressed as

$$r = \frac{dC_L}{dt} = -\frac{dC_K}{dt} = k_1 C_I C_{H_2}, \quad (1.1)$$

where  $k_1$  is the rate constant of the rate determining step,  $C_L$ ,  $C_K$ ,  $C_I$ , and  $C_{H_2}$  are the concentrations of linear aldehyde **L**, rhodium species **K**, **I**, and  $H_2$  in the reaction media, respectively. Because of the fast equilibrium approximation before the rate determining step, the rate law can then be expressed as

$$r = \frac{dC_L}{dt} = -\frac{dC_K}{dt} = k_L C_C C_{H_2} C_{CO}, \quad (1.2)$$

where  $k_L$  is the observed rate constant for the production of linear aldehyde,  $C_C$  and  $C_{CO}$  are the concentrations of rhodium species **C** and CO in the reaction media, respectively. At any given time  $t$ , we have

$$\int_0^c dC_L = C_L = k_L \int_0^t C_C C_{H_2} C_{CO} dt. \quad (1.3)$$

Similarly, for the concentration of branch aldehyde  $C_B$ , we have

$$\int_0^c dC_B = C_B = k_B \int_0^t C_C C_{H_2} C_{CO} dt, \quad (1.4)$$

where  $k_B$  is the observed rate constant for the branched aldehyde. Since the formations of linear and branched aldehydes are two competitive reactions from the same starting point, the observed ratio of  $k_L/k_B$  is directly proportional to the concentration of linear aldehyde to that of branched aldehyde at any given time  $t$ . Dividing equation 1.3 to equation 1.4, we

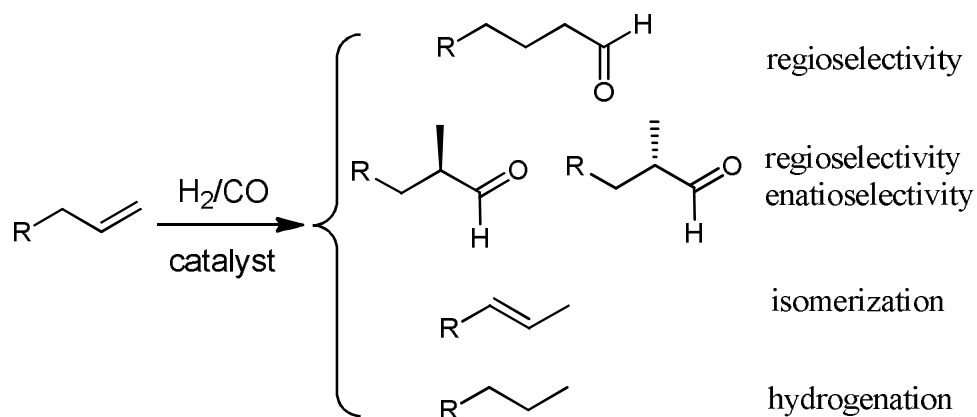
can obtain equation 1.5, which relates the observed rate constants to the concentrations of observed linear and branched aldehyde for two parallel and competitive reaction steps.

$$\frac{C_L}{C_B} = \frac{k_L}{k_B}. \quad (1.5)$$

In the above derivation, we have assumed that the rate determining step is the oxidative addition of H<sub>2</sub> to the rhodium species **I** (or **H**) in the catalytic cycle. This assumption is not a necessary condition for the derivation of equation 1.5. The same conclusion can be reached if one of other steps is assumed to be the rate determining step. It can be shown that equation 1.5 is in general valid for two parallel and competitive reactions that start from the same starting material.<sup>14</sup> We will use this relation to study the Hammett plots in Chapter 2.

#### 1.4 Advances in the Development of Phosphorus Ligands

The current challenge of hydroformylation reaction is to control selectivity for a wide range of diverse substrates (Scheme 1.7). The controlling of selectivity includes 1) chemoselectivity (hydroformylation versus isomerization and hydrogenation), 2) regioselectivity (linear isomer versus branched isomer), and 3) enantioselectivity (selective production of a particular enantiomer when the branched isomer is the desired product).

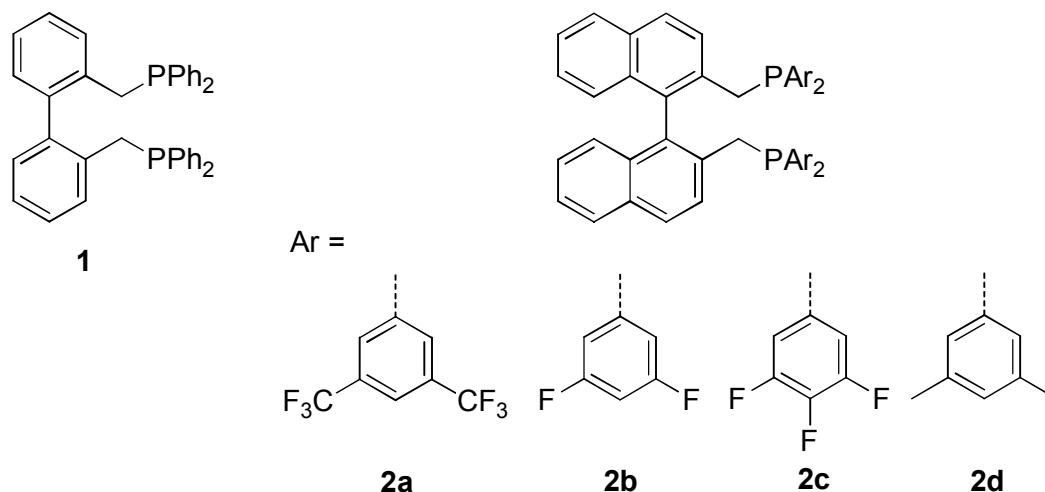


**Scheme 1.7.** Selectivity and side reactions of olefin hydroformylation.

The typical process parameters that will influence the hydroformylation selectivity include temperature, pressure, solvent,  $\text{CO}/\text{H}_2$  ratio, concentration, metal catalyst precursor, ligand, and substrate structure. Although the process has been commercialized for many decades, it is still under constant development in order to address and improve reaction speed, catalyst stability and product selectivity.<sup>15</sup> In the past several decades, many ligand systems were developed to address the issue of regioselectivity and stereoselectivity. In this research, we will particularly focus our efforts on the development of tetraphosphorus ligands to address the regioselectivity.

Commercial rhodium-catalyzed hydroformylation processes use monophosphines as the supporting ligands.  $\text{HRh}(\text{CO})(\text{PPh}_3)_3$  and  $\text{Rh}(\text{acac})(\text{CO})_2$  (acac: acetoacetone) are most commonly used rhodium precursors. Triphenylphosphine is commonly used monodentate ligand, and a large excess of phosphine ligands is usually applied in order to create an active, selective, and stable catalyst system.<sup>1</sup> Recently, bidentate ligands have attracted much more attention because they generally afford higher regioselectivity than monophosphines without the need to load excess amount of ligands. In this section, we will briefly review the recent advances in the development of phosphorus ligands for

regioselective hydroformylation of olefins. We will focus on those ligands that can afford high regioselectivity.



**Figure 1.1.** Bidentate phosphine ligands Bisbi and Naphos.

The first example of applying a bidentate phosphorus ligand for regioselective rhodium-catalyzed hydroformylation was reported in 1987. The chelating bisphosphine ligand is known as Bisbi **1** (Figure 1.1), which was developed by Devon and coworkers at Eastman Kodak. The ligand provided exceptionally high regioselectivity for the hydroformylation of propene.<sup>16</sup>

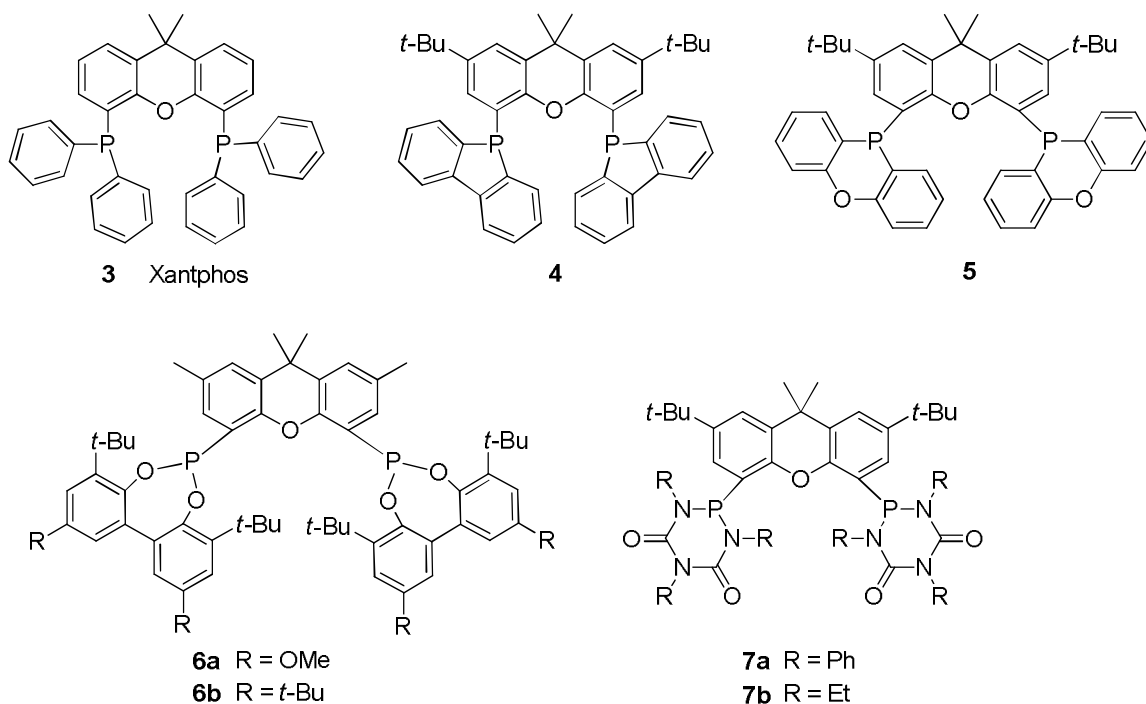
In an effort to understand this phenomenal improvement, Casey and coworkers have studied the correlation between ligand bite angles and the regioselectivity in hydroformylation systematically. They found that ligands with a natural bite angle of about  $120^\circ$ , such as Bisbi **1**, are capable of forming equatorial-equatorial coordination geometry at the rhodium center, which leads to high regioselectivity in the olefin hydroformylation.<sup>17</sup> In a subsequent development, Beller and coworkers reported that the NaPhos ligands **2a-2c** with strong electron-withdrawing substituents are excellent ligands



for regioselective hydroformylation of internal olefins to produce linear aldehydes, and linear to branched ratios of up to 9.5:1 were observed for the hydroformylation of 2-butene, 2-pentene, and 2-octene.<sup>18</sup>

A number of highly regioselective phosphorus ligands have been developed based on the natural bite angle concept. A well known ligand is the Xantphos **3** (Figure 1.2), which was developed by van Leeuwen and coworkers. This ligand has proved to be one of the best ligands for regioselective hydroformylation. For example, a linear to branched ratios of up to 53:1 have been achieved with Xantphos **3** in the hydroformylation of 1-octene.<sup>19</sup> Later on, van Leeuwen and coworkers have carefully examined the correlations between the ligand chelating geometry, bite angle, and the regioselectivity. Their detailed structural study showed that despite that the linear selectivity correlates well to the natural bite angle, the coordination mode in the rhodium complexes does not determine the regiochemistry in the hydroformylation reaction. For example, they found that several Xantphos family ligands that prefer equatorial-axial coordination can also produce aldehyde products with high linear selectivity. This experimental discovery is in contrast to Casey's proposal that equatorial-equatorial coordination mode is a prerequisite for highly regioselective hydroformylation. The bite angle effect on regioselectivity is now believed to influence steric interactions between ligands and substrates in the steps of olefin coordination and alkyl migration. Widening the bite angle leads to an increase in steric congestion around the rhodium center which results in the formation of the sterically less demanding linear rhodium alkyl complexes.<sup>20</sup> Based on the success of Xantphos, van Leeuwen and coworkers later developed dibenzophospholyl and phenoxaphosphanyl-substituted Xantphos type ligands **4** and **5**.<sup>21</sup> These ligands showed high catalytic activity and

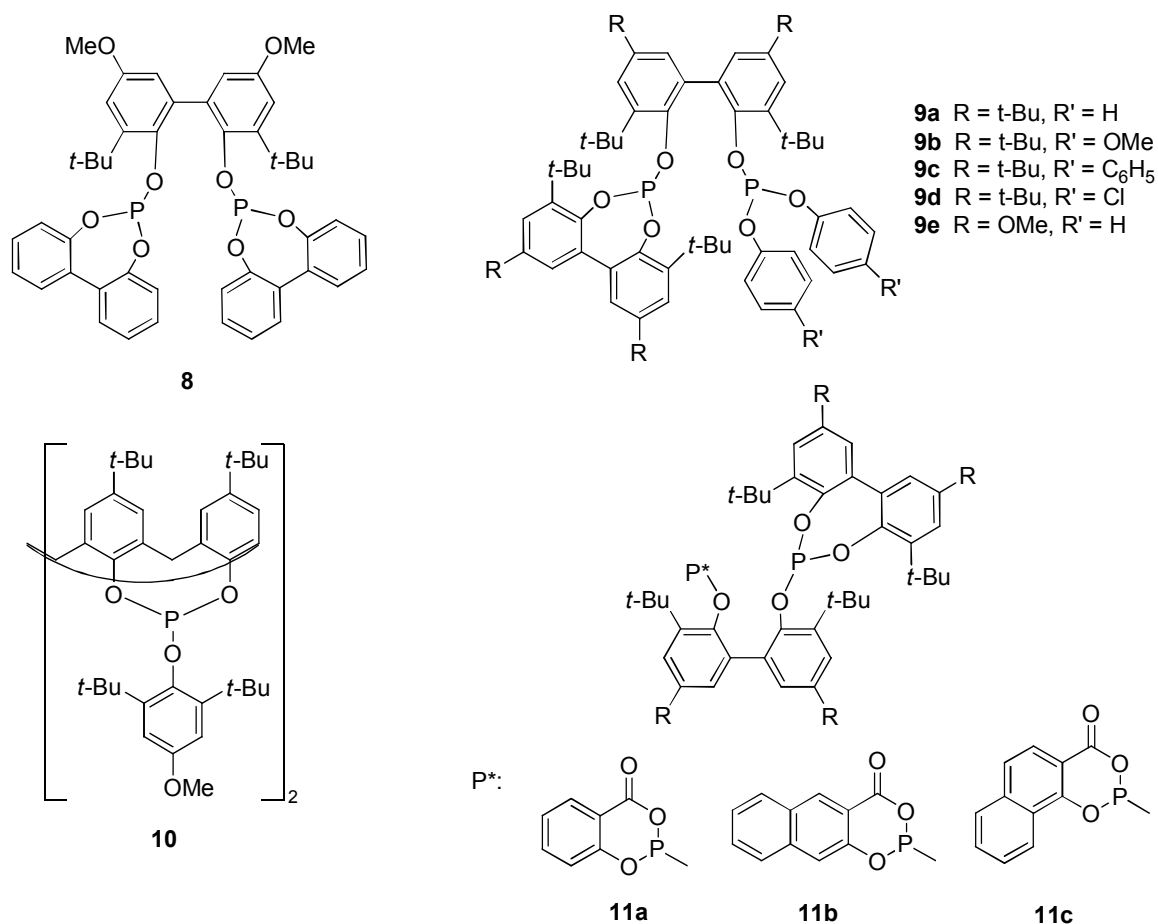
regioselectivity in the rhodium-catalyzed hydroformylation of both terminal and internal octenes. In addition, bulky diphosphite ligands **6a-6b** and phosphorus diamide ligands **7a-7b** that are based on the xanthene backbone were also developed by van Leeuwen's group.<sup>22, 23</sup> Nevertheless, these xanthene phosphites did not afford good regioselectivity.



**Figure 1.2.** Xantphos based bidentate phosphorus ligands.

Another important family of ligands for highly regioselective hydroformylation is the bulky diphosphite ligands (Figure 1.3). A typical representative ligand is Biphephos **8**, which was originally developed by Billig and coworkers at Union Carbide.<sup>24</sup> With this ligand, Buchwald and coworkers studied the hydroformylation of some functionalized olefins under mild reaction conditions, and observed high linear selectivity.<sup>25</sup> Typically, linear to branched ratios of over 40:1 were achieved for terminal olefins having functional groups four or more bonds away from the  $\alpha$ -carbon, and linear to branched ratios ranging from 1.8 to 18 were observed for substrates with an allylic functional group. The catalyst

system tolerates ketones, carboxylic acids, halides, acetals and thioacetals. As variations of Biphephos **8**, unsymmetrical Biphephos derivatives **9a-9e** were developed by van Leeuwen and coworkers. These ligands also showed high regioselectivity in the hydroformylation of terminal olefins.<sup>26</sup> For example, a linear to branched ratio of 24 was observed in the hydroformylation of 1-octene using ligand **9b**.

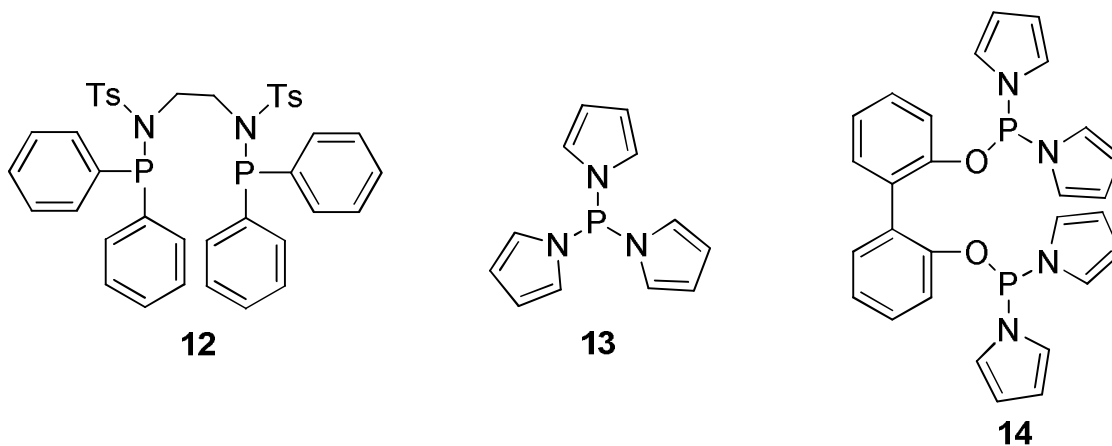


**Figure 1.3.** Bulky diphosphite ligands.

On the basis of molecular modeling calculations, Paciello and coworkers designed and synthesized a chelating diphosphite ligand **10** that is based on the *p*-tert-butyl calix[4]arene backbone.<sup>27</sup> With this ligand, very high regioselectivity has been observed in the rhodium-catalyzed hydroformylation of 1-octene.

Börner and coworkers also have designed and synthesized some unsymmetrical phosphite-acylphosphite ligands **11a-11c** for the isomerization/hydroformylation of internal octene mixtures, and a maximum linear selectivity of 69% *n*-nonanal was obtained with ligand **11c**.<sup>28</sup>

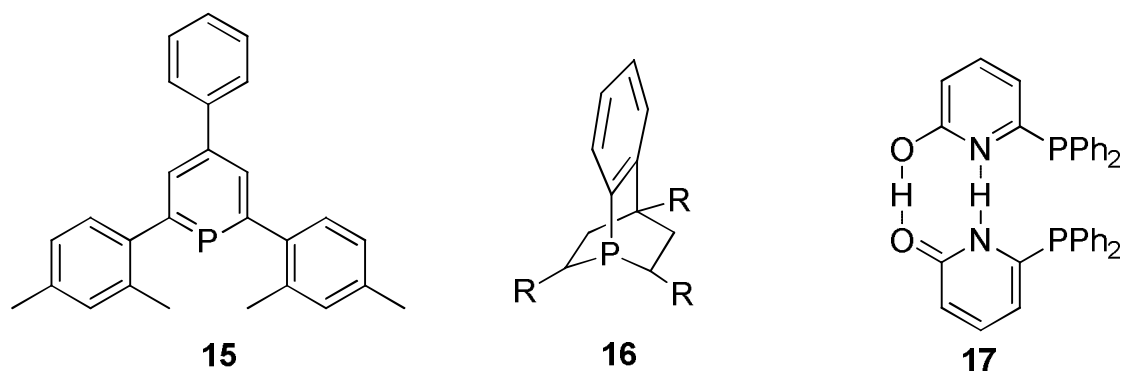
Bisbi derivatives, Xantphos derivatives and bulky diphosphites are the three major types of ligands for controlling regioselectivity in olefin hydroformylation. In the last decade, several other types of phosphorus ligands have been developed and applied in the regioselective hydroformylation of olefins. These examples are listed in Figures 1.4 and 1.5.



**Figure 1.4.** Phosphorus ligands containing P-N bonds.

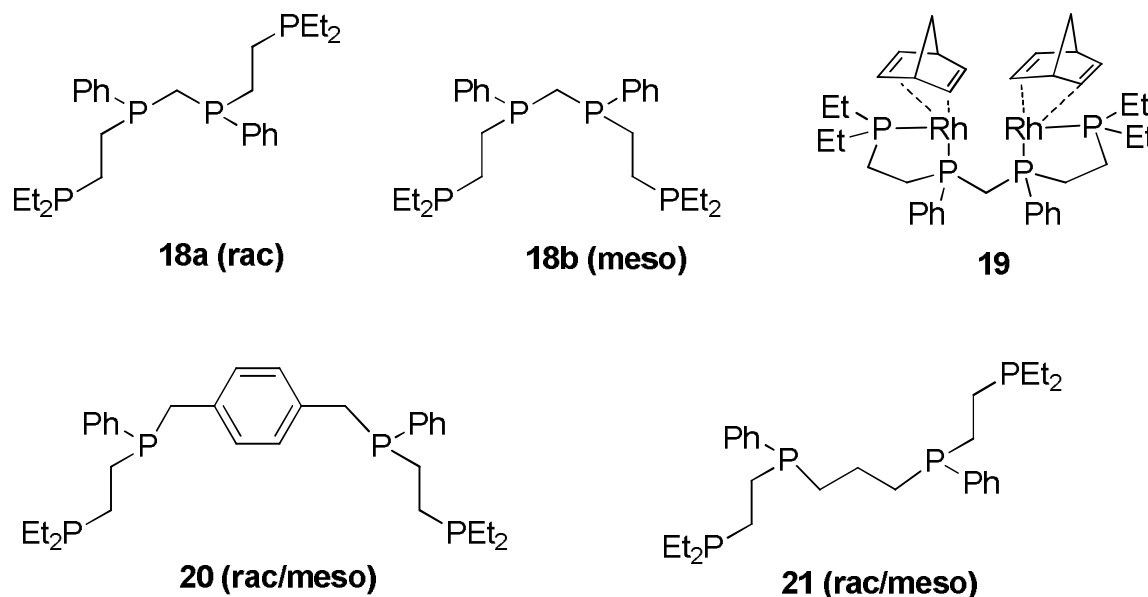
Electron-withdrawing N-sulfonylphosphoramidate ligand **12** was developed by Hersh and coworkers.<sup>29</sup> With this ligand, moderate regioselectivity with a linear to branched ratio of up to 15.8 was obtained in the hydroformylation of 1-hexene. Ziółkowski and coworkers first reported pyrrole based monodentate ligand **13** in regioselective hydroformylation of 1-hexene,<sup>30</sup> and they observed a linear to branched ratio of up to 30 using  $\text{P}(\text{NC}_4\text{H}_4)_3$ . They noted that the strong  $\pi$ -acidity of ligand **13** is beneficial for the

high regioselectivity. Later, van Leeuwen and coworkers developed bidentate pyrrole-based phosphoramidite ligand **14** for the hydroformylation of 1-octene.<sup>31</sup> Very high regioselectivity for the linear aldehyde (a linear to branched of about 100) was achieved together with moderate isomerization to 2-octene.



**Figure 1.5.** Phosphabenzene phosphabarrelene and self-assembled phosphines.

Breit and coworkers have developed phosphabenzene ligand **15** and applied it in the rhodium-catalyzed hydroformylation reactions. The catalyst exhibited very high reactivity, and even tetra substituted olefins were under hydroformylation with noticeable reaction rates.<sup>32</sup> Phosphabarrelene **16** has been synthesized and tested in the hydroformylation of internal olefins by Breit and coworkers. Interestingly, unlike other known catalysts designed for the hydroformylation of internal alkenes that usually undergo isomerization before hydroformylation, using the rhodium/phosphabarrelene catalyst, an internal double bond was hydroformylated without olefin isomerization.<sup>33</sup> Recently, Breit and coworkers have developed another ligand **17**. This ligand was formed by self-assembly through the hydrogen bonding of 6-(diphenylphosphino) pyridin-2(1H)-one with its hydroxypyridine tautomer.<sup>34</sup> With this ligand, high regioselectivity has been observed for the hydroformylation of a variety of terminal olefins.



**Figure 1.6.** Tetraphosphines for bimetallic catalyst system.

The last ligand system we want to discuss is the development of tetraphosphorus ligands (Figure 1.6). These tetraphosphorus ligands were reported by Stanley and coworkers.<sup>35-37</sup> Ligands **18a** and **18b** can form bimetallic rhodium complexes which have been demonstrated to be highly active and regioselective hydroformylation catalysts under mild conditions. Using the bimetallic rhodium complex **19**, the hydroformylation of 1-hexene afforded a linear to branch ratio of 33:1 and an initial turnover frequency of 30 per minute. However, replacing ligand **18a** or **18b** with the spaced bimetallic complexes formed from ligand **20** or **21**, the hydroformylation gave extremely poor rates and regioselectivities. In addition, the corresponding monometallic rhodium complex prepared from Rh(nbd)(BF<sub>4</sub>)<sub>2</sub> and dppe (diphenylphosphinoethane) also gave poor reaction rate and regioselectivity. This indicated that the two rhodium centers did not work independently. Stanley and coworkers have proposed a cooperative bimetallic hydroformylation mechanism that involved dicationic bimetallic rhodium(II) complexes,

which were supported by spectroscopic studies. A uniqueness of the Stanley's mechanism is the cooperative intramolecular hydride transfer from the rhodium hydride to the rhodium acyl species, which was thought to enhance the elimination of the aldehyde from the acyl intermediate.<sup>36</sup>

## 1.5 Objectives

The current challenge of hydroformylation reaction is to control selectivity for a wide range of diverse substrates. In this dissertation research, we will particularly focus our efforts on the development of new tetraphosphorus ligands for the regioselective hydroformylation of terminal and internal olefins with a variety of functional groups. Our main objective is to develop new catalyst systems that can afford high linear selectivity and catalyst stability at high operating temperatures.

In Chapter 2, we will report our research on the development of new tetraphosphoramidite ligands and their applications in the hydroformylation of functionalized allyl, vinyl, and styrene derivatives. The tetra phosphoramidite ligands have showed remarkable high linear selectivity for a diversity of functionalized alkenes. To the best of our knowledge, the linear selectivity achieved with the tetraphosphoramidite ligands is the highest ever reported for allyl cyanide, styrene and several other substrates. We have also investigated the ligand and substrate structural effects on the regioselectivity and catalytic activity systematically for the hydroformylation of allyl cyanide, styrene and 2-octene. We will use Hammett plots to discuss the structure-regioselectivity/activity relationships.

In Chapter 3, we will report our research on the development of new tetraphosphine ligands and their applications in the hydroformylation of terminal alkenes, and isomerization/hydroformylation of internal alkenes. These new tetraphosphine ligands have showed very high linear selectivity at high operating temperatures, which is desirable for the hydroformylation of long chain olefins. The mechanism of isomerization/hydroformylation of internal alkenes will be discussed.



## References

1. For recent reviews and monographs, see: a) *Rhodium Catalyzed Hydroformylation*; Claver, C.; van Leeuwen, P. W. N. M., Eds.; Kluwer Academic Publishers: Dordrecht, The Netherlands, 2000. b) Ungvary, F. *Coord. Chem. Rev.* **2005**, *249*, 2946-2961. c) Clarke, M. L. *Curr. Org. Chem.* **2005**, *9*, 701-718. d) Dieguez, M.; Pamies, O.; Claver, C. *Tetrahedron: Asymm.* **2004**, *15*, 2113-2122. e) Breit, B.; Seiche, W. *Synthesis*, **2001**, 1. f) Beller, M.; Cornils, B.; Frohning, C. D.; Kohlpainter, C. W. *J. Mol. Cat. A*, **1995**, *104*, 17.
2. a) Roelen, O. (Chemische Verwertungsgesellschaft, mbH Oberhausen) German Patent DE 849548, **1938/1952**. b) Roelen, O. (Chemische Verwertungsgesellschaft, mbH Oberhausen) U.S. Patent 2327066, **1943**.
3. a) Jennerjahn, R.; Piras, I.; Jackstell, R.; Franke, R.; Wiese, K.-D.; Beller, M. *Chem. Eur. J.* **2009**, *15*, 6383. b) Gruenanger, C. U.; Breit, B. *Angew. Chem., Int. Ed.* **2010**, *49*, 967. c) Makado, G.; Morimoto, T.; Sugimoto, Y.; Tsutsumi, K.; Kagawa, N.; Kakiuchi, K. *Adv. Synth. Catal.* **2010**, *352*, 299. d) Dabbawala, A. A.; Jasra, R. V.; Bajaj, H. C. *Catal. Commun.* **2010**, *11*, 616. e) Panda, A. G.; Bhor, M. D.; Ekbote, S. S.; Bhanage, B. M. *Catal. Lett.* **2009**, *131*, 649. f) Liu, W.; Yuan, M.; Fu, H.; Chen, H.; Li, R.; Li, X. *Chem. Lett.* **2009**, *38*, 596. g) Goudriaan, P. E.; Kuil, M.; Jiang, X.-B.; van Leeuwen, P. W. N. M.; Reek, J. N. H. *Dalton Trans.* **2009**, 1801. h) Simaan, S.; Marek, I. *J. Am. Chem. Soc.* **2010**, *132*, 4066. i) Spangenberg, T.; Breit, B.; Mann, A. *Org. Lett.* **2009**, *11*, 261. j) Worthy, A. D.; Gagnon, M. M.; Dombrowski, M. T.; Tan, K. L. *Org. Lett.* **2009**, *11*, 2764. h) Wang, X.; Buchwald, S. J. *Am. Chem. Soc.* **2011**, *133*, 19080.
4. a) Evans, D. A.; Osborn, J. A.; Wilkinson, G. *J. Chem. Soc. A*, **1968**, 3133. b) Brown, C. K.; Wilkinson, G. *J. Chem. Soc. A* **1970**, *17*, 2753. c) Wilkinson, G. *Bull. Soc. Chim. Fr.* **1968**, 5055. d) Osborn, J. A.; Jardine, F. H.; Young, J. F.; Wilkinson, G. *J. Chem. Soc. A*, **1966**, 1711.
5. a) Stille, J. K. In *Comprehensive Organic Synthesis*; Trost, B. M.; Fleming, I., Eds.; Pergamon: Oxford, **1991**. b) Wiese, K.-D.; Obst, D. *Top. Organomet. Chem.* **2006**, *18*, 1. c) Eilbracht, P.; Schmidt, A. M. *Top. Organomet. Chem.* **2006**, *18*, 65.
6. Heck, R. F.; Breslow, D. S. *J. Am. Chem. Soc.* **1961**, *83*, 4023.
7. a) van Rooy, A.; Orij, E. N.; Kamer, P. C. J.; van Leeuwen, P. W. N. M. *J. Organometallics*, **1995**, *14*, 34. b) Van Rooy, A.; Orij, E. N.; Kamer, P. C. J.; van den Aardweg, F.; van Leeuwen, P. W. N. M. *J. Chem. Soc., Chem. Commun.* **1991**, 1096. c) Jongsma, T.; Challa, G.; van Leeuwen, P. W. N. M. *J. Organometal.* **1991**, *421*, 121.
8. a) Buisman, G. J. H.; van der Veen, L. A.; Kamer, P. C. J.; van Leeuwen, P. W. N. M. *J. Organometallics*, **1997**, *16*, 5681. b) Buisman, G. J. H.; Vos, E.; Kamer, P. C. J.; van Leeuwen, P. W. N. M. *J. Chem. Soc., Dalton Trans.* **1995**, 409.

9. a) Casey, C. P.; Whiteker, G. T. *Isr. J. Chem.* **1990**, *30*, 299. b) Dierkes, P.; van Leeuwen, P. W. N. M. *J. Chem. Soc., Dalton Trans.* **1999**, 1519.
10. a) Brown, J. M.; Kent, A. G. *J. Chem. Soc. Perkin Trans. II*, **1987**, 1597. b) Gregorio, G.; Montrasi, G.; Tanipieri, M.; Cavalieri d'Oro, P.; Pagani, G.; Andreetta, A. *Chim. Ind. (Milan)*, **1980**, *62*, 389.
11. Moser, W. R.; Papile, C. J.; Brannon, D. A.; Duwell, R. A.; Weininger, S. J. *J. Mol. Catal.*, **1987**, *41*, 271.
12. Kastrup, R. V.; Merola, J. S.; Oswald, A. A. In *ACS Advances in Chemistry Series*; Eds: Alyea, E. L.; Meek, D. W., ACS, Washington D. C., **1982**, Vol. *196*, Chapter 3, p. 43.
13. Unruh, J. D.; Christenson, J. R. *J. Mol. Catal.* **1982**, *14*, 19.
14. a) Connors, K. *Chemical Kinetics, the study of reaction rates in solution*, John Wiley & Sons, New York, **1990**. b) Fogler, H. S. *Elements of Chemical Reaction Engineering*, 2<sup>nd</sup> ed., Prentice Hall, New Jersey, **1992**.
15. a) van der Veen, L. A.; Kamer, P. C. J.; van Leeuwen, P. W. N. M. *Angew. Chem. Int. Ed.*, **1999**, *38*, 336. b) van der Veen, L. A.; Kamer, P. C. J.; van Leeuwen, P. W. N. M. *Organometallics*, **1999**, *18*, 4765. c) Klein, H.; Jackstell, R.; Wiese, K.-D.; Borgmann, C.; Beller, M. *Angew. Chem. Int. Ed.*, **2001**, *40*, 3408. d) Selent, D.; Hess, D.; Wiese, K.-D.; Röttger, D.; Kunze, C.; Börner, A. *Angew. Chem. Int. Ed.*, **2001**, *40*, 1696. e) Billig, E.; Abatjoglou, A. G.; Bryant, D. R. (UCC) EP 213639, **1987**, US 4748261, **1988**. f) Burke, P. M.; Garner, J. M.; Kreutzer, K. A.; Teunissen, A. J. J. M.; Snijder, C. S.; Hansen, C. B. (DSM/Du Pont) WO 97/33854, **1997**. g) Klein, H.; Jackstell, R.; Beller, M. *Chem. Commun.*, **2005**, 2283.
16. Devon, T. J.; Phillips, G. W.; Puckette, T. A.; Stavinoha, J. L.; Vanderbilt, J. J. US Patent 4 694 109, **1987**.
17. a) Casey, C. P.; Whiteker, G. T.; Melville, M. G.; Petrovich, L. M.; Gavey, J. A.; Powell, D. R. *J. Am. Chem. Soc.* **1992**, *114*, 5535. b) Casey, C. P.; Paulsen, E. L.; Beuttenmueller, E. W.; Proft, B. R.; Matter, B. A.; Powell, D. R. *J. Am. Chem. Soc.* **1999**, *121*, 63.
18. Klein, H.; Jackstell, R.; Wiese, K.; Borgmann, C.; Beller, M. *Angew. Chem. Int. Ed.* **2001**, *40*, 3408.
19. a) Kranenburg, M.; van der Burgt, Y. E. M.; Kamer, P. C. J.; van Leeuwen, P. W. N. M. *Organometallics* **1995**, *14*, 3081. b) Kamer, P. C. J.; van Leeuwen, P. W. N. M.; Reek, J. N. H. *Acc. Chem. Res.* **2001**, *34*, 895.
20. a) van der Veen, L. A.; Keeven, P. H.; Schoemaker, G. C.; Reek, J. N. H.; Kamer, P. C. J.; van Leeuwen, P. W. N. M.; Lutz, M.; Spek, A. L. *Organometallics* **2000**, *19*, 872. b) van der Veen, L. A.; Boele, M. D. K.; Bregman, F. R.; Kamer, P. C. J.; van Leeuwen,

- P. W. N. M.; Goubitz, K. ; Fraanje, J. ; Schenk, H. ; Bo, C. *J. Am. Chem. Soc.* **1998**, *120*, 11616. c) Dieleman, C. B.; Kamer, P. C. J.; Reek, J. N. H.; van Leeuwen, P. W. N. M. *Helvetica Chimica Acta* **2001**, *84*, 3269.
21. a) van der Veen, L. A.; Kamer, P. C. J.; van Leeuwen, P. W. N. M. *Angew. Chem. Int. Ed.* **1999**, *38*, 336. b) van der Veen, L. A.; Kamer, P. C. J. ; van Leeuwen, P. W. N. M. *Organometallics* **1999**, *18*, 4765. c) Bronger, R. P. J.; Kamer, P. C. J.; van Leeuwen, P. W. N. M. *Organometallics* **2003**, *22*, 5358.
22. Dieleman, C. B.; Kamer, P. C. J.; Reek, J. N. H.; van Leeuwen, P. W. N. M. *Helvetica Chimica Acta*, **2001**, *84*, 3269.
23. van der Slot, S.C.; Kamer, P. C. J.; van Leeuwen, P. W. N. M.; Fraanje, J.; Goubitz, K.; Lutz, M.; Spek, A. L. *Organometallics* **2000**, *19*, 2504.
24. Billig, E.; Abatjoglou, A. G.; Bryant, D. R. (UCC) US Patent 4769498, **1988**.
25. Cuny, G. D.; Buchwald, S. L. *J. Am. Chem. Soc.* **1993**, *115*, 2066.
26. Van Rooy, A. ; Kamer, P. C. J. ; van Leeuwen, P. W. N. M.; Goubitz, K.; Fraanje, J.; Veldman, N.; Spek, A. L. *Organometallics* **1996**, *15*, 835.
27. Paciello, R.; Siggel, L.; Röper, M. *Angew. Chem. Int. Ed.* **1999**, *38*, 1920.
28. Selent, D.; Hess, D.; Wiese, K.; Röttger, D.; Kunze, C.; Börner, A. *Angew. Chem. Int. Ed.* **2001**, *40*, 1696.
29. Magee, M. P.; Luo, W.; Hersh, W. H. *Organometallics* **2002**, *21*, 362.
30. Trzeciak, A. M. Głowiak, T. Grzybek, R. Ziółkowski, J. J. *J. Chem. Soc., Dalton Trans.*, **1997**, 1831.
31. van der Slot, S. C.; Duran, J.; Luten, J.; Kamer, P. C. J.; van Leeuwen, P. W. N. M. *Organometallics*, **2002**, *21*, 3873.
32. Breit, B.; Winde, R.; Mackewitz, T.; Paciello, R.; Harms, K. *Chem. Eur. J.* **2001**, *7*, 3106.
33. Breit, B.; Fuchs, E. *Chem. Commun.*, **2004** , 694.
34. a) Breit, B.; Seiche, W. *J. Am. Chem. Soc.* **2003**, *125*, 6608. b) Seiche, W.; Schuschkowski, A.; Breit, B. *Adv. Synth. Catal.* **2005**, *347*, 1488.
35. Brousard, M. E.; Juma, B.; Train, S. G.; Peng, W.-J.; Laneman, S. A.; Stanley, G. G. *Science*, **1993**, *260*, 1784.
36. Matthews, R. C.; Howell, D. K.; Peng, W.-J.; Train, S. G.; Treleaven, W.; S. A.; Stanley, G. G. *Angew. Chem. Int. Ed.* **1996**, *35*, 2253.

37. Aubry, D. A.; Bridges, N. N.; Ezell, K.; Stanley, G. G. *J. Am. Chem. Soc.* **2003**, *125*, 11180.

## Chapter 2 Tetraphosphoramidite Ligands for Regioselective

### Hydroformylation of Olefins

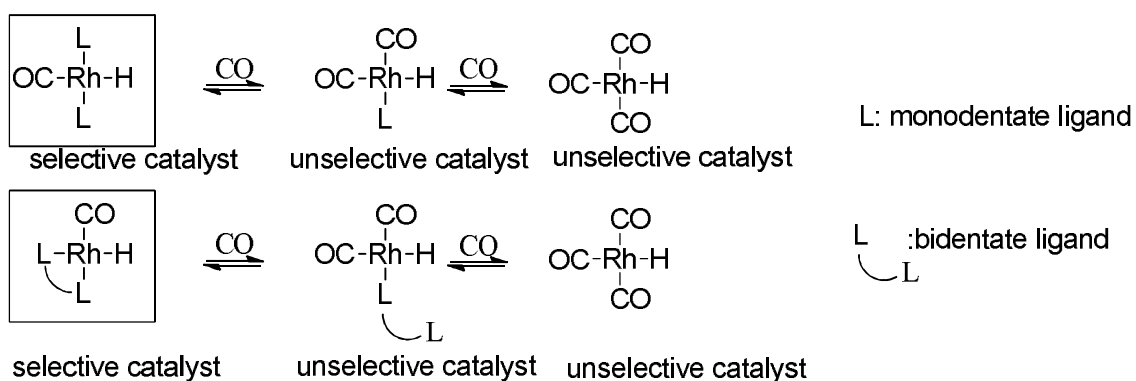
#### 2.1 Introduction

As we pointed out in Chapter 1, the current challenge of hydroformylation is to control chemoselectivity, regioselectivity and enantioselectivity for a wide range of diverse substrates.<sup>1-2</sup> Over the past decades, many ligand systems have been developed to address these issues. Some elegant examples include Devon's bisbi,<sup>3</sup> van Leeuwen's xantphos and bisphosphoramidite,<sup>4</sup> Beller's naphos,<sup>5</sup> Union Carbide's biphephos,<sup>6</sup> and DuPont/DSM's bulky phosphites.<sup>7</sup> A practicable and good hydroformylation catalyst should afford reasonable reaction speed, catalyst stability and product selectivity with minimal cost.

The regioselective hydroformylation of functionalized alkenes is a highly substrate dependent process. Vinyl, allyl, and styrene derivatives have intrinsic properties to afford branched aldehydes; therefore, they are usually good substrates for enantioselective asymmetric hydroformylation. For example, styrene, vinyl acetate and allyl cyanide are often applied as benchmark substrates for asymmetric hydroformylation.<sup>8</sup> On the other hand, it will be a challenging task to develop catalyst systems that can afford highly linear aldehydes for these substrates. In this chapter, we will report and discuss our research on the development of a new class of tetraphosphoramidite ligands, their applications in the regioselective hydroformylation of functionalized terminal olefins and internal olefins, and the structure regioselectivity/activity relationships.

## 2.2 Design of Tetraphosphoramidite Ligands

A major problem encountered in achieving high regioselectivity in hydroformylation is the issue of ligand dissociation (Scheme 2.1). In commercial hydroformylation processes that use monophosphorus ligands, the catalytic species with two phosphines coordinating to the metal center is the desired regioselective catalytic species.<sup>1</sup> The dissociation of phosphorus ligands from the metal center followed by replacement with CO leads to the formation of highly reactive yet unselective catalytic species. In order to prevent the formation of unselective catalytic species and achieve high regioselectivities, a large excess of ligand is employed.

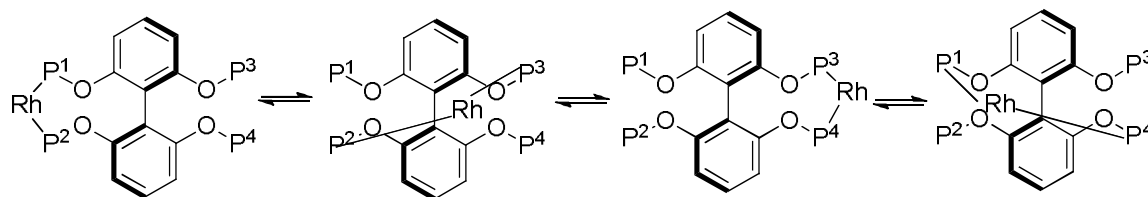


**Scheme 2.1.** Rhodium/ligand complexes and ligand dissociation under the influence of CO in hydroformylation.

For known bidentate bisphosphorus ligands capable of affording high regioselectivities in hydroformylation, typically eight or nine-membered chelating rings are formed. The chelating effects of eight or nine-membered rings are weaker than that of five and six-membered chelating rings. We reasoned that the dissociation of bisphosphorus ligands from the metal in eight or nine-membered chelating rings can also happen under

some hydroformylation conditions. Moreover, in the hydroformylation of functionalized alkenes, after alkene coordination to the metal center, a neighboring group, such as a phenyl group, a cyano group, or an oxygen atom, can coordinate to the open coordination site left by the ligand dissociation and form a multidentate chelating metal/substrate complex, and thus resulting in undesired regioselectivity.

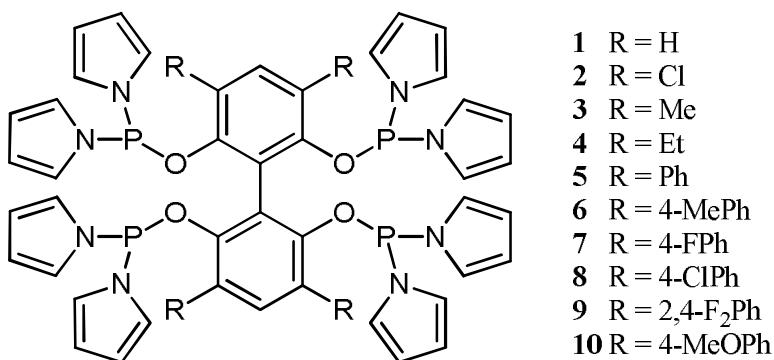
In order to achieve high regioselectivity in the hydroformylation of functionalized olefins, a new strategy to enhance the chelating ability of ligands is needed. We envision that the chelating ability could be enhanced by using ligands capable of forming multiple chelating modes. As illustrated in Scheme 2.2, there are four identical chelating modes when a tetraphosphorus ligand is complexed with rhodium. Therefore, when the tetraphosphorus ligand coordinates with the metal, the existing free phosphorus atoms can effectively increase the local phosphorus concentration around the metal center and enhance the coordination ability of the tetraphosphorus ligand compared with the corresponding bisphosphorus ligands. Furthermore, this local enhancement of phosphorus concentration will not be diluted by reaction volume.



**Scheme 2.2.** Enhanced chelating ability of tetraphosphorus ligands through dynamic multiple chelating modes and increased local phosphorus concentration.

Our group has previously reported the development of pyrrole based tetraphosphorus ligands for highly linear selective hydroformylation of simple olefins and styrene.<sup>9</sup> The

structures of the pyrrole based tetraphosphoramidite ligands are depicted in Figure 2.1. The ligands are based on a biphenyl backbone, and have four equivalent phosphorus groups, which can greatly enhance the local phosphorus concentration around the coordinating center.



**Figure 2.1.** Tetraphosphoramidite ligands.

Ligands **1-7** were found to be effective for the hydroformylation of 1-hexene, 2-hexene, 1-octene, and 2-octene with linear selectivity up to 99.7%. In particular, ligands **5-7** were found to be effective for the hydroformylation of styrene with linear selectivity up to 95.7%. This result is unique in that styrene usually favors branched aldehyde because the Rh-styrene complex linked at the  $\alpha$ -carbon is stabilized by an  $\eta^2$  coordination from the nearby phenyl ring;<sup>1</sup> however, ligands **5-7** are able to override this ortho direction and to afford high linear selectivity. Encouraged by this result, we have continued to develop new tetraphosphorus ligands aiming to higher linear selectivity and catalyst activity for functionalised olefins.

In our efforts to further expand and explore the utility of tetraphosphoramidite ligands, ligands **8-10**, which bear strong electron-withdrawing and electron-donating groups at the phenyl substituent, were synthesized and subsequently applied in the hydroformylation of

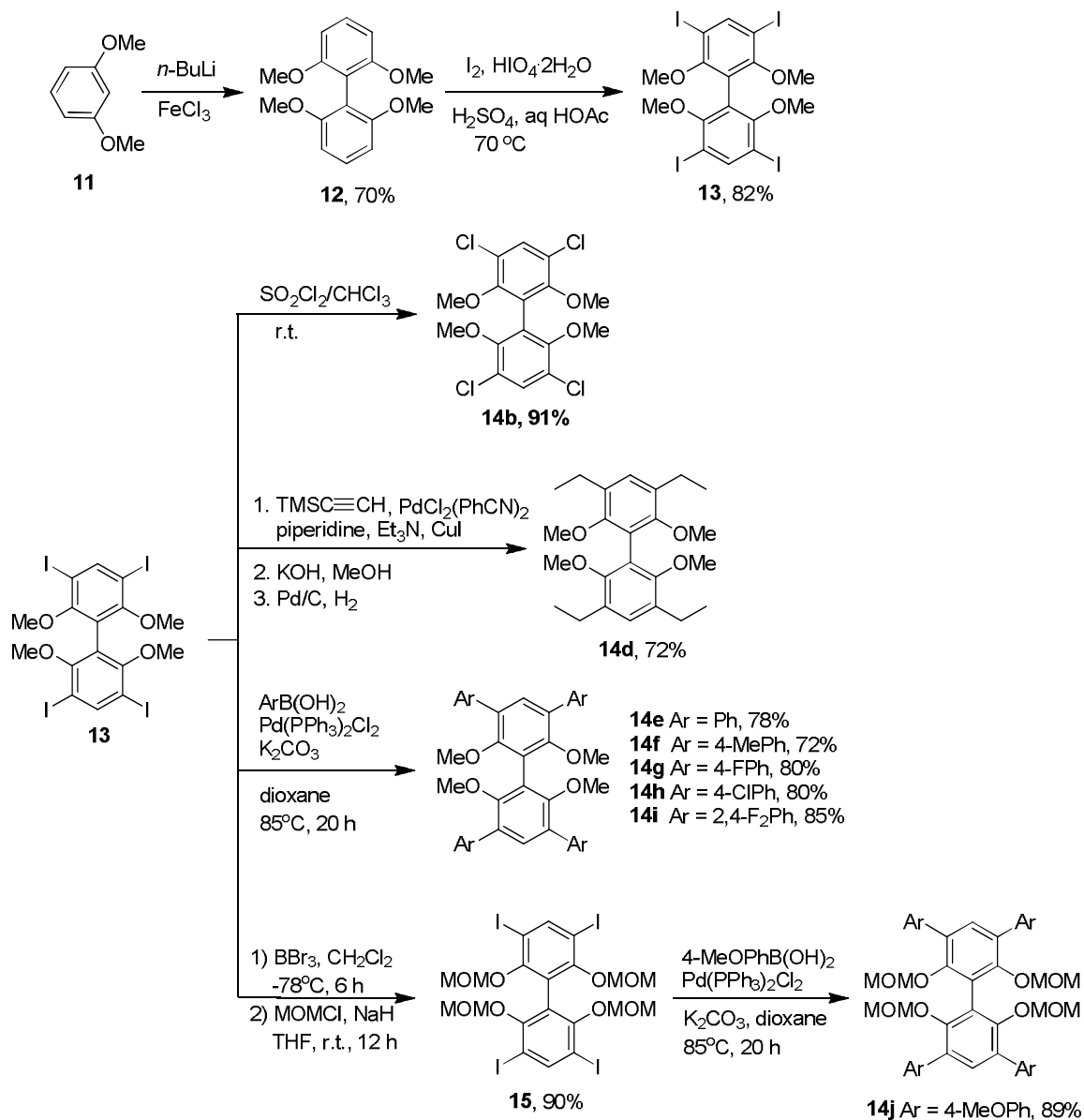


a variety of functionalized allyl, vinyl, and styrene derivatives. We are pleased to find that ligand **9** is highly effective and linear selective for many functionalized allyl, vinyl, and styrene derivatives, and in general affords higher linear selectivity than other ligands previously reported.

### 2.3 Synthesis of Tetraphosphoramidite Ligands

The tetraphosphoramidite ligands can be prepared by coupling of biphenyl tetraols with chlorodipyrrolylphosphine. The substituent group variety in the biphenyl backbone requires us to synthesize a series of tetra substituted biphenyl tetraols. The syntheses of these tetraol precursors are shown in Schemes 2.3. Starting from commercially available 1,3-dimethoxy benzene, the deprotonation of 1,3-dimethoxybenzene was immediately followed by an oxidative homocoupling reaction using  $\text{FeCl}_3$  as the catalyst, which afforded tetramethoxy biphenyl **12** in 70% yield. Iodination of biphenyl **12** under strong acidic conditions afforded tetraiodide **13**, which was subsequently coupled with a variety of substituent groups under various conditions to give a series of tetra substituted biphenyl **14**. Starting from tetraiodide **13**, the chlorination of **13** with sulfuryl chloride in chloroform at room temperature affords tetra chloro substituted biphenyl **14b** in 91% yield. The Sonogashira coupling of tetraiodide **13** with trimethylsilyl acetylene, followed by the deprotection of trimethylsilyl group by KOH and hydrogenation of the alkyne bond catalyzed by Pd/C afforded the tetra ethyl substituted biphenyl **14d** in 72% yield. The tetra substituted compounds **14e** to **14i** were prepared by Suzuki coupling of tetraiodide **13** with the corresponding boronic acids using  $\text{Pd}(\text{PPh}_3)_2\text{Cl}_2$  or  $\text{Pd}(\text{PPh}_3)_4$  as the catalyst. Tetra 4-methoxyphenyl substituted biphenyl **14j** was prepared by first changing the methoxy protection of tetraiodide **13** with the methoxymethyl ether (MOM) protection, followed by

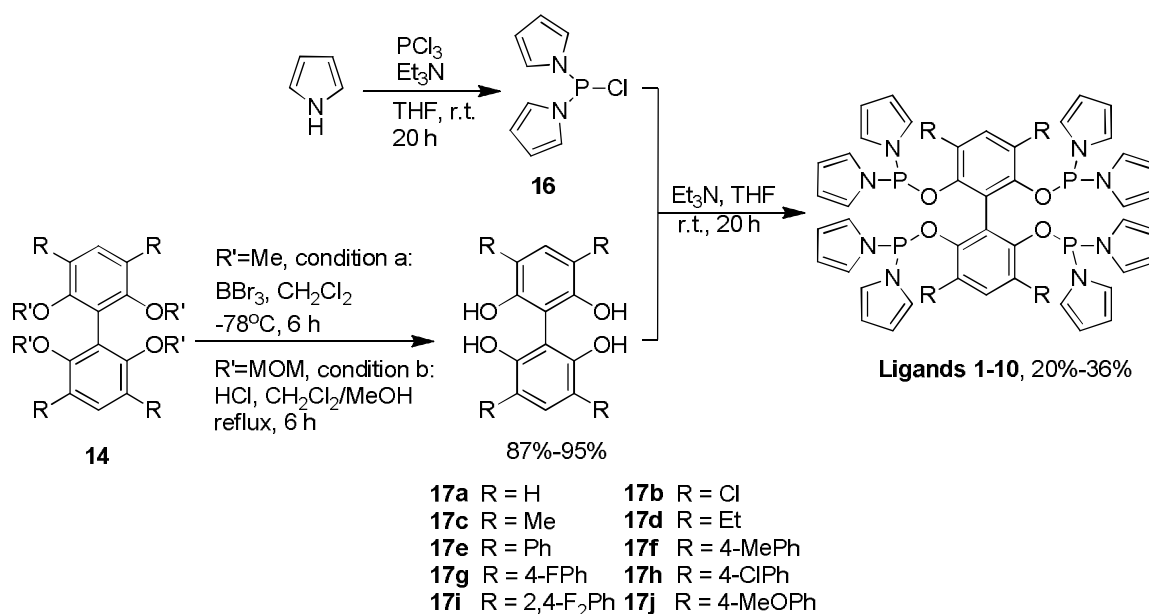
Suzuki coupling of tetraiodide **13** with 4-methoxyphenyl boronic acid. The MOM groups can be removed under mild conditions with 4-methoxyphenyl groups untouched.



**Scheme 2.3.** Synthesis of tetra substituted biphenyls.

The final synthesis of ligands **1** to **10** is shown in Scheme 2.4. Treatment of tetraiodides **12**, **14b**, and **14d** to **14i** with boron tribromide removed the methoxy protection and afforded tetra substituted biphenyl tetraols **17** in 87% to 95% yields. Treatment of biphenyl

**14j** with concentrated HCl removed the MOM protection and afforded the corresponding tetra 4-methoxyphenyl substituted biphenyl tetraol. Ligand **3** was prepared from 2,6,2',6'-tetrahydroxy-3,5,3',5'-tetramethylbiphenyl, which was directly synthesized from *m*-xylorcinol by a two-phase oxidation at the presence of ferric chloride.<sup>10</sup> Chlorodipyrrolylphosphine **16** was prepared by reacting pyrrole with PCl<sub>3</sub> in a stoichiometric ratio under the presence of triethylamine,<sup>3</sup> and it was freshly distilled before an immediate use in the next step. Finally, the couplings of tetraols **17** with chlorodipyrrolylphosphine afforded the tetraphosphoramidite ligands **1** to **10** in yields ranging from 20% to 36%.



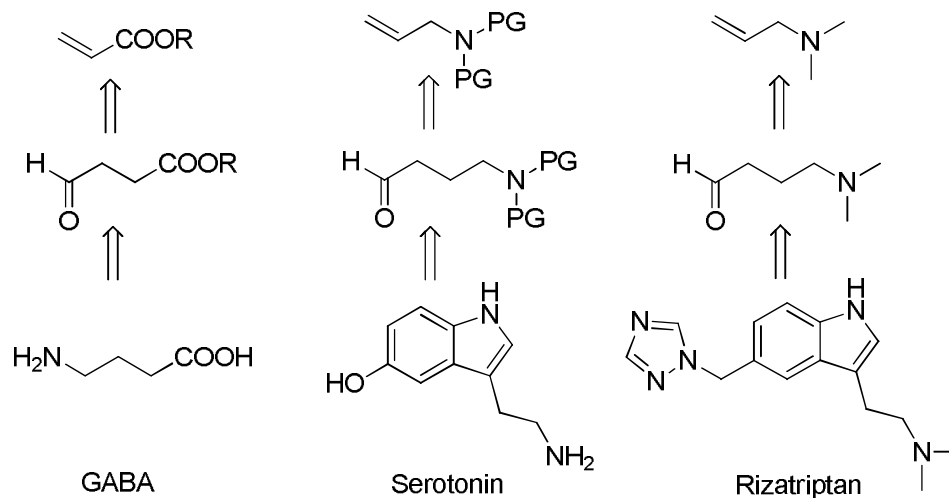
**Scheme 2.4.** Synthesis of Ligands **1-10**.

## 2.4 Hydroformylation of Functionalized Olefins

Hydroformylation of functionalized olefins is a cost effective process to produce functionalized linear or branched aldehydes from readily available cheap starting

materials. The functionalized aldehydes produced from the hydroformylation process can be further converted to dialdehydes, diols, diacids, amino aldehydes, amino alcohols or amino acids, which can be used as versatile building blocks in organic synthesis such as indolization, alkylation, amination and amide coupling to make polymers, macrocycles and pharmaceutical intermediates.<sup>11</sup> In early 1990s, Buchwald et al. reported the regioselective hydroformylation of a variety of functionalized terminal olefins by employing Union Carbide's biphosphos ligand.<sup>12</sup> They observed a typical linear to branch (*l:b*) ratio of  $\geq 40$  for terminal olefins having functional groups four or more bonds away from the  $\alpha$ -carbon and a *l:b* ratio ranging from 1.8 to 18 for substrates with an allylic functional group. In the past decades, while extensive efforts have been put on the development of asymmetric hydroformylation catalyst for the preparation of chiral aldehydes from functionalized alkenes, little attention has been paid on the development of catalyst to prepare linear aldehydes from functionalized alkenes. However, such a catalyst is desirable in situations that functionalized terminal aldehydes are requisite. For example, several biological important compounds in Figure 2.2 can be prepared via hydroformylation of functionalized terminal olefins.  $\gamma$ -aminobutyric acid (GABA) and 5-hydroxytryptamine (Serotonin) are two important naturally occurring neurotransmitters, which have important regulation roles in central nervous system of human being.<sup>13</sup> Rizatriptan is a selective 5-hydroxytryptamine<sub>1</sub> receptor agonist drug developed by Merck and used for the treatment of migraine headaches.<sup>14</sup> The development of hydroformylation technology on functionalized olefins can provide a variety of functionalized aldehydes as building blocks to explore potential chemical structure space in drug optimization. As shown in Figure 2.2, the indole pharmacophore motif in Serotonin and Rizatriptan can be

conveniently explored through Fischer indole synthesis using a variety of functionalized terminal aldehydes.



**Figure 2.2.** Biological active compounds can be prepared via hydroformylation of functionalized olefins. PG: protection group.

### 2.4.1 Hydroformylation of Allyl Cyanide

After the preparation of ligands **1** to **10**, the hydroformylations of functionalized allyl and vinyl substrates were then investigated. Allyl cyanide, which usually gives branched aldehyde in hydroformylation, was selected as the model substrate to test the effectiveness of these ligands. The hydroformylation reaction was conducted in toluene with *n*-decane as the internal standard. The rhodium catalyst was prepared *in situ* by mixing the tetraphosphoramidite with Rh(acac)(CO)<sub>2</sub> in toluene. The substrate to catalyst ratio was 1000 and the catalyst concentration was 1.0 mM. The reaction was terminated after 1 h. Ligand **1** was first applied to optimize the hydroformylation conditions of allyl cyanide with respect to parameter changes of CO/H<sub>2</sub> pressure, temperature and ligand-to-rhodium (L/Rh) ratio. The effect of CO/H<sub>2</sub> pressure was tested with CO/H<sub>2</sub> pressure ranging from

5/5 to 30/30 atm (Table 2.1, entries 1-4). With the increase of CO/H<sub>2</sub> pressure, the regioselectivity decreases. The highest regioselectivity was obtained under a CO/H<sub>2</sub> pressure of 5/5 atm with a linear to branch (*l:b*) ratio of 5.2 (Table 2.1, entry 1). However, slight higher percentage of isomerization was observed under this pressure, indicating the  $\beta$ -H elimination was facilitated under low CO/H<sub>2</sub> pressures. The facilitation of  $\beta$ -H elimination made the reaction more reversible to the starting material, thus may also contribute to the improvement of regioselectivity. Also under high CO/H<sub>2</sub> pressure, the bidentate ligand in the Rh complex can be partially displaced by CO, resulting in unselective catalyst species and lower linear selectivity. The effects of reaction temperature on hydroformylation reaction were also investigated (Table 2.1, entries 4-7). There is a slight increase in *l:b* ratio when the reaction temperature increased from 60 to 100 °C. For temperatures above 100 °C, the *l:b* ratio is nearly constant. Finally, the effect of L/Rh ratio was studied (Table 2.1, entries 1, 8, 9). A moderate increase of *l:b* ratio and slight increase in isomerization were observed when the L/Rh ratio was varied from 2:1 to 4:1 to 6:1. The highest linear selectivity was 88% by employing an L/Rh ratio of 6:1; however, at this ratio, the catalyst activity is impaired with a turnover number (TON) of 742 compared to that of 855 when an L/Rh ratio of 4:1 is employed.

**Table 2.1.** Optimization of reaction conditions for the hydroformylation of allyl cyanide using ligand **1**.<sup>[a]</sup>

Entry	L/Rh	T (°C)	CO/H <sub>2</sub> (atm)	<i>l:b</i> <sup>[b]</sup>	Linear <sup>[c]</sup> (%)	Iso. <sup>[d]</sup> (%)	TON <sup>[e]</sup>
1	4:1	100	5/5	5.2	84	8.0	855
2	4:1	100	10/10	2.8	74	7.6	802
3	4:1	100	20/20	2.1	68	5.7	846
4	4:1	100	30/30	1.9	66	5.4	840
5	4:1	60	5/5	4.0	80	9.6	800
6	4:1	80	5/5	4.3	81	8.1	819
7	4:1	120	5/5	5.2	84	3.3	857
8	2:1	100	5/5	4.8	83	10.3	828
9	6:1	100	5/5	7.1	88	13.9	742

<sup>[a]</sup> S/C = 1000, [Rh] = 1.0 mM, reaction time = 1 h, toluene as solvent, decane as internal standard. <sup>[b]</sup> Linear/branched ratio, determined by GC. <sup>[c]</sup> Percentage of linear aldehyde in all aldehydes. <sup>[d]</sup> Percentage of isomerization of starting material. <sup>[e]</sup> Turnover number to all aldehydes, determined by GC.

#### 2.4.2. Ligand Structural Effects on the Hydroformylation of Allyl Cyanide

After a good set of hydroformylation conditions has been identified, ligands **1-10** were applied to the rhodium-catalyzed hydroformylation of allyl cyanide to investigate the ligand structural effects. The results are listed in Table 2.2. The steric effect was studied by varying the substituents at the 3,3',5,5'-positions of the biphenyl backbone. Ligand **1** is the

first ligand in this series that does not have any modification in the 3,3',5,5'-positions. With this ligand, a linear to branch (*l:b*) ratio of 5.3 and a turnover number (TON) of 828 were obtained after 30 minutes at 100 °C (Table 2.2, entry 1). Ligands **2-5** are modified with the attachment of chloro, methyl, ethyl and phenyl, respectively. The attachment of chloro group at the 3,3',5,5'-positions in ligand **2** lowered the linear selectivity significantly with a *l:b* ratio of only 2.2 (Table 2.2, entry 2). The attachment of methyl, ethyl or phenyl group in ligands **3-5** did not result in a significant change in linear selectivity (Table 2.2, entries 3 to 5), indicating that the steric variation in this series of ligands has little effect on the hydroformylation regioselectivity of allyl cyanide.

**Table 2.2.** Hydroformylation of allyl cyanide with ligands **1-10**.<sup>[a]</sup>

Entry	Ligand	R group in ligand	<i>l:b</i> <sup>[b]</sup>	Linear <sup>[c]</sup> (%)	Iso. <sup>[d]</sup> (%)	TON <sup>[e]</sup>
1	<b>1</b>	H	5.3	84	10	828
2	<b>2</b>	Cl	2.2	68	10	845
3	<b>3</b>	Me	5.1	84	12	779
4	<b>4</b>	Et	4.3	81	14	769
5	<b>5</b>	Ph	5.0	83	10	789
6	<b>6</b>	4-MePh	5.4	87	9	751
7	<b>7</b>	4-FPh	6.7	87	11	783
8	<b>8</b>	4-ClPh	7.9	89	11	778
9	<b>9</b>	2,4-F <sub>2</sub> Ph	10.3	91	16	728
10	<b>10</b>	4-MeOPh	4.6	82	9	779



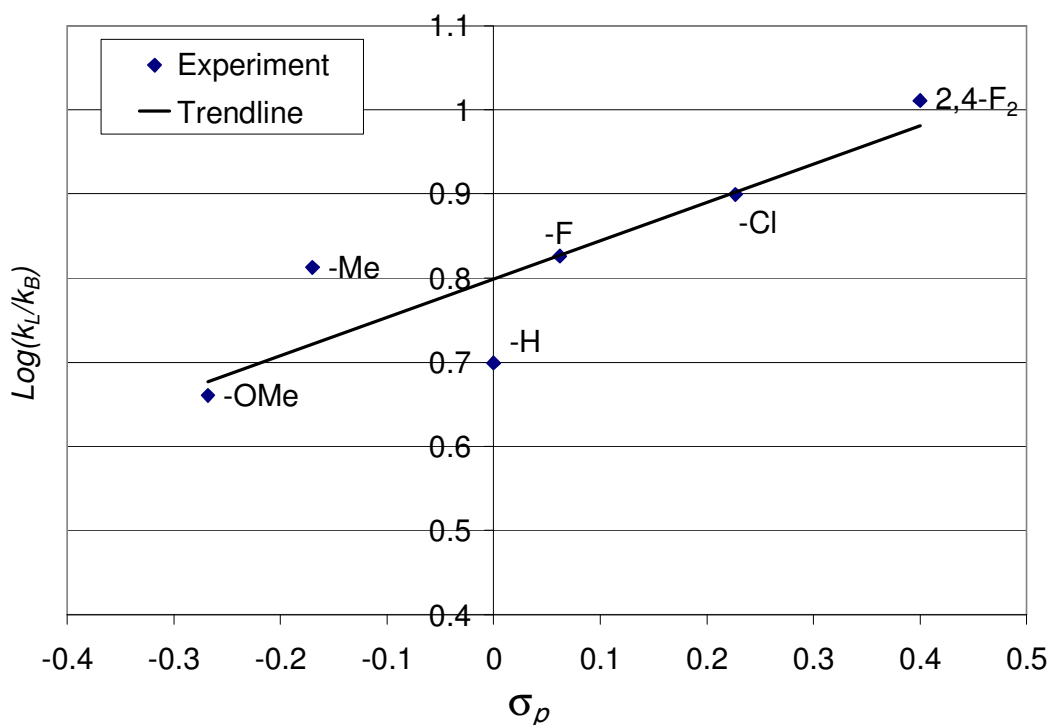
<sup>[a]</sup> S/C = 1000, [Rh] = 1.0 mM, L/Rh ratio = 4:1, CO/H<sub>2</sub> = 5/5 atm, reaction time = 30 min, 100 °C, toluene as solvent, decane as internal standard. <sup>[b]</sup> Linear/branched ratio, determined by GC. <sup>[c]</sup> Percentage of linear aldehyde in all aldehydes. <sup>[d]</sup> Percent of isomerization of starting material. <sup>[e]</sup> Turnover number to all aldehydes, determined by GC. <sup>[f]</sup> Turnover frequency to all aldehydes, determined by GC.

The electronic effect of a ligand is often coupled with and complicated by its steric effect. In order to keep the steric effect a constant factor, ligands **6-10** were designed to minimize the confounding effects. They are modifications of ligand **5** but have substituents varying at the *para* positions of all four phenyl groups. Because the substituents are small and at distance to the coordination center, the steric effect incurred by the substituents is minimal; therefore, the electronic effect can be studied without being confounded by the steric effect. The performance of ligands **6-10** on the hydroformylation of allyl cyanide are also listed in Table 2.2 (entries **6** to **10**). It was found that the attachment of substituents at the *para* position of the phenyl moiety indeed affected both regioselectivity and catalyst activity. The substituents in ligands **5-10** have Hammett constant  $\sigma_p$  ranging from -0.3 to +0.4.<sup>15</sup> Let  $k_L$  and  $k_B$  be the observed rate constants for the formation of linear aldehyde and branched aldehyde, respectively. The Hammett equation of reactions influenced by aromatic substituents can be simply expressed as

$$\log \frac{k_L}{k_B} = \rho \sigma_p + \log \left( \frac{k_L}{k_B} \right)_0, \quad (2.1)$$

where  $\rho$  is a constant, and  $(k_L/k_B)_0$  is the ratio when there is no substituent on the phenyl group. The formations of linear and branched aldehydes are two competitive parallel reactions from the same start, and as we shown in Chapter 1, equation 1.5, the ratio of observed rate constant for the formation of linear aldehyde to that of branched aldehyde

( $k_L/k_B$ ) can be approximated by the ratio of concentrations of linear aldehyde to that of branched aldehyde.<sup>16</sup> The electronic effect was thus treated by Hammett plot in terms of  $\log(k_L/k_B)$  versus  $\sigma_p$  of substituents, which was plotted in Figure 2.3. It is clearly demonstrated that an electron-withdrawing group has a positive effect on the linear selectivity and an upward trend line of linear selectivity was obtained with the increase of  $\sigma_p$ . The highest linear selectivity was afforded by ligand **9** (Table 2.2, entry 9, an *l:b* ratio of 10.3), which bears two strong electron-withdrawing fluoro groups on the phenyl ring; in contrast, the methoxy group, which is strong electron-donating, afforded the lowest linear selectivity in this series of ligands (Table 2.2, entry 10, an *l:b* ratio of 4.6). As for the catalyst activity in terms of TON, under the given hydroformylation conditions, the electronic effect is not large, and a slight decrease of TON was observed with increased electron-withdrawing property (Table 2.2, entries 5 to 10). The results show that a subtle change in ligand electronic property can improve the linear selectivity. It is well documented in the literature that allyl cyanide is a substrate that is commonly applied in the asymmetric hydroformylation and favors branched aldehyde formation.<sup>8</sup> As a sharp contrast, the tetraphosphoramidite ligands **1-10** afforded linear aldehyde with very high selectivities. To the best of our knowledge, ligand **9** afforded the highest linear selectivity for the hydroformylation of allyl cyanide ever reported.



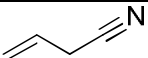
**Figure 2.3.** Hammett plot of  $\log(k_L/k_B)$  versus  $\sigma_p$  values of substituents in ligands **5-10** for the hydroformylation of allyl cyanide.

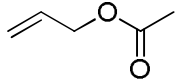
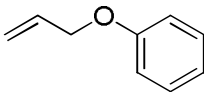
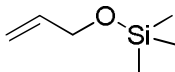
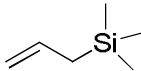
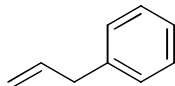
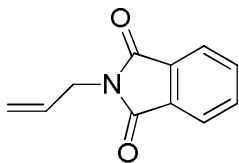
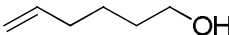
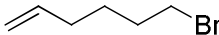
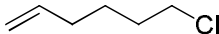
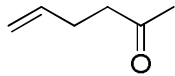
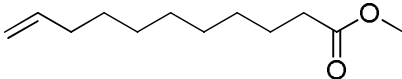
### 2.4.3 Hydroformylation of Functionalized Allyl and Vinyl Derivatives

In general, functionalized allyl and vinyl derivatives have intrinsic tendency to produce branched aldehydes. It will be complementary to the current technology if we can develop a new catalyst system that can reverse the regioselectivity and make linear aldehydes in high yields for these substrates. To this aim, ligand **9**, which afforded the highest linear selectivity for the hydroformylation of allyl cyanide, was applied in the hydroformylation of a variety of functionalized allyl and vinyl derivatives. The results of allyl derivatives are summarized in Table 2.3. We are pleased to find that ligand **9** is effective and highly regioselective to produce the linear aldehydes for allyl olefins with various functions.

Under the given reaction conditions (even at a reaction temperature as high as 120°C), allyl ether, ester and alcohol were well tolerated, and linear selectivities greater than 95% were obtained (Table 2.3, entries 2-4, 8 and 12). In addition, silyl group, ketone and halogens were also tolerated, and the allyl derivatives with these functions were converted to the corresponding aldehydes with linear selectivities greater than 97% (Table 2.3, entries 5, 9-11). Long chain terminal olefins, such as 6-bromo-1-hexene, 6-chloro-1-hexene and 10-undecenoic acid methyl ester, afforded aldehydes with greater than 98% linear selectivities but with about 20 to 40% isomers, which are thermodynamically more stable, steric hindered, and therefore much less reactive (Table 2.3, entries 9-10, 12). Free amines usually gave unclear reactions because of the potential further reactions of amino group with the aldehyde; however, protected amino olefins gave clean and linear aldehydes in high selectivities (Table 2.3, entry 7). For allyl olefins with the functional groups three or more bonds distance away from the double bond (Table 2.3, entries 8-12), the linear selectivities are by and large much higher than those olefins with the functional groups two bonds away, indicating that the functional groups which are remote to the reaction center have little effect on the linear selectivity.

**Table 2.3.** Hydroformylation of functionalized allyl derivatives with ligand **9**.<sup>[a]</sup>

$\text{CH}_2=\text{CHCH}_2\text{R} \xrightarrow[\text{CO/H}_2]{[\text{Rh}]/\text{ligand}} \text{RCH}_2\text{CH}_2\text{CH}_2\text{CHO} + \text{RCH}_2\text{CH}(\text{CH}_3)\text{CHO}$					
Entry	Substrate	<i>l:b</i> <sup>[b]</sup>	Linear <sup>[c]</sup> (%)	Isomer <sup>[d]</sup> (%)	TON <sup>[e]</sup>
1 <sup>[f]</sup>		10	91	16	728

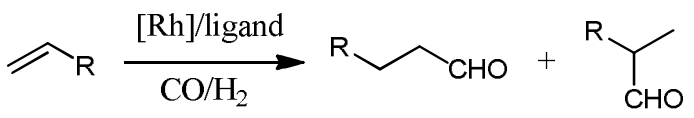
2		26	96	0	947
3		18	95	10	895
4		51	98	14	450
5		43	98	2	514
6		36	97	31	653
7		13	93	0	930
8		518	99.8	0	875
9		47	98	19	548
10		77	99	30	494
11		70	99	0	838
12		79	99	40	450

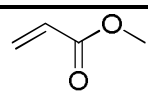
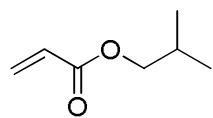
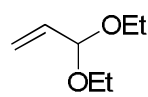
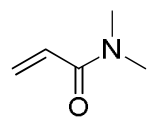
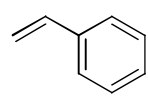
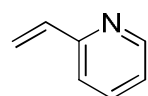
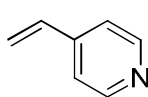
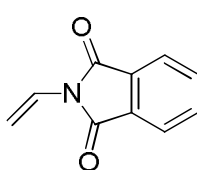
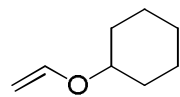
<sup>[a]</sup> S/C = 1000, [Rh] = 1.0 mM, ligand/Rh ratio = 4:1, CO/H<sub>2</sub> = 5/5 atm, 120 °C, reaction time = 2 h, toluene as solvent, decane as internal standard. <sup>[b]</sup> Linear/branched ratio, determined by GC or NMR. <sup>[c]</sup> Percentage of linear aldehyde in all aldehydes. <sup>[d]</sup> Percent of Isomerization of starting material. <sup>[e]</sup> Turnover number to all aldehydes, determined by GC or isolated yield. <sup>[f]</sup> Reaction time = 0.5 h.

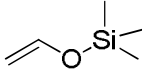
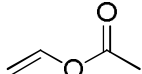
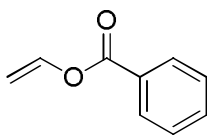
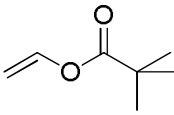
The hydroformylation results of functionalized vinyl derivatives catalyzed by Rh/ligand **9** catalyst were summarized in Table 2.4. As expected, the catalyst is very effective and highly linear selective for the hydroformylation of a variety of vinyl

derivatives. For vinyl acrylic substrates (Table 2.4, entries 1-4), linear selectivities greater than 99% were obtained with high turn over numbers after 2 hours at 120 °C. The catalyst was also found to be highly linear selective for the hydroformylation of styrene and vinyl pyridines; linear selectivities greater than 95% were obtained for these substrates (Table 2.4, entries 5-7). Of them, 2-vinylpyridine was much less reactive than 4-vinylpyridine and styrene. The turn over number of 2-vinylpyridine is only 149 after 2 hours at 120 °C compared to turn over numbers of 639 and 811 of 4-vinylpyridine and styrene, respectively, under the same reaction conditions. This is likely due to the extra stabilization of Rh-vinylpyridine complex by the ortho nitrogen atom, which makes 2-vinylpyridine less labile in the subsequent migratory insertion steps, and hence slows down the overall reaction rate. Moreover, about 20% and 30% hydrogenation products were observed for 2- and 4-vinylpyridines, respectively, probably due to the large excess presence of vinylpyridine and the  $\eta^1$  binding of nitrogen which could displace CO completely from the Rh complex and therefore enhance hydrogenation product. Vinylphthalimide was tested as protected amino vinyl derivatives (Table 2.4, entry 8). The hydroformylation of N-vinylphthalimide afforded linear aldehyde in 90% selectivity. The conversion is high with a turn over number of 954, but with 40% hydrogenation product. Lastly, vinyl ethers and esters were investigated for their regioselectivities (Table 2.4, entries 9-13). The hydroformylation of cyclohexyl and trimethylsilyl ethers afforded aldehydes with linear selectivities of 69% and 72%, respectively (entries 9-10). But for vinyl acetate, vinyl benzoate and vinyl pivalate, the linear selectivities are poor and ranging from 33% to 44% (entries 11-13).

**Table 2.4.** Hydroformylation of functionalized vinyl derivatives with ligand **9**.<sup>[a]</sup>



Entry	Substrate	<i>l:b</i> <sup>[b]</sup>	Linear <sup>[c]</sup> (%)	Hydr <sup>[c]</sup> (%)	TON <sup>[f]</sup>
1		345	99.7	0	807
2		66	99	0	771
3		107	99	0	910
4		464	99.8	12	884
5		26	97	8	811
6		74	99	21	149
7		20	95	31	639
8		9.4	90	40	554
9		2.2	69	0	519

10		2.6	72	0	450
11		0.8	44	20	801
12		0.5	33	0	735
13		0.6	38	0	782

<sup>[a]</sup> S/C = 1000, [Rh] = 1.0 mM, ligand/Rh ratio = 4:1, CO/H<sub>2</sub> = 5/5 atm, 120 °C, reaction time = 2 h, toluene as solvent, decane as internal standard. <sup>[b]</sup> Linear/branched ratio, determined by GC or NMR. <sup>[c]</sup> Percentage of linear aldehyde in all aldehydes. <sup>[d]</sup> Percent of hydrogenation of starting material. <sup>[e]</sup> Turnover number to all aldehydes, determined by GC or isolated yield.

To summarize the regioselectivities of allyl and vinyl derivatives catalyzed by the Rh/ligand **9** system listed in Tables 2.3 and 2.4, several structural features of the functionalized olefins are worth to mention: 1) for an olefin where the  $\gamma$ -atom is carbon, terminal aldehyde is obtained with high linear selectivity, 2) for an olefin where the  $\gamma$ -atom is nitrogen, the primary amine need to be protected and terminal aldehyde is obtained with high linear selectivity, and 3) for an olefin that its  $\gamma$ -atom is oxygen, mild to poor linear selectivity is obtained. For example, allyl acetate, vinyl acetate and methyl acrylate are compounds with high structural similarity; however, the high linear selectivities of allyl acetate (96%, Table 2.3, entry 2) and methyl acrylate (99%, Table 2.4, entry 1) are in sharp contrast with the low linear selectivity of vinyl acetate (44%, Table 2.4, entry 11). This sharp contrast indicates that under the influence of ligand **9**, the  $\gamma$ -ketone in methyl acrylate and the  $\delta$ -oxygen in allyl acetate are not able to coordinate to the Rh center effectively and



hence stabilize the branched Rh-alkyl complex as the  $\gamma$ -oxygen in vinyl acetate does; therefore, high linear selectivities were obtained for allyl acetate and methyl acrylate but not for vinyl acetate. These structural features of functionalized terminal olefins and broad tolerance of various functional groups make it possible the syntheses of  $C_n$  ( $n \geq 3$ ) functionalized terminal aldehydes by hydroformylation using our Rh/tetraphosphoramidite catalyst system.

The reaction mechanism of the hydroformylation of simple olefins catalyzed by Rh/ $Ph_3P$  has been well studied over decades. Wilkinson's dissociation mechanism is generally accepted, and the regioselectivity has been explained to arise from the energy difference for the formations of linear and branched metal-alkyl complexes.<sup>17</sup> Although it will be very convincing to illustrate a reaction mechanism by quantum chemical calculations, currently the computation models are still limited to overly simplified Rh/ $PH_3$  and the like systems, and are not computationally feasible to calculate and construct a complete energy profile versus the reaction coordinate for the Rh/tetraphosphoramidite catalyst system, which the geometric shape of the bulky tetraphosphoramidite ligand can not simply be ignored. Nevertheless, our observations hereinabove are in general consistent with and can be explained by the established Wilkinson's mechanism. From our results, it is clear that, for our tetraphosphoramidite ligand system, ligands with strong electron-withdrawing moieties favor the formation of the linear aldehydes. Further studies are required to completely elucidate the mechanism in detail.

#### 2.4.4 Summary

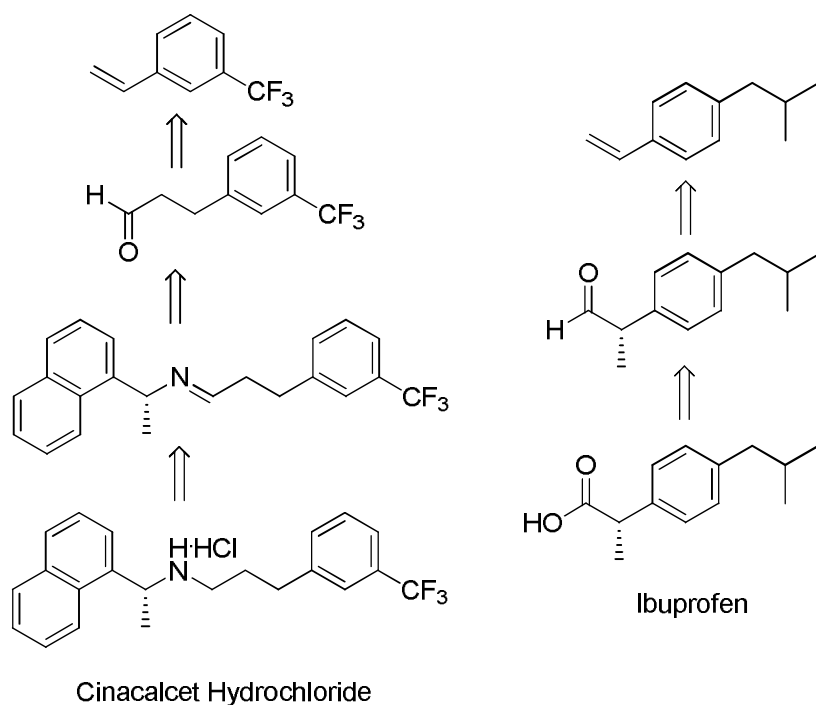
In summary, new tetraphosphoramidite ligands with various substituents to tune their steric and electronic properties have been developed and applied in the rhodium-catalyzed regioselective hydroformylation of a series of functionalized allyl and vinyl derivatives. For the hydroformylation of allyl cyanide, compared with the commonly observed branch selectivity reported in literature, remarkable high linear selectivity that is up to 91% was obtained by these tetraphosphoramidite ligands. The strong electron-withdrawing 2,4-difluorophenyl substituted ligand **9** is particularly effective to afford high linear selectivity. The electronic effect of the ligands on the regioselectivity has been studied with Hammett plots and is following a linear trend. It was found that with the increase of electron-withdrawing ability of the ligands, the linear selectivity increases but the catalyst activity decreases. The Rh/ tetraphosphoramidite catalyst system reported herein is aimed to produce terminal aldehydes, which is desirable and complementary to other catalyst systems that mainly produce branched aldehydes.

As a summary for the extensiveness of the reaction scope, functional groups containing ester, ether, ketone, amine, nitrile and halogens are well tolerated under the aforementioned hydroformylation conditions. Ligand **9** is highly effective to produce linear aldehydes for allyl derivatives with substituents containing heteroatom such as O, N, Si and halogen either directly adjacent to or at distance to the allyl group. For functional groups remote to the ally group, there is little effect on the regioselectivity. For vinyl derivatives, ligand **9** is highly linear selective for acrylic derivatives, styrene, vinylpyridine, and vinyl phthalimide, moderate linear selective for vinyl ethers, and poor linear selective for vinyl esters. The Rh/tetraphosphoramidite catalyst system makes it possible to prepare

C<sub>n</sub> (n ≥ 3) functionalized terminal aldehydes from readily available vinyl and allyl derivatives by hydroformylation with high linear selectivities.

## 2.5 Hydroformylation of Styrene and Its Derivatives

Hydroformylation of styrenes and its derivative can provide a variety of aromatic aldehydes, which can serve as building blocks for constructing complex molecules. For example, as illustrated in Figure 2.4, the asymmetric hydroformylation of a styrene derivative can be used to prepare ibuprofen,<sup>18</sup> a common anti-inflammatory drug for relief of symptoms of arthritis and fever. The regioselective hydroformylation of 3-trifluoromethylstyrene can be used to prepare cinacalcet hydrochloride, which is used to treat secondary hyperparathyroidism.<sup>19</sup> Both linear and branched aldehydes may be desired. However, the regioselectivity and enantioselectivity need to be controlled. In this research, we will focus our studies on the development of new tetraphosphoramidite ligands to produce linear aldehydes from styrene and its derivatives.



**Figure 2.4.** Drugs can be synthesized via hydroformylation of styrene derivatives.

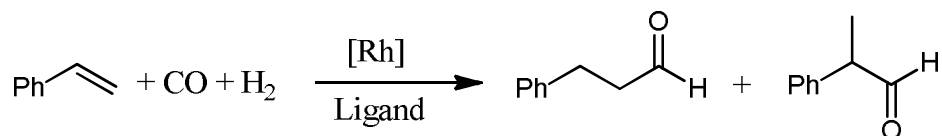
Styrene is a well studied substrate that favors branched aldehyde in hydroformylation because the branched Rh-styrene complex linked at the  $\alpha$ -carbon is stabilized by an  $\eta^2$  coordination from the phenyl ring ortho to the Rh-C( $\alpha$ ) link. The bulky diphosphites, which usually have high linear selectivity for alkyl terminal olefins, afforded typical linear to branched ratios around 1.0 for the hydroformylation of styrene compared to generally higher than 90% branched aldehyde when monodentate ligands are applied. Most recently, Reek et al. reported a linear selectivity of 72% for the hydroformylation of styrene by employing SUPRAPHos ligands.<sup>2g</sup> Therefore, developing catalyst system that can produce linear aldehydes with high selectivity for styrene and the like substrates that have intrinsic branch preferences is a challenging and unsolved problem.

In the previous sections of this chapter, we have reported that the tetraphosphoramidite ligand **9** were very effective for the hydroformylations of a variety of functionalized vinyl

and allyl derivatives to produce linear aldehydes. To expand our study, ligands **1** to **10** were evaluated for the regioselective hydroformylation of a series of styrene and its derivatives with varied electronic properties. We intended to study the structure activity/regioselectivity relationships with regards to the structural variations of both ligands and substrates.

### 2.5.1 Hydroformylation of Styrene

Our group has previously studied the effects of reaction temperature, CO/H<sub>2</sub> pressure and ligand-to-rhodium (L/Rh) ratio on the reaction activity and regioselectivity for the hydroformylation of styrene using the unsubstituted ligand **1**.<sup>9</sup> For the Rh/tetraphosphoramidite system, a good set of reaction conditions are: L/Rh = 4.0, 80 °C, CO/H<sub>2</sub> = 5/5 atm, toluene as solvent. Therefore, our further evaluations of ligands **2** to **10** for the hydroformylation of styrene were conducted under these reaction conditions. As part of our standard procedure, the rhodium catalyst was prepared *in situ* by mixing the tetraphosphoramidite ligand with Rh(acac)(CO)<sub>2</sub> before charging the reactants. The reactions were terminated after immersing the reactor to an 80 °C oil bath for only 30 min so that the differences in catalyst performance can be observed. The results are listed in Table 2.5. Ligands **5** to **10** are found to be highly effective, affording 94% to 96% linear aldehyde. This high linear selectivity by the tetraphosphoramidite ligands is unique for the hydroformylation of styrene when compared to literature precedents in that ligands **5** to **10** were able to override the intrinsic branch preference of styrene and afforded highly linear selectivity. To the best of our knowledge, ligands **8** to **10** afforded the highest linear selectivity for the hydroformylation of styrene ever reported.

**Table 2.5.** Hydroformylation of styrene with ligands **1-10**.<sup>[a]</sup>

Entry	Ligand	R group in ligand	$\sigma_p$ <sup>[b]</sup>	$\sigma_I$ <sup>[c]</sup>	$l:b$ <sup>[d]</sup>	Linear <sup>[e]</sup> (%)	TOF <sup>[f]</sup> (h <sup>-1</sup> )
1	<b>10</b>	4-MeOPh	-0.27	n/a	19.7	95	791
2	<b>6</b>	4-MePh	-0.17	n/a	16.9	94	764
3	<b>5</b>	Ph	0	0.12	18.9	95	552
4	<b>7</b>	4-FPh	0.062	n/a	22.0	96	650
5	<b>8</b>	4-ClPh	0.227	n/a	24.2	96	517
6	<b>9</b>	2,4-F <sub>2</sub> Ph	0.4	n/a	26.2	96	281
7	<b>1</b>	H	n/a	0	4.2	81	368
8	<b>2</b>	Cl	n/a	0.47	10.6	91	727
9	<b>3</b>	Me	n/a	-0.01	13.1	93	155
10	<b>4</b>	Et	n/a	-0.01	12.8	93	148

<sup>[a]</sup> S/C = 1000, [Rh] = 1.0 mM, L/Rh ratio = 4:1, CO/H<sub>2</sub> = 5/5 atm, 80 °C, reaction time = 30 min, toluene as solvent, decane as internal standard. <sup>[b]</sup> Hammett *para* substituent constant, data from reference 15.  $\sigma_p$  is for the substitution group on the R group, not on the biphenyl. By a rigid definition,  $\sigma_p$  is not applicable to entry 6; however, since the 2,4-difluoro groups are remote to the phosphorus coordination center, the value of ( $\sigma_p + \sigma_m$ ) was used to estimate the electron-withdrawing capacity of 2,4-difluoro groups even this treatment is not accurate. <sup>[c]</sup> Hammett substituent inductive parameter, data from reference 15.  $\sigma_I$  is for the substitution group at the 3,3',5,5'-positions of the biphenyl backbone. <sup>[d]</sup> Linear/branched ratio, determined by GC. <sup>[e]</sup> Percentage of linear aldehyde in all aldehydes. <sup>[f]</sup> Turnover frequency, determined by GC.

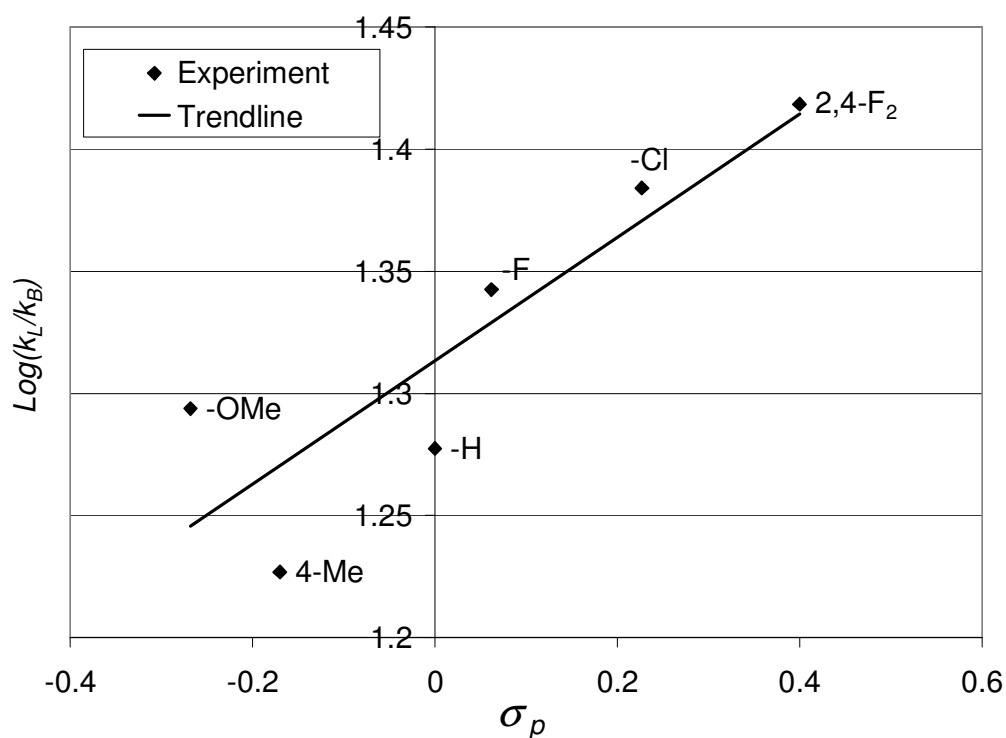
### 2.5.2 Ligand Structural Effects on the Hydroformylation of Styrene

The electronic effects of ligands on the catalyst activity and regioselectivity were studied by changing the substituent at para-position of the phenyl group systematically from strong electron-donating groups to strong electron-withdrawing groups. In many situations, the electronic effect is complicated with the steric effect and cannot be completely isolated. In order to minimize the steric effect, the substituent in variation needs to be small and placed at some distance away from the reaction center. For this reason, in ligands **6** to **10** were designed such that small substituents (F, Cl, Me and MeO) are attached to the phenyl group at the *para* position, which is remote to the chelating phosphorus atoms. The substituent groups in ligands **5** to **10** have Hammett constant  $\sigma_p$  ranging from -0.3 to +0.4.<sup>15</sup> Let  $k_L$  and  $k_B$  be the observed rate constants for the formation of linear aldehyde and branched aldehyde, respectively. The Hammett equation of reactions influenced by aromatic substituents can be simple expressed as

$$\log \frac{k_L}{k_B} = \rho \sigma_p + \log \left( \frac{k_L}{k_B} \right)_0, \quad (2.1)$$

Where  $\rho$  is a constant, and  $(k_L/k_B)_0$  is the ratio when there is no substituent on the phenyl group. The formations of linear and branched aldehydes are two parallel and competitive reactions from the same start, and as we showed in Chapter 1, equation 1.5, the ratio of observed rate constant for the formation of linear aldehyde to that of branched aldehyde ( $k_L/k_B$ ) can be approximated by the ratio of concentrations of linear aldehyde to that of branched aldehyde.<sup>16</sup> The Hammett plot of  $\log(k_L/k_B)$  versus  $\sigma_p$  values of substituents was plotted in Figure 2.5. It is apparent that an electron-withdrawing group has a positive effect on the linear selectivity. An upward trend line of linear selectivity was obtained with the increase of  $\sigma_p$ . The highest linear selectivity was afforded by ligand **9** (Table 2.5, entry 6, a

*l:b* ratio of 26.2), which bears 2 strong electron-withdrawing fluoro groups on the phenyl ring. In contrast, ligand **6** which has electron-donating methyl groups attached on the phenyl ring afforded the lowest linear selectivity among ligands **5** to **10** (Table 2.5, entry 2, a *l:b* ratio of 16.9). Compared to the methyl group, the methoxy group has lower  $\sigma_p$  but affording a higher linear selectivity. This is most likely due to the inductive effect of the methoxy group which is able to pull electrons from the phenyl ring and therefore counteracts its electron-donating ability by the resonance effect.

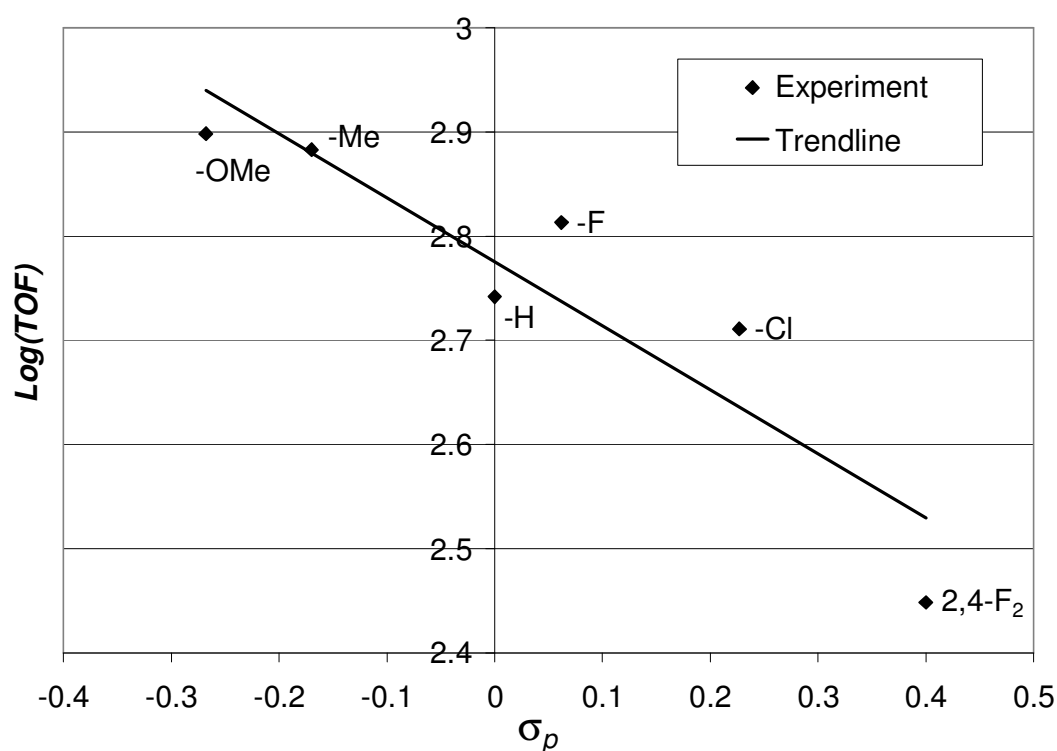


**Figure 2.5.** Hammett plot of  $\log(k_L/k_B)$  versus  $\sigma_p$  values of substituents in ligands **5-10** for the hydroformylation of styrene.

The steric effect of the ligand on the regioselectivity is significant too. It was found that the introduction of substituents at the 3,3',5,5'-positions of the biphenyl backbone greatly



increased the regioselectivity for the linear aldehyde. The unsubstituted ligand **1** afforded a *l:b* ratio of only 4.2 (Table 2.5, entry 7). The use of ligands **2** to **4** that are bearing chloro, methyl or ethyl substituents ortho to the pyrrolyl phosphorus groups increased the linear to branch ratios to 10.6 and above in all cases. (Table 2.5, entries 8-10); as another comparison, the use of ligands **5** to **10** that are bearing varied phenyl substituents ortho to the pyrrolyl phosphorus groups increased the linear to branch ratios to 16.9 and above in all cases. (Table 2.5, entries 1-6).



**Figure 2.6.** Turn over frequency (TOF, in logarithm scale) versus  $\sigma_p$  values of substituents in ligands **5-10** for the hydroformylation of styrene.

The catalyst activity in terms of the turn over frequency (TOF) versus the Hammett constant  $\sigma_p$  was plotted in Figure 2.6. Contrary to the upward trend in the linear selectivity,

a downward trend was observed for the catalyst activity with the increase of electron-withdrawing ability of the substituent in the phenyl group. While ligand **9** afforded the highest linear selectivity, its catalyst activity was the lowest among ligands **5** to **10** (Table 2.5, entry 6). However, this electronic effect trend is only valid for ligands **5** to **10** which all have the phenyl moiety at the 3,3',5,5'-positions of the biphenyl backbone. The electronic effect on the catalyst activity is different if we look at the electronic donating or withdrawing property of the substituents directly at the 3,3',5,5'-positions of the biphenyl backbone. The unsubstituted ligand **1** afforded TOF of 368 after 30 minutes at 80°C (Table 2.5, entry 7). Despite that the substituent electronic effect at the 3,3',5,5'-positions is complicated by the steric effect, the electronic donating or withdrawing ability can still be characterized by the Hammett inductive parameter ( $\sigma_I$ ). The use of ligands **2**, **5**, **3** and **4** that are bearing chloro, phenyl, methyl and ethyl substituents with increasing electron-donating ability as indicated by their  $\sigma_I$  values afforded TOFs in the decreasing order of 727, 552, 155 and 148, respectively, under the same conditions (Table 2.5, entries 3, 8-10).

### 2.5.3 Electronic and Steric Effects of Styrene Substrates

It has been well known that the catalyst performance is substrate dependent. The electronic effects of substrates on the catalyst activity and regioselectivity were studied by employing a series of *para*-substituted styrenes. The results are listed in Table 2.6. Ligands **5**, **7** and **10**, which bear phenyl, 4-fluorophenyl and 4-methoxyphenyl in the structure, respectively, were applied in the hydroformylation of substituted styrenes. Overall, all these ligands afforded high linear selectivity for all substrates listed in Table 2.6. In all reactions, remarkable high linear to branch ratios (*l:b*) were obtained, ranging from 11.1

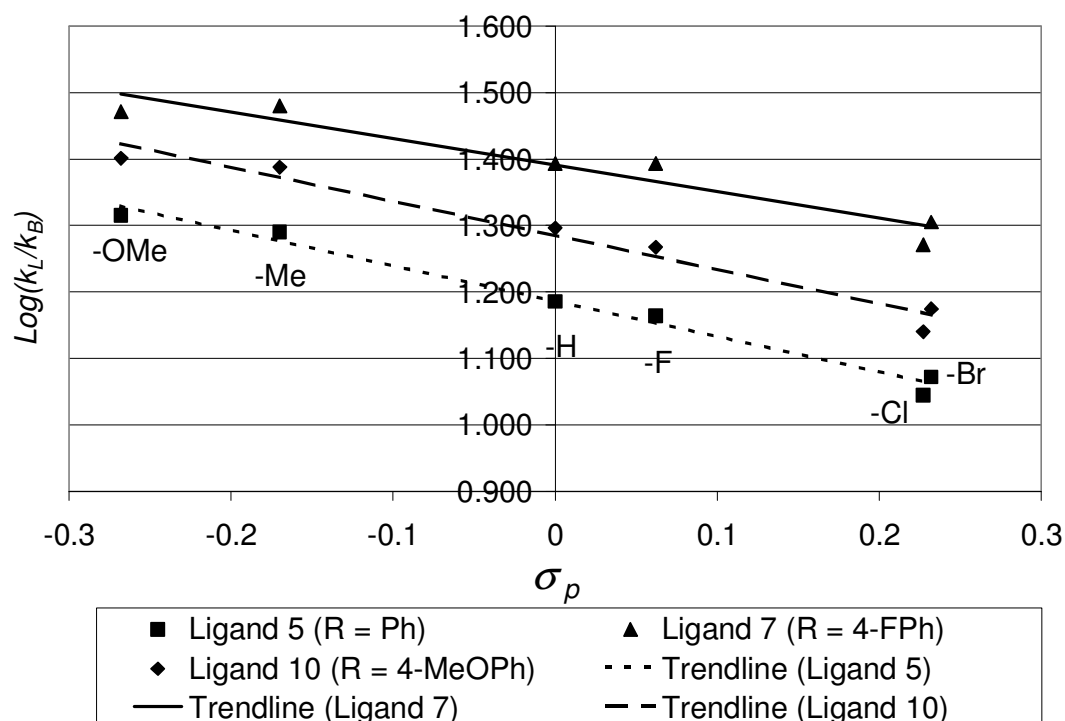
(Table 2.6, entry 3, ligand **5**) to 29.6 (Table 2.6, entry 6, ligand **7**), and this corresponds to a linear selectivity that is above 92% and up to 97%. When substrate to substrate is compared, 4-methoxystyrene afforded the highest linear selectivity (Table 2.6, entry 6,  $l:b = 20.7, 25.2, 29.6$ ), and 4-chlorostyrene gave the lowest (Table 2.6, entry 3,  $l:b = 11.1, 13.8, 18.7$ ). The corresponding Hammett plots of  $\log(k_L/k_B)$  versus  $\sigma_p$  are shown in Figure 2.7. The *para*-substituted styrenes have  $\sigma_p$  ranging from -0.268 to 0.232.<sup>15</sup> With the increase of  $\sigma_p$ , upward trends are observed for all three series of experimental data (ligand **5**, **7** and **10**), the linear selectivity increases in the order of 4-chlorostyrene  $\approx$  4-bromostyrene < 4-fluorostyrene < styrene < 4-methylstyrene < 4-methoxystyrene. The similar upward trends in linear selectivity by all three ligands indicate that no underlying changes in reaction mechanism take place if the ligands are only to be modulated by electronic property at distant substituents. Furthermore, consistent with and complementary to the results in Table 2.5, for every single substituted styrene, the linear selectivity decreases in the order of ligand **7** > ligand **10** > ligand **5**.

**Table 2.6.** Hydroformylation of styrene derivatives with ligands **5**, **7** and **10**.<sup>[a]</sup>

$\text{Ar}-\text{CH}=\text{CH}_2 + \text{CO} + \text{H}_2 \xrightarrow[\text{Ligand}]{[\text{Rh}]} \text{Ar}-\text{CH}_2\text{CH}_2\text{CHO} + \text{Ar}-\text{CH}(\text{CH}_3)\text{CHO}$								
			Ligand <b>5</b>		Ligand <b>7</b>		Ligand <b>10</b>	
			(R=Ph)		(R=4-FPh)		(R=4-MeOPh)	
entry	substrate	$\sigma_p^{[b]}$	TOF <sup>[d]</sup>		TOF <sup>[d]</sup>		TOF <sup>[d]</sup>	
			$l:b^{[c]}$		$l:b^{[c]}$		$l:b^{[c]}$	
			(h <sup>-1</sup> )		(h <sup>-1</sup> )		(h <sup>-1</sup> )	
1	Styrene	0	15.3	769	24.7	697	19.8	865

2	4-F-styrene	0.062	14.6	902	24.7	674	18.5	971
3	4-Cl-styrene	0.227	11.1	1113	18.7	726	13.8	1192
4	4-Br-styrene	0.232	11.8	1334	20.2	938	14.9	1453
5	4-Me-Styrene	-0.17	19.5	808	30.2	605	24.4	933
6	4-MeO-styrene	-0.268	20.7	627	29.6	530	25.2	774

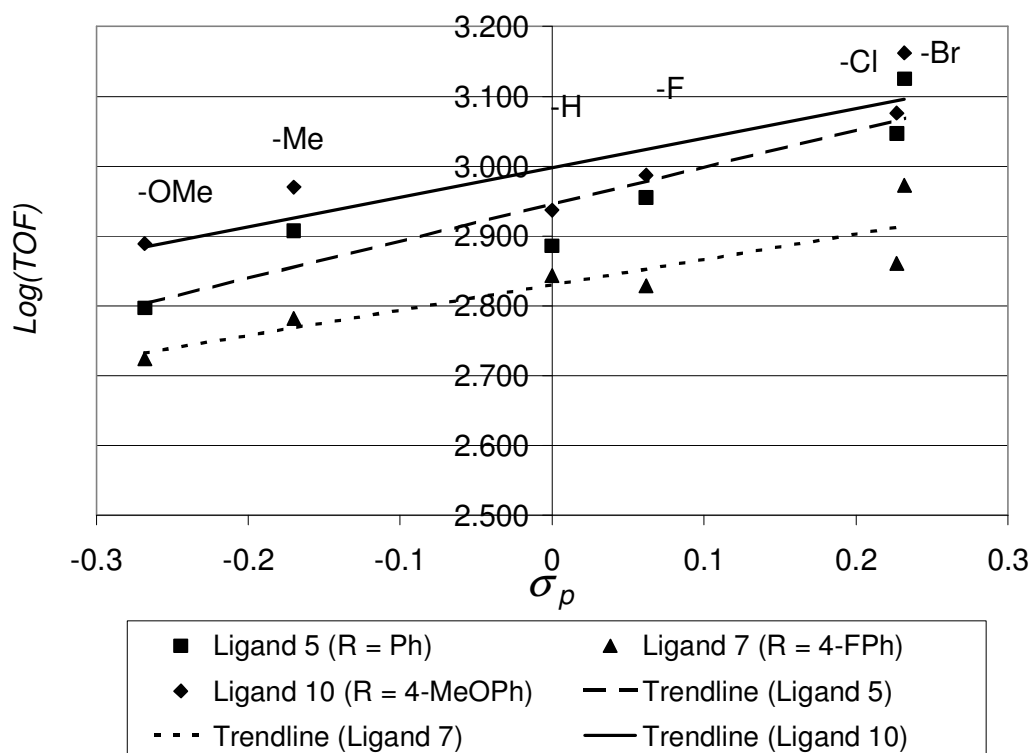
<sup>[a]</sup> S/C = 1000, [Rh] = 1.0 mM, L/Rh ratio = 4:1, CO/H<sub>2</sub> = 5/5 atm, 80 °C, reaction time = 20 min, toluene as solvent, decane as internal standard. <sup>[b]</sup> Hammett *para* substituent constant, data from reference 15. <sup>[c]</sup> Linear/branched ratio, determined by GC. <sup>[d]</sup> Turnover frequency, determined by GC.



**Figure 2.7.** Hammett plot of  $\log(k_L/k_B)$  versus  $\sigma_p$  value of substituent on styrene.

The electronic effects of substrates on the catalyst activity were compared in terms of turn over frequency (TOF). The data were also listed in Table 2.6. The correlations between the TOF and  $\sigma_p$  were plotted in Figure 2.8. In contrast to the downward trend in

the linear selectivity observed in Figure 2.7, an upward trend was observed for the catalyst activity with the increase of electron-withdrawing ability of the substrates. In all three cases, 4-bromostyrene resulted in the highest TOF and is the most reactive substrate (Table 2.6, entry 4), and 4-methoxystyrene resulted in the lowest TOF and is the least reactive substrate (Table 2.6, entry 6). Again, this trend was observed consistently across ligands **5**, **7** and **10**, confirming that these ligands are operating under the same mechanism. With the increase of  $\sigma_p$  values of the substituents, the reactivity of the styrenes increases in the order of 4-methoxystyrene < 4-methylstyrene < styrene < 4-fluorostyrene < 4-chlorostyrene < 4-bromostyrene.



**Figure 2.8.** Turn over frequency (TOF, in logarithm scale) versus  $\sigma_p$  values of substituents on styrene.

The steric effect of the styrene derivatives on the regioselectivity and reactivity is also remarkable. The hydroformylation results of styrene derivative with substituents at the *ortho*, *meta*, and *para* positions are listed in Table 2.7. When a substituent group was introduced to the *ortho* position of the styrene, the reactivity and regioselectivity were improved dramatically. For example, the hydroformylation of 4-Cl-styrene, 3-Cl-styrene, and 2-Cl-styrene afforded linear to branch ratios of 19, 15 and 134 and TOFs of 484, 605, and 1310, respectively (Table 2.7, entries 1-3). For the hydroformylation of bromo, fluoro, methyl, and methoxy substituted styrenes, in all cases, the *ortho* substituted styrenes afforded much better linear selectivities and TOFs than the corresponding *para* substituted styrenes (Table 2.7, entries 4-11).

**Table 2.7.** Hydroformylation of styrene derivatives with ligand 7.<sup>[a]</sup>

$$\text{Ar-CH=CH}_2 + \text{CO} + \text{H}_2 \xrightarrow[\text{Ligand}]{[\text{Rh}]} \text{Ar-CH}_2\text{-CH}_2\text{-CHO} + \text{Ar-CH(CH}_3\text{)-CHO}$$

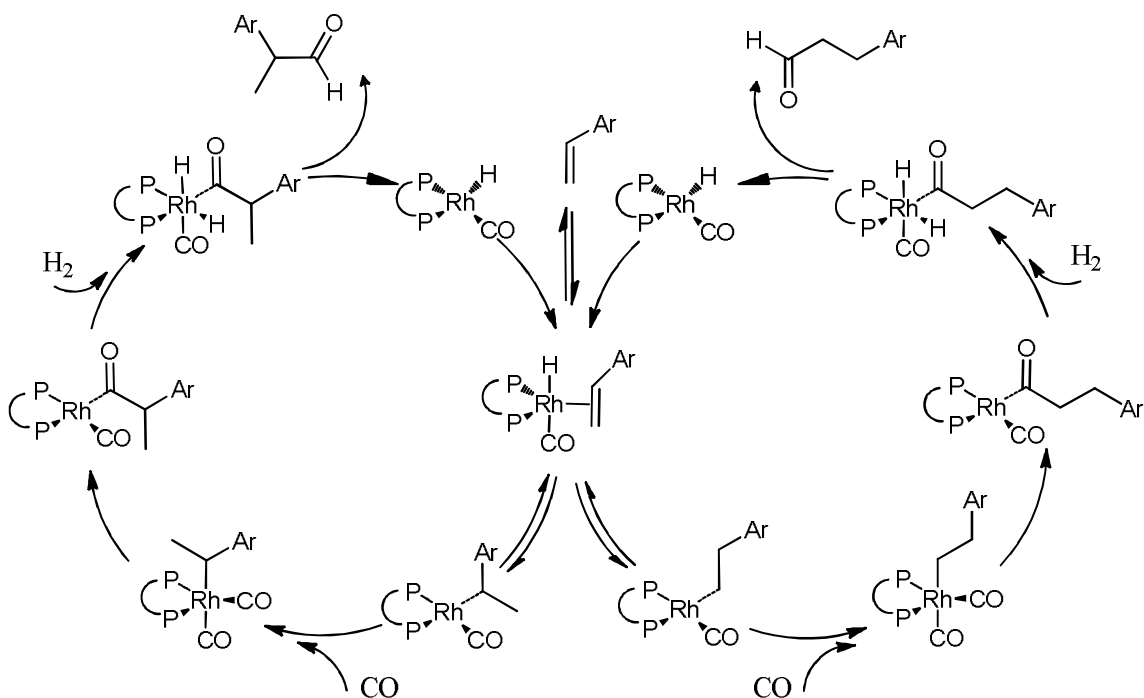
Entry	Substrate	<i>l</i> : <i>b</i> <sup>[b]</sup>	Linear <sup>[c]</sup> (%)	TOF <sup>[d]</sup> (h <sup>-1</sup> )
1	4-Cl-styrene	19	95	726
2	3-Cl-styrene	15	94	907
3	2-Cl-styrene	134	99.3	1965
4	4-F-styrene	25	96	674
5	2-F-styrene	35	97	1618
6	4-Br-styrene	20	95	938
7	2-Br-styrene	236	99.6	1427

8	4-Me-styrene	30	96	605
9	2-Me-styrene	496	99.8	1433
10	4-MeO-styrene	30	97	530
11	2-MeO-styrene	62	98	1368

<sup>[a]</sup> S/C = 1000, [Rh] = 1.0 mM, L/Rh ratio = 4:1, CO/H<sub>2</sub> = 5/5 atm, 80 °C, reaction time = 20 min, toluene as solvent, decane as internal standard. <sup>[b]</sup> Linear/branched ratio, determined by GC. <sup>[c]</sup> Percentage of linear aldehyde in all aldehydes. <sup>[d]</sup> Turnover frequency, determined by GC.

As we briefly explained in Chapter1, Wilkinson's dissociation mechanism is generally accepted for the rhodium-catalyzed hydroformylation of alkenes, where the regioselectivity arises from the formation of linear and branched metal-alkyl complexes.<sup>17</sup> For a bidentate ligand (L<sup>Λ</sup>L) catalyst system, the 16-electron square-planar intermediate HRh(CO)(L<sup>Λ</sup>L) was proposed to be the regioselective catalyst species. As shown in Scheme 2.5, starting from this species, the catalytic cycle consists of the following steps: 1) coordination of alkenes to form a Rh-alkene complex, 2) migratory insertion of alkenyl to Rh-H bond to form Rh-alkyl complex, 3) coordination of CO, 4) migratory insertion of CO to Rh-alkyl bond, 5) oxidative addition of H<sub>2</sub> to form an octahedral Rh-ketyl hydride complex, and 6) reductive elimination to generate the linear and branched aldehydes and regenerate the catalyst. Except the last step, all other steps in the catalytic cycle could be reversible. The linear/branch ratio are determined by the following steps: 1) the forward reaction to form the linear Rh-alkyl complex, 2) the forward reaction to form the branched Rh-alkyl complex, and 3) the β-H elimination of either linear or branched Rh-alkyl complexes to form the starting alkene again or its isomers with shifted double bond. For styrene, the β-H elimination leads back to the starting material; while this reverse process is continuing, it will enrich the linear aldehyde, therefore improve the linear selectivity.

The steric hindrance at the *ortho* position can inhibit the formation of the  $\eta^2$  benzylic Rh coordination that would favor branched aldehyde, and therefore resulted in better linear regioselectivity. Furthermore the steric hindrance at the *ortho* position facilitates the reductive elimination, and therefore better reactivity was observed.



**Scheme 2.5.** The catalytic cycles of styrene and derivatives to form linear and branched aldehydes.

## 2.5.4 Summary

In conclusion, new tetraphosphoramidite ligands with various substituents to tune their electronic properties have been developed and applied in the rhodium-catalyzed regioselective hydroformylation of a series of substituted styrenes. Compared with the commonly observed branch selectivity reported in literature, remarkable high linear selectivity that is greater than 92% and up to 97% was obtained by these



tetraphosphoramidite ligands. The strong electron-withdrawing 2,4-difluorophenyl substituted ligand **9** afforded the highest linear selectivity. The electronic effects on catalyst activity and regioselectivity by both ligands and styrene derivatives have been studied with Hammett plots. It was found that with the increase of electron-withdrawing ability of the ligands, the linear selectivity increases but the catalyst activity decreases. For the series of substituted styrenes, with the increase of electron-withdrawing ability of the substrate, the linear selectivity decreases but the catalyst activity increases.

## 2.6. Hydroformylation of Simple Terminal Olefins

Simple terminal olefins are relative easy substrates for regioselective hydroformylation. Previously, our group has already reported that highly regioselective hydroformylation of 1-hexene and 1-octene was obtained using the unsubstituted ligand **1**.<sup>9</sup> As a comparison, ligand **9** was also tested in the hydroformylation of simple terminal olefins. The results were listed in Table 2.8. As expected, this ligand afforded almost exclusively linear aldehyde for all simple olefins tested (Table 2.8, all entries). As the olefin chain length increasing from 1-pentene to 1-undecene, the reactivity of the substrates decreases due to the steric hindrance, and the percentages of isomerization of olefins increase. After 20 minutes at 120°C, the isomerization percentages of 1-octene, 1-nonene, and 1-undecene were 24%, 30%, and 29%, respectively (Table 2.8, entries 3-5). No internal isomer of 1-pentene was observed (Table 2.8, entry 1), and only 5% of internal isomers was observed for 1-hexene (Table 2.8, entry 2) under the same conditions. Since the isomerization has been commonly observed for olefins using the Rh/tetraphosphoramidite catalyst, the zero or low percentages of isomers indicate that the hydroformylation of internal pentene and hexenes is fast under the reaction conditions. The

hydroformylation of a fluoro substituted olefin  $\text{CF}_3(\text{CF}_2)_5\text{CH}=\text{CH}_2$  afforded almost exclusively linear aldehyde with high TOF after 20 minutes at 120°C (Table 2.8, entry 6, 90% assay yield). One reason for the high TOF of this substrate is that it lacks of a  $\gamma$ -hydrogen, so the  $\beta$ -elimination will not produce internal olefins, which are more sterically hindered than terminal olefins and are less reactive.

**Table 2.8.** Hydroformylation of simple terminal using with ligand **9**.<sup>[a]</sup>

Entry	Substrate	<i>l:b</i> <sup>[b]</sup>	Linear <sup>[c]</sup> (%)	Iso. <sup>[d]</sup> (%)	Hydr. <sup>[e]</sup> (%)	TOF <sup>[f]</sup> (h <sup>-1</sup> )
1	1-pentene	588	99.8	0	0	2271
2	1-hexene	574	99.8	5	4	1830
3	1-octene	141	99.3	24	4	1659
4	1-nonene	671	99.9	30	3	1647
5	1-undecene	1386	99.9	29	4	1749
6	$\text{CF}_3(\text{CF}_2)_5\text{CH}=\text{CH}_2$	887	99.9	0	0	2721

<sup>[a]</sup> S/C = 1000, [Rh] = 1.0 mM, ligand/Rh ratio = 4:1, CO/H<sub>2</sub> = 5/5 atm, 120 °C, reaction time = 20 min, toluene as solvent, decane as internal standard. <sup>[b]</sup> Linear/branched ratio, determined by GC. <sup>[c]</sup> Percentage of linear aldehyde in all aldehydes. <sup>[d]</sup> Isomerization to internal olefins. <sup>[e]</sup> Turnover number, determined by GC. <sup>[f]</sup> Turnover frequency, determined by GC.

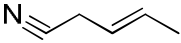
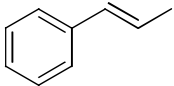
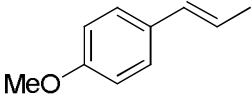
## 2.7. Hydroformylation of Internal Olefins

### 2.7.1 Hydroformylation of $\beta$ - and $\gamma$ -Olefins

Internal olefins are more difficult substrates than the corresponding terminal olefins for the regioselective hydroformylation. Furthermore, the isomerization to internal olefins from the corresponding terminal olefins is a major undesired side reaction that leads to

poor regioselectivity and reduced aldehyde productivity. Therefore, developing catalyst system that can provide high regioselectivity and high catalytic activity is highly desirable but a challenging undertaking. For this reason, ligand **9**, which exhibits the highest regioselectivity for terminal olefins, was tested in the hydroformylation of some common  $\beta$ - and  $\gamma$ -olefins. The results were listed in Table 2.9.

**Table 2.9.** Hydroformylation of internal olefins with ligand **9**.<sup>[a]</sup>

Entry	Substrate	<i>l:b</i> <sup>[b]</sup>	Linear <sup>[c]</sup> (%)	Iso. <sup>[d]</sup> (%)	Hydr. <sup>[e]</sup> (%)	TON <sup>[f]</sup> (h <sup>-1</sup> )
1	2-pentene	940	99.9	4.0	0.1	853
2	2-hexene	60	98.4	16	0.1	639
3	2-octene	53	98.1	35	0	324
4	trans-3-hexene	17	94.5	18	0	236
5		6.8	87.2	33	0	655
6		8.4	89.4	4.0	1.3	67
7		9.0	90.0	4.6	2.0	49

<sup>[a]</sup> S/C = 1000, [Rh] = 1.0 mM, ligand/Rh ratio = 4:1, CO/H<sub>2</sub> = 5/5 atm, 120 °C, reaction time = 2 h, toluene as solvent, decane as internal standard. <sup>[b]</sup> Linear/branched ratio, determined by GC. <sup>[c]</sup> Percentage of linear aldehyde in all aldehydes. <sup>[d]</sup> Isomerization to internal olefins. <sup>[e]</sup> Turnover number, determined by GC. <sup>[f]</sup> Turnover number, determined by GC.

The results show that ligand **9** is highly effective for the regioselective hydroformylation of simple  $\beta$ -olefins. The ligand afforded greater than 87% linear aldehyde for 2-pentene, 2-hexene, and 2-octene. As expected, with the increase olefin

chain length, the reactivity of the  $\beta$ -olefins decreases due to the steric hindrance, and the percentage of isomerization of increases (Table 2.9, entries 1-3). The hydroformylation of a simple  $\gamma$ -olefin (trans-3-hexene) is slow with a TOF of only 236 after 2 h at 120 °C, but the regioselectivity is high, resulting in 94.5% linear aldehyde among all aldehydes produced (Table 2.9, entry 4). To the best of our knowledge, this is the best linear selectivity reported for a  $\gamma$ -olefin.

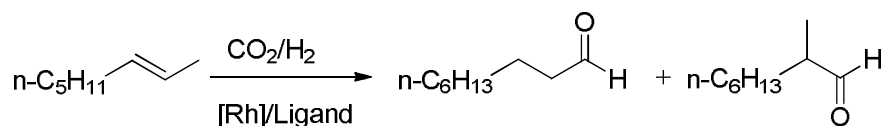
The hydroformylation of several functionalized  $\beta$ -olefins was also tested using ligand **9**. The ligand afforded 87% linear aldehyde for 3-pentenitrile with a TON of 655 after 2 h at 120°C (Table 2.9, entry 5). The hydroformylation of two styrene derivatives (trans- $\beta$ -methylstyrene and trans-anethole) is slow with TONs of only 67 and 47, respectively, after 2 h at 120 °C (Table 2.9, entries 6 and 7); however, about 90% linear selectivity was observed for these two substrates.

### 2.7.2 Ligand Structural Effects on the Hydroformylation of 2-Octene

The ligand structural effects on the hydroformylation of 2-octene was then studied. The evaluations of ligands **2** to **10** for the hydroformylation of 2-octene were conducted under the following reaction conditions: L/Rh = 4.0, 100 °C, CO/H<sub>2</sub> = 5/5 atm, toluene as solvent. As our standard procedure, the rhodium catalyst was prepared *in situ* by mixing the tetraphosphoramidite ligand with Rh(acac)(CO)<sub>2</sub> before charging the reactants. The reactions were terminated after immersing the reactor to an oil bath set at 100 °C for only 30 min so that the differences in catalyst performance can be observed. The results are listed in Table 2.10. The overall turnover frequency is low because of the short reaction time. However, Ligands **1** to **10** are found to be highly regioselective, affording 95% to

99% linear aldehyde. With the variation of the substituent group in the ligands, noticeable changes in both regioselectivity and reactivity were observed.

**Table 2.10.** Hydroformylation of 2-octene with ligands **1-10**.<sup>[a]</sup>



Entry	Ligand	R group in ligand	$\sigma_p$ <sup>[b]</sup>	$\sigma_I$ <sup>[c]</sup>	$l:b$ <sup>[d]</sup>	Linear <sup>[e]</sup> (%)	TOF <sup>[f]</sup> (h <sup>-1</sup> )
1	<b>10</b>	4-MeOPh	-0.27	n/a	58.7	98	196
2	<b>6</b>	4-MePh	-0.17	n/a	67.1	99	282
3	<b>5</b>	Ph	0	0.12	44.0	98	279
4	<b>7</b>	4-FPh	0.062	n/a	25.1	96	169
5	<b>8</b>	4-ClPh	0.227	n/a	22.7	96	180
6	<b>9</b>	2,4-F <sub>2</sub> Ph	0.4	n/a	19.2	95	84
7	<b>1</b>	H	n/a	0	18.3	95	187
8	<b>2</b>	Cl	n/a	0.47	52.7	98	366
9	<b>3</b>	Me	n/a	-0.01	35.9	97	158
10	<b>4</b>	Et	n/a	-0.01	27.8	97	81

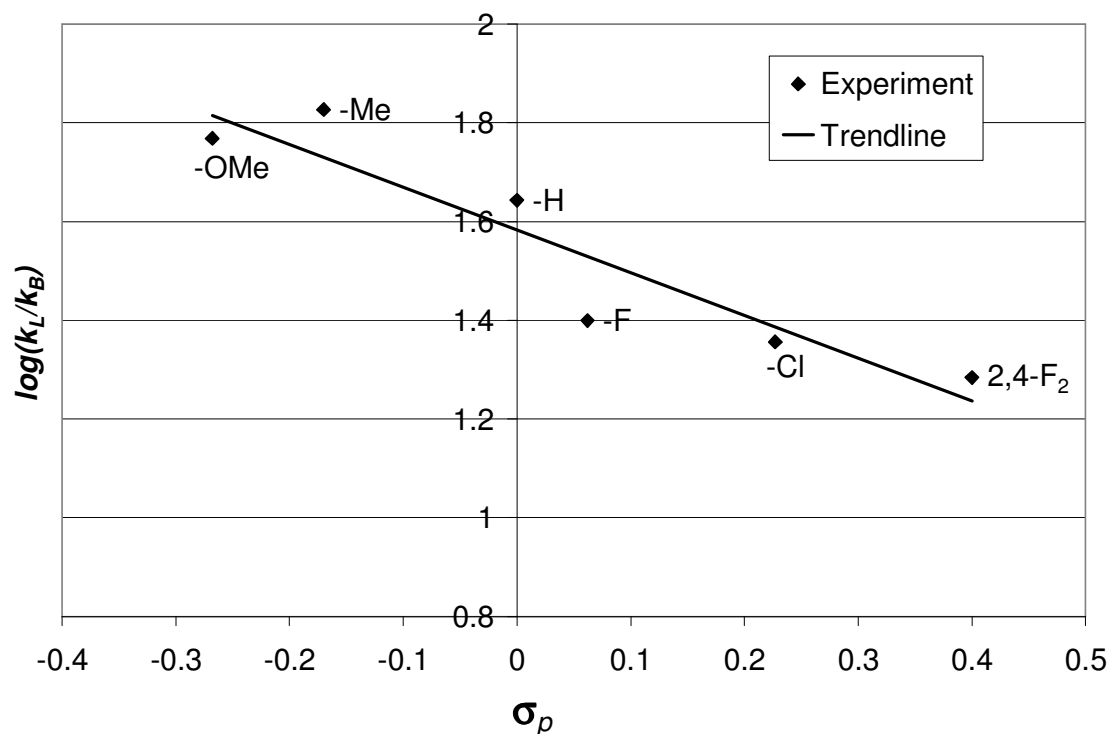
<sup>[a]</sup> S/C = 1000, [Rh] = 1.0 mM, L/Rh ratio = 4:1, CO/H<sub>2</sub> = 5/5 atm, 100 °C, reaction time = 30 min, toluene as solvent, decane as internal standard. <sup>[b]</sup> Hammett *para* substituent constant, data from reference 15.  $\sigma_p$  is for the substitution group on the R group, not on the biphenyl.  $\sigma_p$  of 2,4-difluoro in entry 6 was estimated by the summation of  $\sigma_p$  and  $\sigma_m$  for a single fluoro substituent. <sup>[c]</sup> Hammett substituent inductive parameter, data from reference 15.  $\sigma_I$  is for the substitution group at the 3,3',5,5'-positions of the biphenyl backbone. <sup>[d]</sup> Linear/branched ratio, determined by GC. <sup>[e]</sup> Percentage of linear aldehyde in all aldehydes. <sup>[f]</sup> Turnover frequency, determined by GC.

The electronic effects of ligands on the catalyst activity and regioselectivity were studied by changing the substituent at *para*-position of the phenyl group systematically from strong electron-donating groups to strong electron-withdrawing groups. The electronic effect is usually complicated with the steric effect and cannot be completely isolated. In order to minimize the steric effect, the substituent in variation needs to be small and placed at some distance away from the reaction center. For this reason, our quantitative study on the electronic effect is limited to ligands **5** to **10** that have small substituents (F, Cl, Me and MeO) attached to the phenyl group at the *para* position, which is remote to the chelating phosphorus atoms. As shown in section 2.4.2, the electronic effect of aromatic substituents on the regioselectivity can be treated using the following equation:

$$\log \frac{k_L}{k_B} = \rho \sigma_p + \log \left( \frac{k_L}{k_B} \right)_0, \quad (2.1)$$

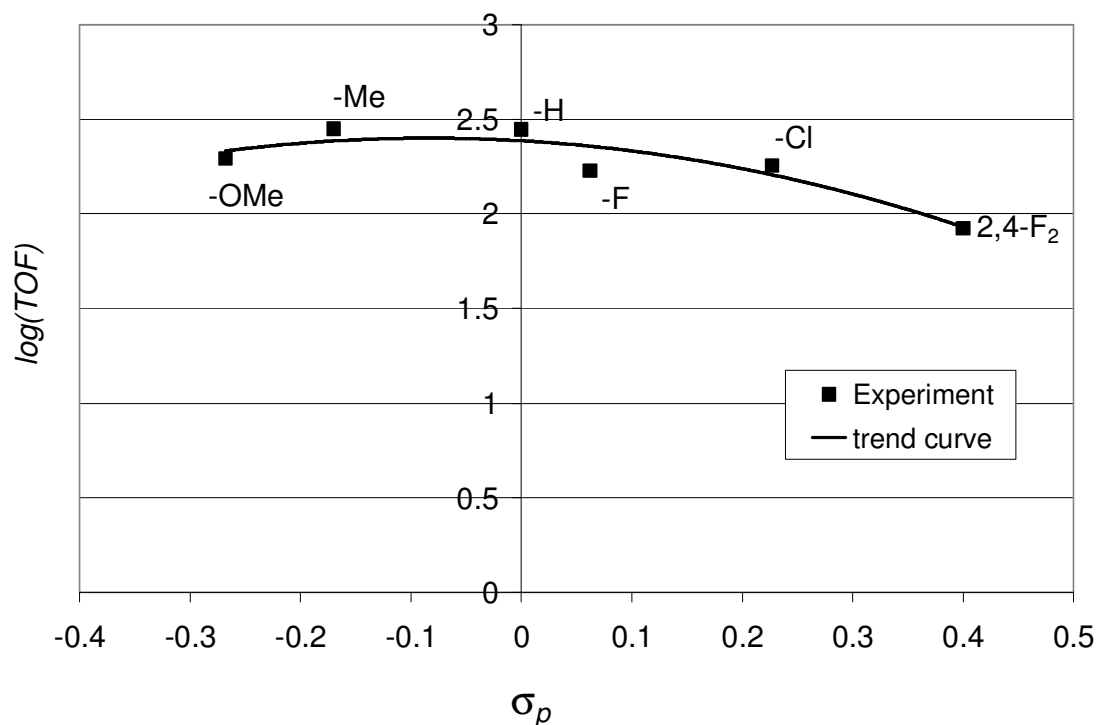
where  $k_L$  and  $k_B$  are the observed rate constants for the formation of linear aldehyde and branched aldehyde, respectively,  $\rho$  is a constant,  $\sigma_p$  is Hammett constant  $\sigma_p$ , and  $(k_L/k_B)_0$  is the linear to branch rate constant ratio when there is no substituent on the phenyl group. The substituent groups in ligands **5** to **10** have Hammett constant  $\sigma_p$  ranging from -0.3 to +0.4.<sup>15</sup> The formations of linear and branched aldehydes are two parallel and competitive reactions from the same rhodium intermediate, and as we showed in Chapter 1, equation 1.5, the ratio of observed rate constant for the formation of linear aldehyde to that of branched aldehyde ( $k_L/k_B$ ) can be approximated by the ratio of concentrations of linear aldehyde to that of branched aldehyde.<sup>16</sup>

The Hammett plot of  $\log(k_L/k_B)$  versus  $\sigma_p$  values of substituents was plotted in Figure 2.9. It is apparent that an electron-withdrawing group has a negative effect on the linear selectivity. A downward trend line of linear selectivity was obtained with the increase of  $\sigma_p$ . The highest linear selectivity was obtained using ligand **6** that has an electron-donating group on the phenyl ring, affording a linear to branch ratio of 67.1 (Table 2.10, entry 2). In contrast, ligand **9** which bears 2 strong electron-withdrawing fluoro groups on the phenyl ring afforded the lowest linear selectivity among ligands **5** to **10** (Table 2.10, entry 6, a *l*:*b* ratio of 19.2).



**Figure 2.9.** Hammett plot of  $\log(k_L/k_B)$  versus  $\sigma_p$  values of substituents in ligands **5-10** for the hydroformylation of 2-octene.

The steric effect of the ligand on the regioselectivity is also significant. The introduction of substituents at the 3,3',5,5'-positions of the biphenyl backbone improved the regioselectivity for the linear aldehyde. The unsubstituted ligand **1** afforded a *l:b* ratio of 18.3 (Table 2.10, entry 7). The use of ligands **5**, **6** and **10** that are bearing phenyl, 4-tolyl, and 4-methoxyphenyl groups ortho to the pyrrolyl phosphorus groups increased the linear to branch ratios to 44.0, 67.1, and 58.7, respectively (Table 2.10, entries 1-3). Improvement on regioselectivity was also observed for ligand **2-4** that bearing chloro, methyl, and ethyl substituents directly on the biphenyl backbone and ortho to the pyrrolyl phosphorus groups (Table 2.10, entries 8-10). Linear to branch ratios of 52.7, 35.9, and 27.8 were observed for ligand **2**, **3**, and **4**, respectively.



**Figure 2.10.** Turn over frequency (TOF, in logarithm scale) versus  $\sigma_p$  values of substituents in ligands **5-10** for the hydroformylation of 2-octene.

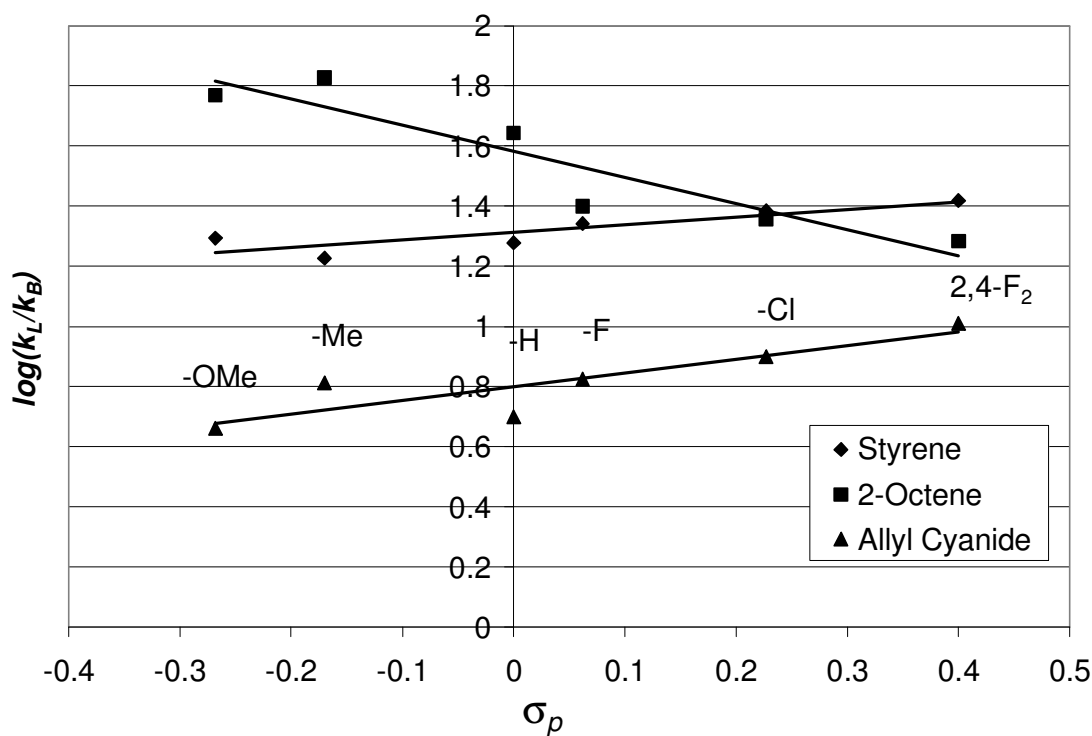


The catalyst activity in terms of the turn over frequency (TOF) versus the Hammett constant  $\sigma_p$  was plotted in Figure 2.10. No single trend line was observed for the catalyst activity with the increase of electron-withdrawing ability of the substituent in the phenyl group. It appears that the electronic effect on the catalyst activity is different within the electron-donating groups and within the electron-withdrawing groups. The phenyl substituted ligand **5** afforded TOF of 279 after 30 minutes at 100°C (Table 2.10, entry 3). For the ligands **7**, **8** and **9** with electron-withdrawing groups, with the increase of  $\sigma_p$ , the catalytic activity decrease. Ligand **9** that bears 2,4-difluorophenyl groups had the lowest TOF among ligands **5** to **10** (Table 2.10, entry 6). On the other side, for ligand **6** that bears 4-methylphenyl groups, there is little improvement in TOF compared to ligand **5**; for ligand **10** that bears 4-methoxyphenyl groups, a noticeable decrease in TOF was observed (Table 2.10, entries 1-2).

The hydroformylation of 2-octene to form a linear aldehyde is complicated with the isomerization of the double bond. In order to obtain highly linear selective terminal aldehyde, the double bond of 2-octene must migrate to the end. However, the migration of the double bond could occur to the opposite direction and produce 3-octene and 4-octene as well. Certainly, the isomerization of 2-octene to these unwanted internal octenes will impair both regioselectivity and reactivity, and also make the interpretation of the ligand effect difficult. In chapter 3, we will discuss further on the olefin isomerization in the hydroformylation of internal olefins.

### 2.7.3 Summary

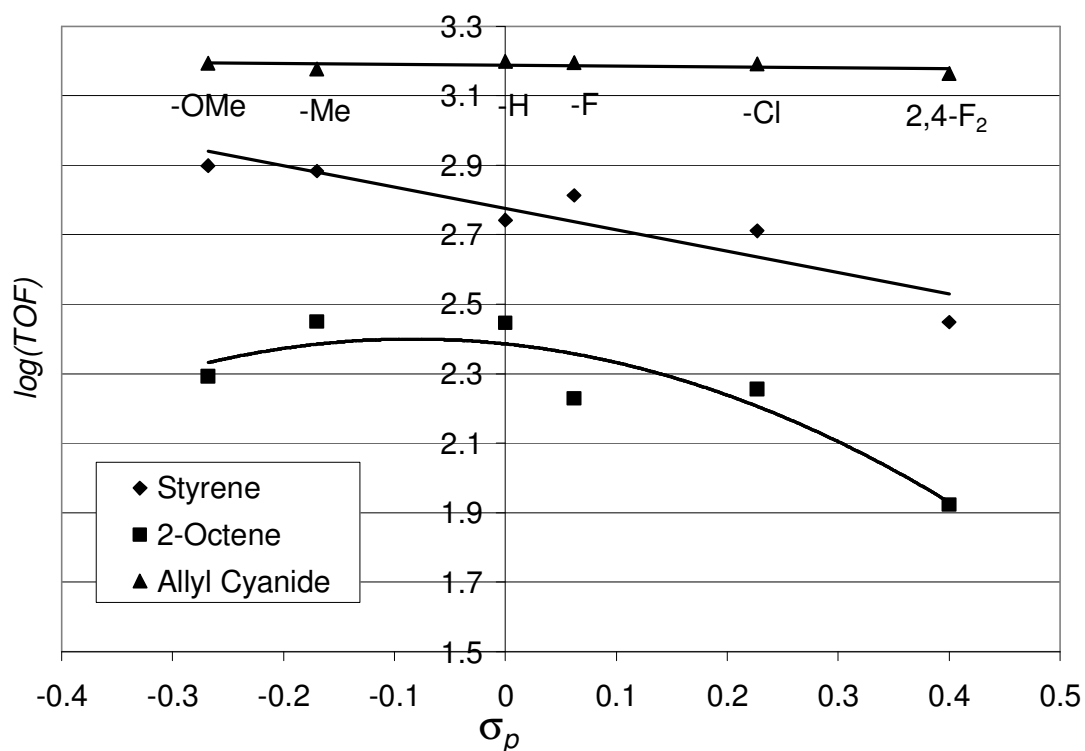
In previous sections, we have discussed the ligand structural effects on the hydroformylation of allyl cyanide, styrene and 2-octene, separately. To summarize the ligand structural effects on varied substrates, we have overlaid the Hammett plots from previous section in Figures 2.11 and 2.12. These plots can provide us some insights on the influence of ligand electronic property on the regioselectivity and catalytic activity, and help us gain understandings on the nature of the interactions between the ligands and olefin substrates.



**Figure 2.11.** Hammett plot of  $\log(k_L/k_B)$  versus  $\sigma_p$  values of substituents in ligands **5-10** for the hydroformylation of styrene, 2-octene, and allyl cyanide.

Figure 2.11 and Figure 2.12 are the overlays of Hammett plots for the regioselectivity and catalytic activity for the hydroformylation of styrene, 2-octene and allyl cyanide,

respectively. It is clear that the ligand electronic effect is varied with the individual substrate under reaction conditions. For the series of ligands **5** to **10**, with the increase of electron-withdrawing capacity, 1) in the case of styrene, the regioselectivity increases, but the catalytic activity decreases; 2) in the case of allyl cyanide, the regioselectivity increases, and the electronic property of a ligand has little effect on the catalytic activity; 3) in the case of 2-octene, the regioselectivity decreases, and the catalytic activity also decreases for ligands bearing electron-withdrawing groups.



**Figure 2.12.** Turn over frequency (TOF, in logarithm scale) versus  $\sigma_p$  values of substituents in ligands **5-10** for the hydroformylation of styrene, 2-octene, and allyl cyanide.

## Experimental Section

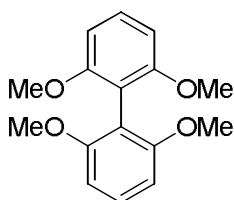
### General methods

All reactions and manipulations were performed in a nitrogen-filled glovebox or using standard Schlenk techniques, unless otherwise noted. All reagents and solvent were purchased from commercial vendors (Aldrich or TCI) unless otherwise noted. The reagents were used as is without further purification. Solvents were dried with standard procedures and degassed with N<sub>2</sub>. Column chromatography was performed using 200~400 mesh silica gel supplied by Natland International Corporation. Thin layer chromatography (TLC) was performed on 0.25 mm silica 60-F plates. <sup>1</sup>H NMR, <sup>13</sup>C NMR, <sup>19</sup>F NMR, and <sup>31</sup>P NMR spectra were recorded on Bruker Avance 400 (or 300) MHz or Varian Mercury 500 MHz NMR spectrometers. All chemical shifts are reported in ppm. GC analysis was carried on a Hewlett-Packard 6890 gas chromatograph using capillary columns.

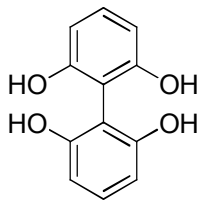
### Experimental procedures and compound data

**General procedure for the hydroformylation of olefins:** To an 8 mL glass vial with a magnetic stirring bar was charged tetraphosphorus ligand (4 μmol) and Rh(acac)(CO)<sub>2</sub> (1 μmol in 100 μL toluene, charged as stock solution). The mixture was stirred for 5 minutes. Then allyl cyanide (1 mmol) was added, followed by the addition of *n*-decane (100 μL) as internal standard. Additional toluene was added to bring the total reaction volume to 1 mL. The reaction mixture was transferred to an autoclave. The autoclave was sealed and purged with nitrogen for three times and subsequently charged with CO (5 atm) and H<sub>2</sub> (5 atm). The autoclave was then immersed in a preheated oil bath and was well stirred. After the desired reaction time, the autoclave was taken out of the oil bath and cooled in ice water.

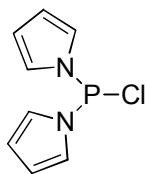
The pressure was carefully released in a well ventilated hood. The reaction mixture was immediately analyzed by GC, HPLC, and/or proton NMR to determine regioselectivity, conversion and turnover number. The reactions were repeated several times to ensure reproducibility.



**Synthesis of 2,6,2',6'-tetramethoxy-1,1'-biphenyl (12):** To a 250 mL Schlenk flask was added 1, 3-dimethoxybenzene (8.26 g, 60 mmol). The flask was degassed and charged with nitrogen. To the flask was added THF (40 mL). The resulting solution was cooled to  $-78^{\circ}\text{C}$  in a dry ice/acetone bath. To the cooled solution was added *n*-BuLi (26.4 mL, 2.5 M solution in hexane, 66 mmol). The reaction mixture was allowed to warm to room temperature and stirred for 4 h. the mixture was cooled again to  $-78^{\circ}\text{C}$  and added through cannula to a cold ( $-78^{\circ}\text{C}$ ) solution of  $\text{FeCl}_3$  (13.5 g, 83 mmol) in THF (40 mL). The reaction mixture was allowed to warm to room temperature and stirred for 16 h. The reaction mixture was concentrated under reduced pressure. To the residue was added aqueous 2N HCl solution (100 mL),  $\text{CH}_2\text{Cl}_2$  (60 mL). After stirring for 5 min, the organic phase was separated. The organic phase was washed with aqueous 2N HCl solution (2 x 20 mL), dried over  $\text{Na}_2\text{SO}_4$  and passed through a short silica gel plug. The pure title product was obtained by recrystallization from EtOH. (5.7 g, 70 %).  $^1\text{H}$  NMR (300 MHz,  $\text{CDCl}_3$ )  $\delta$  7.31 (t,  $J = 8.30$  Hz, 2H), 6.68 (d,  $J = 8.33$  Hz, 4H), 3.73 (s, 12H);  $^{13}\text{C}$  NMR (75 MHz,  $\text{CDCl}_3$ )  $\delta$  158.3, 128.7, 112.4, 104.4, 56.1.

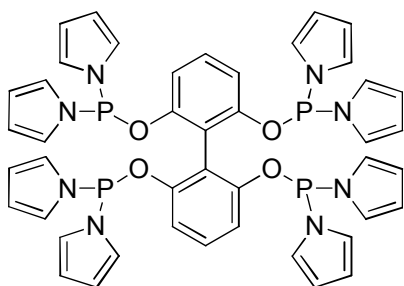


**General procedure for the synthesis 1,1'-biphenyl -2,6,2',6'-tetraol (17a):** To a 250 mL Schlenk flask was added 2, 2', 6, 6'-tetramethoxy-1,1'-biphenyl (5.48 g, 20 mmol). The flask was degassed and charged with nitrogen. To the flask was added  $\text{CH}_2\text{Cl}_2$  (100 mL). The resulting solution was cooled to  $-78^\circ\text{C}$  in a dry ice/acetone bath. To the cooled solution was added boron tribromide (7.7 mL) dropwise. The reaction mixture was allowed to warm to room temperature and stirred for 5 h. After cooled to  $0^\circ\text{C}$ , water (50 mL) was added dropwise to quench the reaction. The organic phase was separated and the aqueous phase was extracted with ether (3 x 25 mL). The combined organic layers was dried over  $\text{Na}_2\text{SO}_4$  and concentrated under reduced pressure. The crude product was purified by recrystallization from ethanol to give the title compound (3.57 g, 81%).  $^1\text{H}$  NMR (300 MHz,  $\text{CDCl}_3$ )  $\delta$  7.59 (s, 4H), 7.02 (t,  $J = 8.13$  Hz, 2H), 6.48 (d,  $J = 8.10$  Hz, 4H);  $^{13}\text{C}$  NMR (75 MHz,  $\text{CDCl}_3$ )  $\delta$  207.0, 157.2, 129.8, 108.1.

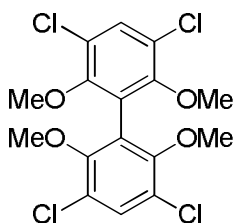


**Synthesis of chlorodipyrrolylphosphine (16):** To a 100 mL flask was charged THF (60 mL) followed by  $\text{PCl}_3$  (2.71 mL, 0.03 mol). The resulting solution was then cooled to  $0^\circ\text{C}$  in an ice bath. To the cooled solution was added dropwise a solution of pyrrole (4.20 mL, 0.06 mol) and  $\text{NEt}_3$  (3 mL) in THF (15 mL) while maintaining the temperature at  $0^\circ\text{C}$ . The precipitation of triethylamine·HCl salt was formed immediately upon addition. After

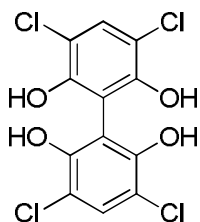
addition, the cold bath was removed and the reaction mixture was allowed to warm to room temperature and stirred for 6 h. The reaction mixture was diluted with THF (30 ml) and filtered to remove the salts. The salts were washed with THF (3 x 10 mL). The combined THF solution affords chlorodipyrrolylphosphine (2.35 g, 39 % yield) as a colorless liquid.  $^1\text{H}$  NMR (300 MHz,  $\text{CDCl}_3$ )  $\delta$  6.51-6.50 (m, 4H), 7.24-7.21 (m, 4H);  $^{31}\text{P}$  NMR (146 MHz,  $\text{CDCl}_3$ )  $\delta$  102.9.



**General procedure for the synthesis of ligand 1,1'-biphenyl-2,6,2',6'-tetrakis(dipyrrolylphosphoramidite) (1):** To a solution of chlorodipyrrolylphosphine (4.4 mmol, 0.87g) in THF (10 mL) was added dropwise triethylamine (1mL) and a solution of biphenyl-2,6,2',6'-tetraol **17a** (1 mmol, 0.218g) in THF (5 mL) at room temperature. The triethylamine.HCl salts were formed immediately after the addition. The reaction mixture was stirred for 6 h at room temperature. The triethylamine.HCl salts were then filtered off and the solvent was removed under vacuum. The crude product was purified by flash chromatography on basic aluminum oxide (eluting with hexane/EtOAc/ $\text{NEt}_3$  6:1:0.1) to afford the pure ligand (0.31 g, 36 %) as an air-stable colorless solid.  $^1\text{H}$  NMR (300 MHz,  $\text{CD}_2\text{Cl}_2$ )  $\delta$  7.23 (t,  $J = 8.3$  Hz, 2H), 6.68 (m, 20H), 6.21 (m, 16H);  $^{13}\text{C}$  NMR (75 MHz,  $\text{CD}_2\text{Cl}_2$ )  $\delta$  152.86 (d,  $J = 12.2\text{Hz}$ ) 131.0, 121.5 (d,  $J = 16.8\text{Hz}$ ), 118.1, 115.3(d,  $J = 13.7$  Hz), 112.7;  $^{31}\text{P}$  NMR (146 MHz,  $\text{CDCl}_3$ )  $\delta$  107.3. HRMS ( $\text{ES}^+$ ) calcd. for  $\text{C}_{44}\text{H}_{39}\text{N}_8\text{O}_4\text{P}_4$  [ $\text{MH}^+$ ] 867.2045, found 867.2021.



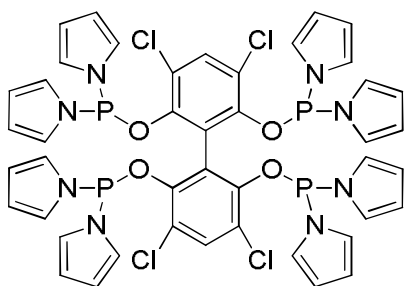
**Synthesis of 3,3',5,5'-tetrachloro-2,2',6,6'-tetramethoxy-1,1'-biphenyl (14b):** A solution of 5 mL (62.5 mmol) of  $\text{SO}_2\text{Cl}_2$  in 5 mL of  $\text{CHCl}_3$  was added dropwise to a solution of 2.8 g (10 mmol) of 2,2',6,6'-tetramethoxybiphenyl **12** in 20 mL of  $\text{CHCl}_3$  at room temperature. The solution was stirred and monitored by TLC plate. After 30 min, saturated NaCl solution was added carefully to the reaction mixture and the organic layer was separated. The water layer was extracted three times with chloroform (20 mL) and the organic layer was combined and dried over anhydrous magnesium sulfate. After filtration, the solvent was evaporated and the residue was passed through a short silica gel plug. The solvent was evaporated and 3.8 g of white solid was obtained in 91% yield.  $^1\text{H}$  NMR (500 MHz,  $\text{CDCl}_3$ )  $\delta$  7.51 (s, 2 H), 3.67 (s, 12 H);  $^{13}\text{C}$  NMR (126 MHz,  $\text{CDCl}_3$ )  $\delta$  153.4, 130.1, 125.1, 123.5, 60.9; IR (film):  $\nu$  1467, 1419, 1284, 1102, 1017, 882  $\text{cm}^{-1}$ ; HRMS ( $\text{ES}^+$ ) calcd for  $\text{C}_{16}\text{H}_{18}\text{Cl}_4\text{O}_4$   $[\text{M}+\text{H}]^+$  427.9990, found 427.9985.



**Synthesis of 3,3',5,5'-tetrachloro-1,1'-biphenyl-2,2',6,6'-tetraol (17b):** To a 250 mL Schlenk flask was added 3,3',5,5'-tetrachloro-2,2',6,6'-tetramethoxybiphenyl **14b** (1.7 g, 4.1 mmol). The flask was degassed and charged with nitrogen. To the flask was added  $\text{CH}_2\text{Cl}_2$  (20 mL). The resulting solution was cooled to  $-78^\circ\text{C}$  in a dry ice/acetone bath. To

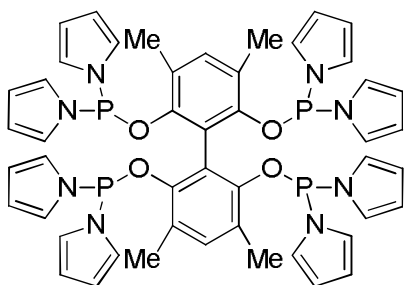


the cooled solution was added boron tribromide (1.5 mL, 18.0 mmol) dropwise. The reaction mixture was allowed to warm to room temperature and stirred for 5 h. After cooled to 0 °C, water (50 mL) was added dropwise to quench the reaction. The organic phase was separated and the aqueous phase was extracted with ethyl acetate (3 x 25 mL). The combined organic layers was dried over Na<sub>2</sub>SO<sub>4</sub> and concentrated under reduced pressure. The crude product was purified by recrystallization from hexanes to give the titled compound **17b** (1.35 g, 92%). <sup>1</sup>H NMR (500 MHz, acetone) δ 7.38 (s, 2H); <sup>13</sup>C NMR (125 MHz, acetone) δ 152.2, 130.20, 130.18, 112.6, 110.6; IR (film): ν 3525, 3503, 1596, 1449, 1423, 1300, 1281, 1172, 783 cm<sup>-1</sup>; HRMS (ES<sup>+</sup>) calcd for C<sub>12</sub>H<sub>5</sub>Cl<sub>4</sub>O<sub>4</sub> [M-H]<sup>+</sup> 352.8942, found 352.8965.

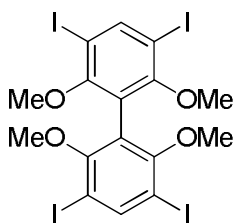


**Synthesis of 3,3',5,5'-tetrachloro-1,1'-biphenyl-2,2',6,6'-tetrakis-(dipyrrolylphosphoramidite) (2):** To a solution of chlorodipyrrolylphosphine (55 mmol, 10.9 g) in THF (50 mL) was added dropwise triethylamine (13 mL) and a solution of 3,3',5,5'-tetrachloro tetraol (10 mmol, 3.6 g) in THF (100 mL) at room temperature. The triethylamine·HCl salts were formed immediately after the addition. The reaction mixture was stirred for 6 h at room temperature. The triethylamine·HCl salts were then filtered off, and the solvent was removed under vacuum. The crude product was purified by recrystallization from hexanes three times to afford the pure ligand **2** (2.2 g, 22%) as an air-stable colorless solid: <sup>1</sup>H NMR (400 MHz, CDCl<sub>3</sub>) δ 7.26 (s, 2 H), 6.65 (brs, 16 H), 6.21 (t, *J* = 2.2 Hz, 16 H); <sup>13</sup>C

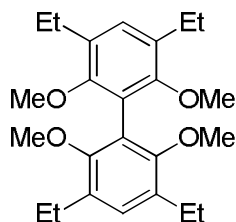
NMR (100 MHz,  $\text{CDCl}_3$ )  $\delta$  147.6, 131.9, 123.0, 121.40, 121.39, 121.33, 121.22, 121.15, 113.7, 113.6, 112.5, 112.4, 112.38, 112.28;  $^{31}\text{P}$  NMR (161 MHz,  $\text{CDCl}_3$ )  $\delta$  109.0; IR (film):  $\nu$  1462, 1188, 1063, 1057, 1031, 731  $\text{cm}^{-1}$ ; HRMS ( $\text{ES}^+$ ) calcd for  $\text{C}_{44}\text{H}_{35}\text{Cl}_4\text{N}_8\text{O}_4\text{P}_4$   $[\text{M}+\text{H}]^+$  1003.0486, found 1003.0463.



**Synthesis of 3,3',5,5'-tetramethyl-1,1'-biphenyl-2,2',6,6'-tetrakis-(dipyrrolylphosphoramidite) (3):** Ligand **3** was prepared according to the general procedure using chlorodipyrrolylphosphine (1.7 g, 8.3 mmol) and 3,3',5,5'-tetramethylbiphenyl-2,2',6,6'-tetraol (0.5 g, 1.9 mmol). Purification by recrystallization from hexanes gave **3** as a white solid in 34% yield (0.6 g).  $^1\text{H}$  NMR (400 MHz,  $\text{CDCl}_3$ )  $\delta$  7.23 (brs, 16 H), 6.72 (s, 2 H), 6.20 (t,  $J = 2.2$  Hz, 16 H), 1.67 (s, 12 H);  $^{13}\text{C}$  NMR (100 MHz,  $\text{CDCl}_3$ )  $\delta$  149.0, 134.1, 126.6, 121.31, 121.25, 121.21, 121.13, 113.2, 113.1, 112.0, 111.9, 111.8, 111.7, 16.3;  $^{31}\text{P}$  NMR (161 MHz,  $\text{CDCl}_3$ )  $\delta$  105.6; IR (film):  $\nu$  1453, 1190, 1179, 1056, 1037, 729  $\text{cm}^{-1}$ ; HRMS ( $\text{ES}^+$ ) calcd for  $\text{C}_{48}\text{H}_{47}\text{N}_8\text{O}_4\text{P}_4$   $[\text{M}+\text{H}]^+$  923.2671, found 923.2651.



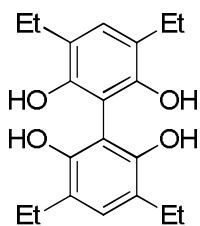
**Synthesis of 3,3',5,5'-tetraiodo-2,2',6,6'-tetramethoxy-1,1'-biphenyl (13):** A 200-ml., three-necked flask is charged with 13.8 g. (50.0 mmol) of 2,2',6,6'-tetramethoxybiphenyl **12**, 9.1 g. (40.0 mmol) of periodic acid dihydrate, and 20.4 g. (80.0 mmol) of iodine. A solution of 3 mL of concentrated sulfuric acid and 20 mL of water in 100 mL of glacial acetic acid is added to this mixture. The resulting purple solution is heated at 80° with stirring for approximately 10 hours until the color of iodine disappears. The reaction mixture is diluted with approximately 250 mL of water, and the white-yellow solid that separates is collected on a Büchner funnel and washed three times with 100-mL portions of water. The product is recrystallized from boiling acetone as colorless, fine needles (31.8 g, 82%). <sup>1</sup>H NMR (500 MHz, CDCl<sub>3</sub>) δ 8.28 (s, 2 H), 3.59 (s, 12 H); <sup>13</sup>C NMR (126 MHz, CDCl<sub>3</sub>) δ 158.9, 147.6, 124.8, 86.7, 61.0; IR (film): ν 1641, 1450, 1397, 1250, 1154, 1059, 921 cm<sup>-1</sup>.



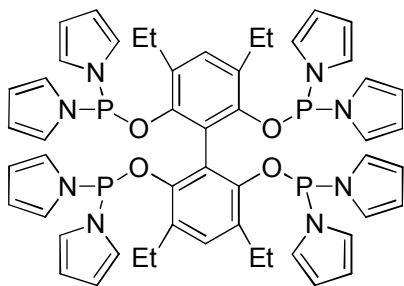
**Synthesis of 3,3',5,5'-tetraethyl-2,2',6,6'-tetramethoxy-1,1'-biphenyl (14d):**

3,3',5,5'-tetraiodo-2,2',6,6'-tetramethoxybiphenyl **13** (7.8 g, 10 mmol) and ethynyltrimethylsilane (8.2 mL g, 58.0 mmol) in a mixture of triethylamine (100 mL) and piperidine (30 mL) was treated with PdCl<sub>2</sub>(PhCN)<sub>2</sub>, (0.4 mg, 1.0 mmol), triphenylphosphine (275 mg, 1.0 mmol), and CuI (80 mg). The originally yellow solution turned to green and then brown. After 3 h at room temperature it was heated at 80 °C for 24 h. The precipitate was filtered and the filtration was passed through a short silica gel plug. The obtained solution was evaporated and treated with a solution of KOH (6.0 g, 108.0

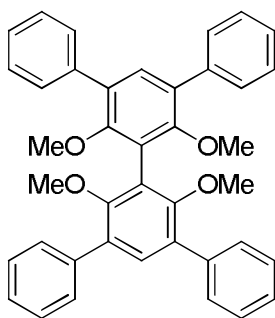
mmol) in methanol (40 mL). The reaction solution was stirred at room temperature for 2 h until TLC analysis indicated that the reaction was complete. Ether-water workup and the obtained yellow liquid was dissolved in 200 mL of mixture of ethyl acetate and methanol and combined with 5 wt% Pd/C (0.5 g) in an autoclave under a 200 psi of hydrogen atmosphere. The reaction was stirred at room temperature for 2 h until no hydrogen absorption was observed. Filtration and flash chromatography afford 2.9 g of white solid in 73% yield.  $^1\text{H}$  NMR (500 MHz,  $\text{CDCl}_3$ )  $\delta$  7.09 (s, 2 H), 3.53 (s, 12 H), 2.69 (q,  $J = 7.5$  Hz, 8 H), 1.27 (t,  $J = 7.5$  Hz, 12 H);  $^{13}\text{C}$  NMR (126 MHz,  $\text{CDCl}_3$ )  $\delta$  154.6, 132.2, 128.8, 123.3, 60.4, 22.9, 15.0; IR (film):  $\nu$  1468, 1425, 1058  $\text{cm}^{-1}$ ; HRMS ( $\text{ES}^+$ ) calcd for  $\text{C}_{24}\text{H}_{35}\text{O}_4$   $[\text{M}+\text{H}]^+$  387.2535, found 387.2526.



**Synthesis of 3,3',5,5'-tetraethyl-1,1'-biphenyl-2,2',6,6'-tetraol (17d):** Tetraol **17d** was prepared according to the general procedure using 3,3',5,5'-tetraethyl-2,2',6,6'-tetramethoxybiphenyl **14d** (2.9 g, 7.3 mmol) and boron tribromide (3.0 mL, 36.0 mmol). Purification by recrystallization from hexanes gave **17d** as a white solid in 92% yield (2.2 g).  $^1\text{H}$  NMR (500 MHz, acetone)  $\delta$  6.92 (s, 2 H), 6.55 (s, 4 H), 2.59 (q,  $J = 7.5$  Hz, 8 H), 1.18 (t,  $J = 7.5$  Hz, 12 H);  $^{13}\text{C}$  NMR (126 MHz, acetone)  $\delta$  152.3, 130.7, 122.8, 107.0, 23.8, 15.1; IR (film):  $\nu$  3530, 3503, 1472, 1173, 1092  $\text{cm}^{-1}$ ; HRMS ( $\text{ES}^+$ ) calcd for  $\text{C}_{20}\text{H}_{27}\text{O}_4$   $[\text{M}+\text{H}]^+$  331.1909, found 331.1905.

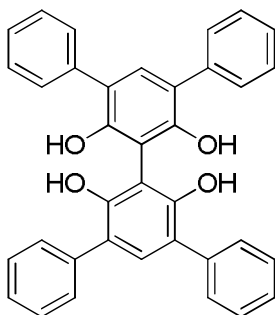


**Synthesis of 3,3',5,5'-tetraethyl-1,1'-biphenyl-2,2',6,6'-tetrakis-(dipyrrolylphosphoramidite) (4):** Ligand **4** was prepared according to the general procedure using 3,3',5,5'-Tetraethylbiphenyl-2,2',6,6'-tetraol **17d** (2.0 g, 6.0 mmol) and chlorodipyrrolylphosphine (5.2 g, 25.4 mmol). Purification by recrystallization from hexanes gave **4** as a white solid in 28% yield (1.6 g).  $^1\text{H}$  NMR (400 MHz,  $\text{CDCl}_3$ )  $\delta$  6.77 (brs, 18 H), 6.21 (t,  $J = 2.2$  Hz, 16 H), 2.01 (q,  $J = 7.6$  Hz, 8 H), 0.90 (t,  $J = 7.6$  Hz, 12 H);  $^{13}\text{C}$  NMR (100 MHz,  $\text{CDCl}_3$ )  $\delta$  148.9, 132.3, 130.7, 121.1, 118.9, 111.8, 22.8, 14.3;  $^{31}\text{P}$  NMR (161 MHz,  $\text{CDCl}_3$ )  $\delta$  105.6; IR (film):  $\nu$  1453, 1174, 1083, 1044, 1025, 729  $\text{cm}^{-1}$ ; HRMS ( $\text{ES}^+$ ) calcd for  $\text{C}_{52}\text{H}_{55}\text{N}_8\text{O}_4\text{P}_4$   $[\text{M}+\text{H}]^+$  979.3297, found 979.3257.

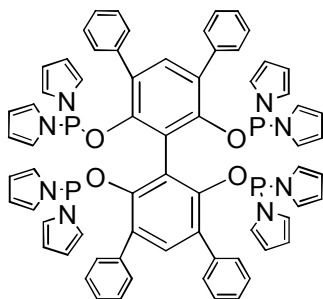


**Synthesis of 3,3',5,5'-tetraphenyl-2,2',6,6'-tetramethoxy-1,1'-biphenyl (14e):** A mixture of phenylboronic acid (14.6 g, 120.0 mmol), 3,3',5,5'-tetraiodo-2,2',6,6'-tetramethoxybiphenyl **13** (7.8 g, 10 mmol), palladium tetrakis(triphenyl)phosphine (1.0 g), and potassium carbonate (24 g, 160 mmol) in dry dioxane (150 mL) was stirred under nitrogen for 24 h at 85  $^{\circ}\text{C}$ . The resulting mixture was cooled and poured into a solution of

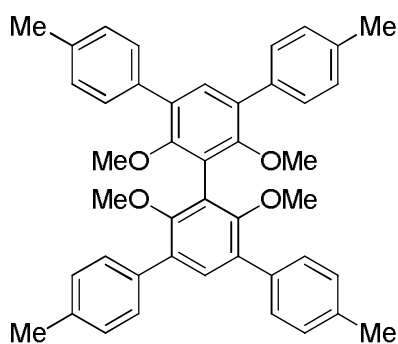
ice with concentrated hydrochloric acid (3:1) and the organic phase was extracted twice with dichloromethane, dried over magnesium sulfate. After evaporation of the solvent, the mixture was subjected to flash chromatography to give 4.5 g (78%) of **14e** as a white solid.  $^1\text{H}$  NMR (500 MHz,  $\text{CDCl}_3$ )  $\delta$  7.66 (d,  $J = 7.5$  Hz, 8 H), 7.44 (d,  $J = 7.5$  Hz, 8 H), 7.42 (s, 2 H), 7.36 (t,  $J = 7.5$  Hz, 4 H), 3.42 (s, 12 H);  $^{13}\text{C}$  NMR (126 MHz,  $\text{CDCl}_3$ )  $\delta$  155.7, 138.7, 132.6, 130.4, 129.0, 128.3, 126.9, 124.1, 60.4; IR (film):  $\nu$  1459, 1410, 1215, 1068, 929, 738  $\text{cm}^{-1}$ ; HRMS ( $\text{ES}^+$ ) calcd for  $\text{C}_{40}\text{H}_{35}\text{O}_4$   $[\text{M}+\text{H}]^+$  579.2535, found 579.2529.



**Synthesis of 3,3',5,5'-tetraphenyl-1,1'-biphenyl-2,2',6,6'-tetraol(17e):** Tetraol **17e** was prepared according to the general procedure using 3,3',5,5'-tetraphenyl-2,2',6,6'-tetramethoxybiphenyl **14e** (4.5 g, 8.0 mmol) and boron tribromide (3.5 mL, 42.0 mmol). Purification by recrystallization from hexanes gave **17e** as a white solid in 89% yield (3.7 g).  $^1\text{H}$  NMR (500 MHz, acetone)  $\delta$  7.69 (d,  $J = 7.5$  Hz, 8 H), 7.52 (s, 4 H), 7.40 (t,  $J = 7.5$  Hz, 8 H), 7.32 (s, 2 H), 7.28 (t,  $J = 7.5$  Hz, 4 H); IR (film):  $\nu$  3523, 1456, 1154, 1033  $\text{cm}^{-1}$ ;  $^{13}\text{C}$  NMR (126 MHz, acetone)  $\delta$  154.1, 140.0, 133.7, 130.3, 129.0, 127.2, 122.5, 108.1; HRMS ( $\text{ES}^+$ ) calcd for  $\text{C}_{36}\text{H}_{27}\text{O}_4$   $[\text{M}+\text{H}]^+$  523.1909, found 523.1914.

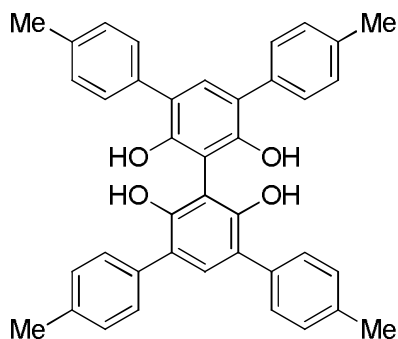


**Synthesis of 3,3',5,5'-tetrakis(dipyrrolylphosphoramidite)-1,1'-biphenyl-2,2',6,6'-tetraol (5):** Ligand **5** was prepared according to the general procedure using 3,3',5,5'-tetrakis(dipyrrolylphosphoramidite)-1,1'-biphenyl-2,2',6,6'-tetraol **4e** (2.6 g, 5.0 mmol) and chlorodipyrrolylphosphine (4.8 g, 24.3 mmol). Purification by recrystallization from hexanes gave **5** as a white solid in 26% yield (1.5 g).  $^1\text{H}$  NMR (400 MHz,  $\text{CDCl}_3$ )  $\delta$  7.26 (s, 2 H), 7.24 (m, 4 H), 7.20 (m, 8 H), 7.12 (m, 8 H), 6.49 (brs, 16 H), 6.07 (t,  $J = 2.0$  Hz, 16 H);  $^{13}\text{C}$  NMR (100 MHz,  $\text{CDCl}_3$ )  $\delta$  149.42, 149.40, 136.7, 135.1, 131.2, 129.5, 128.3, 127.5, 121.0, 120.9, 118.93, 120.86, 120.79, 120.77, 120.0, 111.8;  $^{31}\text{P}$  NMR (161 MHz,  $\text{CDCl}_3$ )  $\delta$  106.5; IR (film):  $\nu$  1451, 1419, 1178, 1054, 1036, 730  $\text{cm}^{-1}$ ; HRMS ( $\text{ES}^+$ ) calcd for  $\text{C}_{68}\text{H}_{55}\text{N}_8\text{O}_4\text{P}_4$   $[\text{M}+\text{H}]^+$  1171.3297, found 1171.3259.



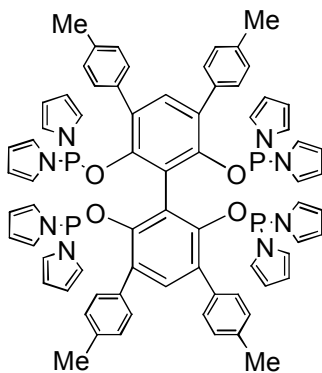
**Synthesis of 3,3',5,5'-tetra-4-methylphenyl-2,2',6,6'-tetramethoxy-1,1'-biphenyl (14f):** 3,3',5,5'-tetra-4-methylphenyl-2,2',6,6'-tetramethoxy-1,1'-biphenyl **14f** was prepared according to the general procedure for synthesis of 3,3',5,5'-tetrakis(dipyrrolylphosphoramidite)-1,1'-biphenyl-2,2',6,6'-tetraol **4e**

by using tolylboronic acid (24.5 g, 180.0 mmol), 3,3',5,5'-tetraiodo-2,2',6,6'-tetramethoxybiphenyl **13** (11.9 g, 15.2 mmol). Purification by flash chromatography gave **14f** as a white solid in 72% yield (6.9 g).  $^1\text{H}$  NMR (500 MHz,  $\text{CDCl}_3$ )  $\delta$  7.57 (d,  $J = 7.5$  Hz, 8 H), 7.44 (s, 2 H), 7.26 (d,  $J = 7.5$  Hz, 8 H), 3.44 (s, 12 H), 2.44 (s, 12 H);  $^{13}\text{C}$  NMR (126 MHz,  $\text{CDCl}_3$ )  $\delta$  155.5, 136.5, 135.9, 132.3, 130.2, 128.97, 128.88, 124.2, 60.3, 21.2; IR (film):  $\nu$  1457, 1413, 1054  $\text{cm}^{-1}$ ; HRMS ( $\text{ES}^+$ ) calcd for  $\text{C}_{44}\text{H}_{43}\text{O}_4$   $[\text{M}+\text{H}]^+$  635.3161, found 635.3133.

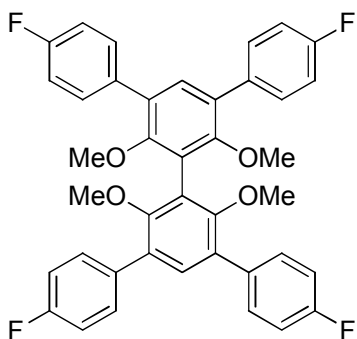


**Synthesis of 3,3',5,5'-tetratolyl-1,1'-biphenyl-2,2',6,6'-tetraol(17f):** Tetraol **17f** was prepared according to the general procedure using 3,3',5,5'-tetratolyl-2,2',6,6'-tetramethoxybiphenyl (5.7 g, 9.0 mmol) and boron tribromide (3.9 mL, 46.8 mmol). Purification by recrystallization from hexanes gave **17f** as a white solid in 89% yield (4.6 g).  $^1\text{H}$  NMR (500 MHz, acetone)  $\delta$  7.56 (d,  $J = 7.5$  Hz, 8 H), 7.36 (s, 4 H), 7.28 (s, 2 H), 7.21 (d,  $J = 7.5$  Hz, 8 H);  $^{13}\text{C}$  NMR (126 MHz, acetone)  $\delta$  153.8, 137.0, 136.5, 133.4, 130.2, 129.6, 122.3, 108.1, 21.2; IR (film):  $\nu$  3520, 1593, 1455, 1155, 1024  $\text{cm}^{-1}$ ; HRMS ( $\text{ES}^+$ ) calcd for  $\text{C}_{40}\text{H}_{35}\text{O}_4$   $[\text{M}+\text{H}]^+$  579.2535, found 579.2532.



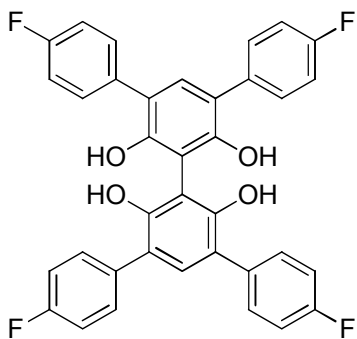


**Synthesis of 3,3',5,5'-tetratolylphenyl-1,1'-biphenyl-2,2',6,6'-tetrakis-(dipyrrolyl-phosphoramidite) (6):** Ligand **6** was prepared according to the general procedure using 3,3',5,5'-Tetratolylbiphenyl-2,2',6,6'-tetraol **17f** (2.8 g, 4.5 mmol) and chlorodipyrrolylphosphine (3.9 g). Purification by recrystallization from hexanes gave **6** as a white solid in 21% yield (1.2 g).  $^1\text{H}$  NMR (400 MHz,  $\text{CDCl}_3$ )  $\delta$  7.20 (s, 2 H), 7.00 (d,  $J = 2.0$  Hz, 8 H), 6.95 (d,  $J = 2.0$  Hz, 8 H), 6.49 (brs, 16 H), 6.05 (t,  $J = 2.0$  Hz, 16 H), 2.34 (s, 12 H);  $^{13}\text{C}$  NMR (100 MHz,  $\text{CDCl}_3$ )  $\delta$  149.3, 137.2, 134.8, 133.7, 131.1, 129.4, 129.0, 120.92, 120.88, 120.85, 120.78, 111.6, 21.2; IR (film):  $\nu$  1449, 1178, 1073, 1054, 1037, 730  $\text{cm}^{-1}$ ;  $^{31}\text{P}$  NMR (161 MHz,  $\text{CDCl}_3$ )  $\delta$  106.8; HRMS ( $\text{ES}^+$ ) calcd for  $\text{C}_{72}\text{H}_{63}\text{N}_8\text{O}_4\text{P}_4$   $[\text{M}+\text{H}]^+$  1227.3923, found 1227.3933.



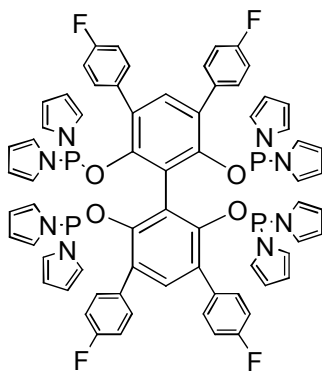
**Synthesis of 3,3',5,5'-tetra(4-fluorophenyl)-2,2',6,6'-tetramethoxy-1,1'-biphenyl (14g):** 3,3',5,5'-tetra(4-fluorophenyl)-2,2',6,6'-tetramethoxybiphenyl **14g** was prepared

according to the general procedure for synthesis of 3,3',5,5'-tetraphenyl-2,2',6,6'-tetramethoxybiphenyl **14e** by using 4-fluorophenylboronic acid (22.8 g, 163.0 mmol), 3,3',5,5'-tetraiodo-2,2',6,6'-tetramethoxybiphenyl **2** (10.6 g, 13.6 mmol). Purification by flash chromatography gave **14g** as a white solid in 80% yield (7.1 g).  $^1\text{H}$  NMR (400 MHz,  $\text{CDCl}_3$ )  $\delta$  7.65-7.60 (m, 8 H), 7.38 (s, 2 H), 7.17-7.11 (m, 8 H), 3.40 (s, 12 H);  $^{19}\text{F}$  NMR (376 MHz,  $\text{CDCl}_3$ )  $\delta$  115.9;  $^{13}\text{C}$  NMR (100 MHz,  $\text{CDCl}_3$ )  $\delta$  163.3, 160.9, 155.6, 134.40, 134.38, 132.3, 130.63, 130.54, 129.6, 124.2, 115.4, 115.1, 60.3; IR (film):  $\nu$  1586, 1461, 1420, 1055  $\text{cm}^{-1}$ ; HRMS ( $\text{ES}^+$ ) calcd for  $\text{C}_{40}\text{H}_{31}\text{F}_4\text{O}_4$   $[\text{M}+\text{H}]^+$  651.2158, found 651.2186.

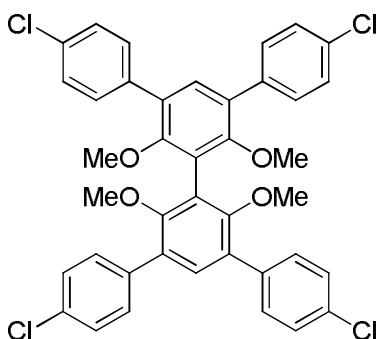


**Synthesis of 3,3',5,5'-tetra(4-fluorophenyl)-1,1'-biphenyl -2,2',6,6'-tetraol (**17g**):**

Tetraol **17g** was prepared according to the general procedure using 3,3',5,5'-tetra(4-fluorophenyl)-2,2',6,6'-tetramethoxybiphenyl (6.6 g, 10.2 mmol) **14g** and boron triboromide (7.7 mL, 81.0 mmol). Purification by recrystallization from hexanes gave **17g** as a white solid in 98% yield (6.0 g).  $^1\text{H}$  NMR (400 MHz, acetone)  $\delta$  7.71 (td,  $J_1 = 7.5$  Hz,  $J_2 = 1.2$  Hz, 8 H), 7.66 (s, 4 H), 7.31 (s, 2 H), 7.16 (td,  $J_1 = 7.5$  Hz,  $J_2 = 1.2$  Hz, 8 H);  $^{19}\text{F}$  NMR (376 MHz, acetone)  $\delta$  113.5;  $^{13}\text{C}$  NMR (100 MHz, acetone)  $\delta$  163.0, 160.6, 153.5, 135.40, 135.37, 132.85, 132.80, 131.50, 131.43, 131.41, 120.8, 114.9, 114.7, 107.2; IR (film):  $\nu$  3526, 1593, 1458, 1157, 1018  $\text{cm}^{-1}$ ; HRMS ( $\text{ES}^+$ ) calcd for  $\text{C}_{36}\text{H}_{23}\text{F}_4\text{O}_4$   $[\text{M}+\text{H}]^+$  595.1532, found 595.1545.

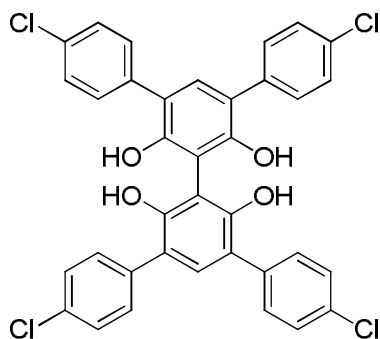


**Synthesis of 3,3',5,5'-tetra(4-fluorophenyl)-1,1'-biphenyl-2,2',6,6'-tetrakis(dipyrrolylphosphoramidite) (7):** Ligand **7** was prepared according to the general procedure using 3,3',5,5'-tetra(4-fluorophenyl)biphenyl-2,2',6,6'-tetraol **17g** (5.0 g, 8.4 mmol) and chlorodipyrrolylphosphine (7.5 g, 37.0 mmol). Purification by recrystallization from hexanes gave **7** as a white solid in 31% yield (3.2 g).  $^1\text{H}$  NMR (400 MHz,  $\text{CDCl}_3$ )  $\delta$  7.11 (s, 2 H), 7.09-6.97 (m, 8 H), 6.87-6.76 (m, 8 H), 6.54 (brs, 16 H), 6.11 (t,  $J = 1.5$  Hz, 16 H);  $^{19}\text{F}$  NMR (470 MHz,  $\text{CDCl}_3$ )  $\delta$  118.6;  $^{13}\text{C}$  NMR (100 MHz,  $\text{CDCl}_3$ )  $\delta$  163.6, 161.2, 149.59, 149.52, 134.9, 132.17, 132.14, 131.13, 131.05, 130.7, 120.76, 120.71, 120.68, 115.2, 115.0, 112.0; IR (film):  $\nu$  1453, 1152, 1011  $\text{cm}^{-1}$ ;  $^{31}\text{P}$  NMR (162 MHz,  $\text{CDCl}_3$ )  $\delta$  106.6; HRMS ( $\text{ES}^+$ ) calcd for  $\text{C}_{68}\text{H}_{51}\text{F}_4\text{N}_8\text{O}_4\text{P}_4$   $[\text{M}+\text{H}]^+$  1243.2920, found 1243.2955.



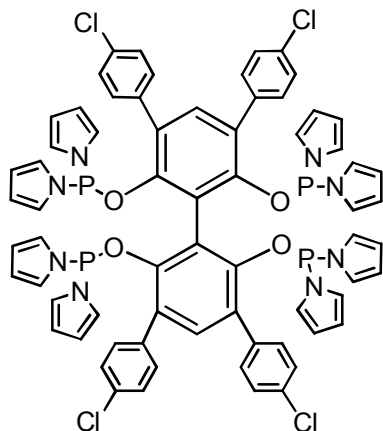
**Synthesis of 3,3',5,5'-tetra(4-chlorophenyl)-2,2',6,6'-tetramethoxy-1,1'-biphenyl (14h):** A mixture of compound **13** (0.5 g, 0.64 mmol), 4-chlorophenyl boronic acid (0.8 g,

5.12 mmol), Pd (PhPh<sub>3</sub>)<sub>4</sub> (0.148 g, 0.128 mmol), and K<sub>2</sub>CO<sub>3</sub> (0.706 g, 5.12 mmol) in dioxane (10 mL) was stirred under N<sub>2</sub> for 24 h at 85 °C. The resulting reaction mixture was diluted by 50 mL water, extracted with EtOAc (3×75 mL). The organic layers were combined, and then dried with MgSO<sub>4</sub> and concentrated to remove solvent. The solid residue was subjected to silica gel flash chromatography (10% DCM in hexane), afforded compound **14h** as white solid (0.44 g, 95% yield). <sup>1</sup>H NMR (400 MHz, CDCl<sub>3</sub>) δ 7.555 (d, J=8.4 Hz, 8H), 7.394 (d, J=8.4 Hz, 8H), 7.346 (s, 2H), 3.363 (s, 12H); <sup>13</sup>C NMR (100MHz, CDCl<sub>3</sub>) δ 156.0, 137.0, 133.3, 132.4, 130.5, 129.6, 128.8, 124.4, 60.7.

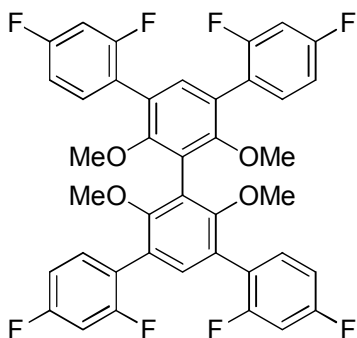


**Synthesis of 3,3',5,5'-tetra(4-chlorophenyl)-1,1'-biphenyl-2,2',6,6'-tetraol (17h):** To a 250 mL Schlenk flask was added compound **14h** (1.75 g, 2.44 mmol) and CH<sub>2</sub>Cl<sub>2</sub> (50 mL). The resulting solution was cooled to -78 °C in a dry ice/acetone bath. To the cooled solution was added boron tribromide (1.05 mL, 10.8 mmol) dropwise. The reaction mixture was allowed to warm to room temperature and stirred for 5 h. After cooled to 0 °C, water (50 mL) was added dropwise to quench the reaction. The organic phase was separated and the aqueous phase was extracted with ether (3 x 50 mL). The combined organic layers was dried over Na<sub>2</sub>SO<sub>4</sub> and concentrated under reduced pressure. The crude product was purified by recrystallization from methanol to give the title compound as white solid (1.4 g, 88%). <sup>1</sup>H NMR (400 MHz, DMSO) δ 8.099 (s, 4H), 7.610 (dd, J<sub>1</sub>=6.8

Hz,  $J_2=2.0$  Hz, 8H), 7.438 (dd,  $J_1=6.8$  Hz,  $J_2=2.0$  Hz, 8H), 7.163 (s, 2H);  $^{13}\text{C}$  NMR (100MHz, DMSO)  $\delta$  153.1, 137.9, 131.4, 131.0, 130.6, 127.9, 120.0, 109.7.

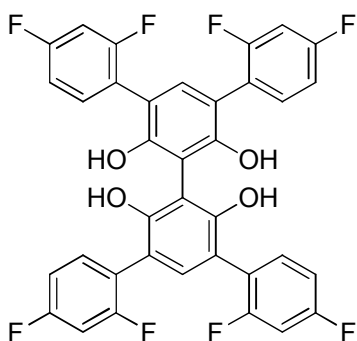


**Synthesis of 3,3',5,5'-tetra(4-chlorophenyl)-1,1'-biphenyl-2,2',6,6'-tetrakis(dipyrrolylphosphoramidite) (8):** To a solution of chlorodipyrrolylphosphine (8.8 mmol, 1.75 g) in THF (10 mL) was added dropwise a solution of triethylamine (1.4 mL) in THF (10 mL) and a solution of compound **17h** (1.321 g, 2 mmol) in THF (30 mL) at room temperature. The  $\text{Et}_3\text{N}\cdot\text{HCl}$  salts were formed immediately after the addition. The reaction mixture was stirred over night (~ 12 h) at room temperature. The  $\text{Et}_3\text{N}\cdot\text{HCl}$  salts were then filtered off and the solvent was removed under vacuum. The crude product was recrystallized from hexane to afford the pure ligand as white solid (0.51 g, 20%).  $^1\text{H}$  NMR (400 MHz,  $\text{CDCl}_3$ )  $\delta$  7.069 (s, 2H), 7.066 (d,  $J=8.5$  Hz, 8H), (s, 2H), 6.893 (d,  $J=8.5$  Hz, 8H), 6.517 (s, 16H), 6.098 (t,  $J=2.1$  Hz, 16H);  $^{13}\text{C}$  NMR (100MHz,  $\text{CDCl}_3$ )  $\delta$  149.6, 134.6, 134.5, 134.0, 130.7, 130.6, 128.4, 120.8, 120.3, 112.1;  $^{31}\text{P}$  NMR (162MHz,  $\text{CDCl}_3$ )  $\delta$  105.7; HRMS ( $\text{ES}^+$ ) calcd for  $\text{C}_{68}\text{H}_{51}\text{N}_8\text{O}_4\text{P}_4\text{Cl}_4$   $[\text{M}]^+$  1307.1738, found 1307.1609.



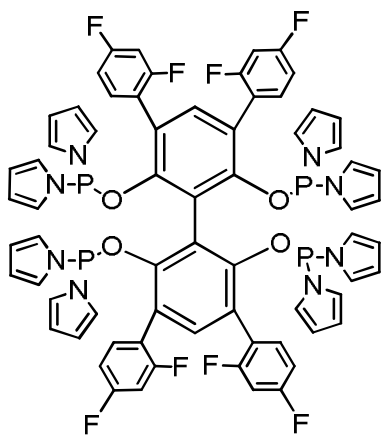
**Synthesis of 3,3',5,5'-tetra(2,4-difluorophenyl)-2,2',6,6'-tetramethoxy-1,1'-biphenyl**

**(14i):** A mixture of compound **13** (5 g, 6.4 mmol), 2,4-difluorophenyl boronic acid (6 g, 38 mmol), Pd(PPh<sub>3</sub>)<sub>2</sub>Cl<sub>2</sub> (0.89 g, 1.28 mmol), and K<sub>2</sub>CO<sub>3</sub> (7.06 g, 51.2 mmol) in dioxane (50 mL) was stirred under N<sub>2</sub> for 24 h at 85 °C. The resulting reaction mixture was diluted by 100 mL water, extracted with EtOAc (3×100 mL). The organic layers were combined, passed through a silica plug and then dried with MgSO<sub>4</sub> and concentrated to remove solvent. The solid residue was recrystallized from DCE to afford compound **14i** as white solid (4.2 g, 90% yield). <sup>1</sup>H NMR (400 MHz, DMSO) δ 7.648 (q, J=8.0 Hz, 4H), 7.368 (dt, J<sub>1</sub>=9.8Hz, J<sub>2</sub>=2.6, 4H), 7.359 (s, 2H), 3.323 (s, 12H); <sup>13</sup>C NMR (100MHz, CDCl<sub>3</sub>) δ 162.6 (d, J<sub>CF</sub>=247.4), 160.6 (d, J<sub>CF</sub>=250.0), 157.1, 133.4, 132.4 (q, J<sub>CF</sub>=4.7), 123.9, 123.4, 122.1 (dd, J<sub>CF</sub>=16.0, 3.7), 111.2 (dd, J<sub>CF</sub>=21.0, 3.6), 104.1 (t, 122.1 (dd, J<sub>CF</sub>=25.7), 60.6; <sup>19</sup>F NMR (376.5MHz, CDCl<sub>3</sub>) δ -109.6, -111.2.



**Synthesis of 3,3',5,5'-tetra(2,4-difluorophenyl)-1,1'-biphenyl-2,2',6,6'-tetraol (17i):**

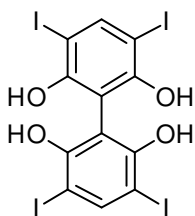
To a 250 mL Schlenk flask was added compound **14i** (4.2g, 5.8 mmol) and CH<sub>2</sub>Cl<sub>2</sub> (50 mL). The resulting solution was cooled to -78 °C in a dry ice/acetone bath. To the cooled solution was added boron tribromide (2.7 mL, 28.6 mmol) dropwise. The reaction mixture was allowed to warm to room temperature and stirred for 5 h. After cooled to 0 °C, water (50 mL) was added dropwise to quench the reaction. The organic phase was separated and the aqueous phase was extracted with EtOAc (3 x 50 mL). The combined organic layers was dried over Na<sub>2</sub>SO<sub>4</sub>, passed through a small pad of silica gel, and concentrated to remove the solvent. The crude product was purified by recrystallization from methanol to give the title compound as white solid (3.8 g, 98%). <sup>1</sup>H NMR (400 MHz, DMSO) δ 8.155 (s, 4H), 7.504 (q, J=8.1Hz, 4H), 7.232 (dt, J<sub>1</sub>=9.9 Hz, J<sub>2</sub>=2.6 Hz, 4H), 7.107 (dt, J<sub>1</sub>=8.7 Hz, J<sub>2</sub>=2.7 Hz, 4H), 6.983 (s, 2H); <sup>13</sup>C NMR (100MHz, DMSO) δ 161.3 (dd, J<sub>CF</sub>=245.0, 11.4), 159.7 (dd, J<sub>CF</sub>=248.1, 12.2), 153.7, 133.6 (dd, J<sub>CF</sub>=9.4, 5.2), 132.6, 122.7, 114.2, 111.1 (dd, J<sub>CF</sub>=20.8, 3.2), 110.1, 103.8 (t, J<sub>CF</sub>=26.3); <sup>19</sup>F NMR (376.5MHz, DMSO) δ -109.3, -112.7.



**Synthesis of 3,3',5,5'-tetra(2,4-difluorophenyl)-1,1'-biphenyl-2,2',6,6'-tetrakis-**

**(dipyrrolylphosphoramidite) (9):** To a solution of chlorodipyrrolylphosphine (8.8 mmol, 1.75 g) in THF (10 mL) was added dropwisely a solution of triethylamine (1.4 mL) in THF

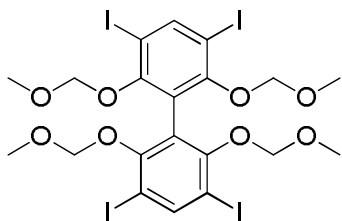
(10 mL) and a solution of compound **17i** (1.333 g, 2 mmol) in THF (30 mL) at room temperature. The Et<sub>3</sub>N·HCl salts were formed immediately after the addition. The reaction mixture was stirred over night (~12 h) at room temperature. The Et<sub>3</sub>N·HCl salts were then filtered off and the solvent was removed under vacuum. The crude product was recrystallized from hexane to afford the pure ligand as off white solid (0.95 g, 36%). <sup>1</sup>H NMR (400 MHz, CDCl<sub>3</sub>) δ 7.168 (s, 2H), 6.706 (dt, J<sub>1</sub>=9.4 Hz, J<sub>2</sub>=2.4 Hz, 4H), 6.638 (m, 4H), 6.554 (m, 4H), 6.530 (s, 16H), 6.079 (t, J=2.1 Hz, 16H); <sup>13</sup>C NMR (100MHz, CDCl<sub>3</sub>) δ 163.2 (dd, J<sub>CF</sub>=250.9, 12.6 Hz), 160.3 (dd, J<sub>CF</sub>=250.0, 12.6 Hz), 151.2, 136.2, 133.1 (dd, J<sub>CF</sub>=10.1, 4.0 Hz), 124.5, 121.0, 120.2, 119.8 (dd, J<sub>CF</sub>=15.1, 3.0 Hz), 112.1, 111.4 (dd, J<sub>CF</sub>=21.1, 4.0 Hz), 104.1 (t, J<sub>CF</sub>=24.7 Hz); <sup>31</sup>P NMR (162MHz, CDCl<sub>3</sub>) δ 105.8; <sup>19</sup>F NMR (376.5MHz, CDCl<sub>3</sub>) δ -108.7, -109.8; HRMS (ES<sup>+</sup>) calcd for C<sub>68</sub>H<sub>47</sub>N<sub>8</sub>O<sub>4</sub>F<sub>8</sub>P<sub>4</sub> [M]<sup>+</sup> 1315.2543, found 1315.2672.



**Synthesis of 3,3',5,5'-tetraiodo-1,1'-biphenyl-2,2',6,6'-tetraol:** To a 250 mL Schlenk flask was added 3,3',5,5'-tetraiodo-2,2',6,6'-tetramethoxy-1,1'-biphenyl (6.4 g, 8.2 mmol). The flask was degassed and charged with nitrogen. To the flask was added CH<sub>2</sub>Cl<sub>2</sub> (40 mL). The resulting solution was cooled to -78 °C in a dry ice/acetone bath. To the cooled solution was added boron tribromide (3.0 mL, 36.0 mmol) dropwisely. The reaction mixture was allowed to warm to room temperature and stirred for additional 5 hours. After cooled to 0 °C, water (50 mL) was added dropwisely to quench the reaction. The organic phase was separated and the aqueous phase was extracted with ethyl acetate (3 x 50 mL).

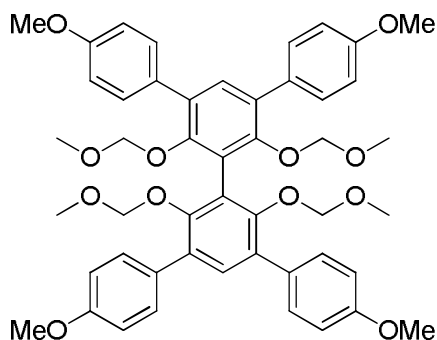


The combined organic layers was dried over  $\text{Na}_2\text{SO}_4$  and concentrated under reduced pressure. The crude product was used in the next step without purification.  $^1\text{H}$  NMR (400 MHz,  $\text{CDCl}_3$ )  $\delta$  8.029 (s, 2H), 5.395 (s, 4H);  $^{13}\text{C}$  NMR (100MHz, DMSO)  $\delta$  155.8, 145.2, 109.8, 75.8.



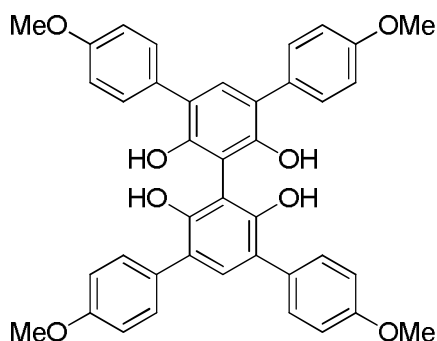
**Synthesis of 3,3',5,5'-tetraiodo-2,2',6,6'-tetra(methoxymethoxy)-1,1'-biphenyl (15):**

To a mixture of THF (15 mL) and NaH (640 mg, 26.6 mmol) in 250 mL round bottom flask in ice bath, a solution of 3,3',5,5'-tetraiodo-1,1'-biphenyl-2,2',6,6'-tetraol (4.0 g, 5.54 mmol) in THF (10 mL) was added dropwisely at  $0^\circ\text{C}$ . After 1 hour, the reaction mixture was allowed to warm to room temperature, and stirred for an additional 3 h. To the resulting reaction mixture, methoxymethyl chloride (2.1g, 26 mmol) in THF (10 mL) was added dropwisely. The reaction mixture was allowed to stir at room temperature for an additional 12 h. TLC indicated a full conversion. The reaction mixture was poured into  $\text{Et}_2\text{O}$  (300 mL) and washed extensively with 3N NaOH (3 $\times$ 75 mL). The organic layers were combined, and then dried with  $\text{MgSO}_4$  and concentrated to give MOM-protected compound **15** as off white solid (4.9 g, 98% yield).  $^1\text{H}$  NMR (400 MHz,  $\text{CDCl}_3$ )  $\delta$  8.289 (s, 2H), 4.914 (s, 8H), 2.987 (s, 12H);  $^{13}\text{C}$  NMR (100MHz,  $\text{CDCl}_3$ )  $\delta$  155.9, 147.4, 126.3, 100.2, 87.8, 56.9.



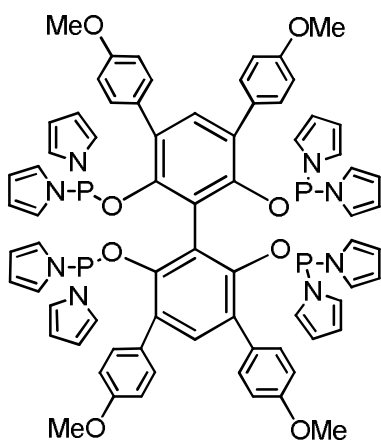
### Synthesis of 3,3',5,5'-tetra(4-methoxyphenyl)-2,2',6,6'-tetra(methoxymethoxy)-

**1,1'-biphenyl (14j):** A mixture of compound **13** (2.95 g, 3.3 mmol), 4-methoxyphenyl boronic acid (5.4 g, 36 mmol), Pd (PhPh<sub>3</sub>)<sub>4</sub> (0.148 g, 0.26 mmol), and K<sub>2</sub>CO<sub>3</sub> (5.1 g, 37 mmol) in dioxane (40 mL) was stirred under N<sub>2</sub> for 24 h at 85 °C. The resulting reaction mixture was diluted by 50 mL water, extracted with EtOAc (3×75 mL). The organic layers were combined, dried with MgSO<sub>4</sub> and passed through a silica gel plug. The solvent was then evaporated to afford compound **14j** as off white solid (2.4 g, 89% yield). <sup>1</sup>H NMR (400 MHz, CDCl<sub>3</sub>) δ 7.536 (d, J=8.8 Hz, 8H), 7.325 (s, 2H), 6.955 (dd, J<sub>1</sub>=6.8 Hz, J<sub>2</sub>=2.0 Hz, 8H), 4.607 (s, 8H), 3.845 (s, 12H), 2.859 (s, 12H); <sup>13</sup>C NMR (100MHz, CDCl<sub>3</sub>) δ 158.9, 152.8, 132.3, 131.3, 131.2, 130.6, 125.1, 114.0, 98.5, 56.3, 55.5.



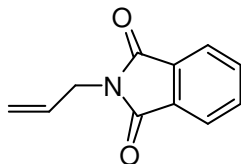
**Synthesis of 3,3',5,5'-tetra(4-methoxyphenyl)-1,1'-biphenyl-2,2',6,6'-tetraol (17j):** To a 250 mL flask was added compound **14j** (1.75g, 5.8 mmol) and CH<sub>2</sub>Cl<sub>2</sub> (16 mL) and MeOH (24 mL), followed by 36% concentrated HCl (16 mL). The reaction mixture was

stirred and refluxed for 6 h. After that, the reaction mixture was concentrated, diluted with 20 mL water and extracted with CH<sub>2</sub>Cl<sub>2</sub> (3 x 50 mL). The combined organic layers were dried over Na<sub>2</sub>SO<sub>4</sub>, passed through a small pad of silica gel. The solvent was then removed under reduced pressure to afford the tetraol product as white solid (1.3 g, 95%). <sup>1</sup>H NMR (400 MHz, CDCl<sub>3</sub>) δ 7.508 (d, J=8.4 Hz, 8H), 7.346 (s, 2H), 6.989 (d, J=8.8 Hz, 8H), 5.428 (s, 4H), 3.848 (s, 12H); <sup>13</sup>C NMR (100MHz, CDCl<sub>3</sub>) δ 159.0, 150.7, 132.9, 130.4, 129.3, 121.5, 114.3, 105.3, 55.4.

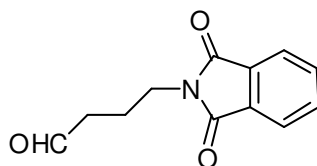


**Synthesis of 3,3',5,5'-tetra(4-methoxyphenyl)-1,1'-biphenyl-2,2',6,6'-tetrakis(dipyrrolylphosphoramidite) (10):** To a solution of chlorodipyrrolylphosphine (8.8 mmol, 1.75 g) in THF (10 mL) was added dropwisely a solution of triethylamine (1.4 mL) in THF (10 mL) and a solution of compound **17j** (1.285 g, 2 mmol) in THF (30 mL) at room temperature. The Et<sub>3</sub>N·HCl salts were formed immediately after the addition. The reaction mixture was stirred over night (~12 h) at room temperature. The Et<sub>3</sub>N·HCl salts were then filtered off and the solvent was removed under vacuum. The crude product was recrystallized from hexane to afford the pure ligand as white solid (0.75 g, 29%). <sup>1</sup>H NMR (400 MHz, CDCl<sub>3</sub>) δ 7.155 (s, 2H), 7.020 (d, J=8.4 Hz, 8H), 6.668 (d, J=8.8 Hz, 8H), 6.510 (s, 16H), 6.061 (t, J=2.0 Hz, 16 H), 3.806 (s, 12H); <sup>13</sup>C NMR (100MHz, CDCl<sub>3</sub>) δ 159.0,

134.8, 130.9, 130.7, 128.9, 121.0, 120.9, 120.8, 113.8, 111.7, 55.3;  $^{31}\text{P}$  NMR (162MHz,  $\text{CDCl}_3$ )  $\delta$  105.7; HRMS ( $\text{ES}^+$ ) calcd for  $\text{C}_{72}\text{H}_{63}\text{N}_8\text{O}_8\text{P}_4$   $[\text{M}]^+$  1291.3719, found 1291.3721.

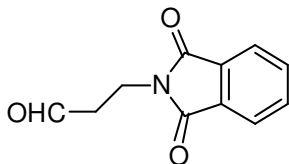


**Synthesis of N-allylphthalimide:** To a 125 mL flask were charged with potassium phthalimide (1.0 g, 5.4 mmol), tetrabutylammonium bromide (30 mg, 0.2 mmol) and DMF (25 mL). Allyl chloride (0.44 mL, 5.4 mmol) was added dropwise over 10 min. The reaction mixture was stirred at room temperature for 12 h. The reaction was quenched by water (20 mL) and was stirred at 0°C for 10 min. The resulting precipitate was filtered off, washed with water and recrystallized from ethanol to yield the desired product as white solid (0.9 g, 90%).  $^1\text{H}$  NMR (400 MHz,  $\text{CDCl}_3$ )  $\delta$  7.861 (m, 2H), 7.725 (m, 2H), 5.894 (m, 1H), 5.255 (dd,  $J_1=16.8$  Hz,  $J_2=1.3$  Hz, 1H), 5.199 (dd,  $J_1=10.5$  Hz,  $J_2=1.3$  Hz, 1H), 4.301 (d,  $J=5.6$  Hz, 2H);  $^{13}\text{C}$  NMR (100MHz,  $\text{CDCl}_3$ )  $\delta$  167.9, 134.0, 132.2, 131.6, 123.3, 117.8, 40.1.



**Synthesis of 4-(1,3-dioxisoindolin-2-yl)butanal:** The typical hydroformylation procedure was followed. After the reaction is over, the solvent was removed under vacuum. The product was obtained after flash column chromatography (silica gel, 25% EtOAc/Hexane) as white solid.  $^1\text{H}$  NMR (400 MHz,  $\text{CDCl}_3$ )  $\delta$  9.779 (t,  $J=1.2$  Hz, 1H), 7.840 (m, 2H), 7.733 (m, 2H), 3.742 (t,  $J=7.2$  Hz, 2H), 2.556 (dt,  $J_1=7.3$  Hz,  $J_2=1.2$  Hz,

2H), 2.030 (m, 2H);  $^{13}\text{C}$  NMR (100MHz,  $\text{CDCl}_3$ )  $\delta$  200.8, 168.3, 134.0, 132.0, 123.2, 41.0, 37.1, 21.1.



**Synthesis of 3-(1,3-dioxoisindolin-2-yl)propanal:** The typical hydroformylation procedure was followed. After the reaction is over, the solvent was removed under vacuum. The product was obtained after flash column chromatography (silica gel, 25% EtOAc/Hexane) as white solid.  $^1\text{H}$  NMR (400 MHz,  $\text{CDCl}_3$ )  $\delta$  9.828 (t,  $J=1.2$  Hz, 1H), 7.837 (m, 2H), 7.731 (m, 2H), 4.035 (t,  $J=7.0$  Hz, 2H), 2.893 (dt,  $J_1=7.1$  Hz,  $J_2=1.4$  Hz, 2H);  $^{13}\text{C}$  NMR (100MHz,  $\text{CDCl}_3$ )  $\delta$  199.4, 168.0, 134.1, 132.0, 123.4, 42.4, 31.7.

## References

1. For recent reviews and monographs, see: a) *Rhodium Catalyzed Hydroformylation*; Claver, C.; van Leeuwen, P. W. N. M., Eds.; Kluwer Academic Publishers: Dordrecht, The Netherlands, 2000. b) Ungvary, F. *Coord. Chem. Rev.* **2005**, *249*, 2946-2961. c) Clarke, M. L. *Curr. Org. Chem.* **2005**, *9*, 701-718. d) Dieguez, M.; Pamies, O.; Claver, C. *Tetrahedron: Asymm.* **2004**, *15*, 2113-2122. e) Breit, B.; Seiche, W. *Synthesis*, **2001**, 1. f) Beller, M.; Cornils, B.; Frohning, C. D.; Kohlpainter, C. W. *J. Mol. Cat. A*, **1995**, *104*, 17.
2. a) Jennerjahn, R.; Piras, I.; Jackstell, R.; Franke, R.; Wiese, K.-D.; Beller, M. *Chem. Eur. J.* **2009**, *15*, 6383. b) Gruenanger, C. U.; Breit, B. *Angew. Chem., Int. Ed.* **2010**, *49*, 967. c) Makado, G.; Morimoto, T.; Sugimoto, Y.; Tsutsumi, K.; Kagawa, N.; Kakiuchi, K. *Adv. Synth. Catal.* **2010**, *352*, 299. d) Dabbawala, A. A.; Jasra, R. V.; Bajaj, H. C. *Catal. Commun.* **2010**, *11*, 616. e) Panda, A. G.; Bhor, M. D.; Ekbote, S. S.; Bhanage, B. M. *Catal. Lett.* **2009**, *131*, 649. f) Liu, W.; Yuan, M.; Fu, H.; Chen, H.; Li, R.; Li, X. *Chem. Lett.* **2009**, *38*, 596. g) Goudriaan, P. E.; Kuil, M.; Jiang, X.-B.; van Leeuwen, P. W. N. M.; Reek, J. N. H. *Dalton Trans.* **2009**, 1801. h) Simaan, S.; Marek, I. *J. Am. Chem. Soc.* **2010**, *132*, 4066. i) Spangenberg, T.; Breit, B.; Mann, A. *Org. Lett.* **2009**, *11*, 261. j) Worthy, A. D.; Gagnon, M. M.; Dombrowski, M. T.; Tan, K. L. *Org. Lett.* **2009**, *11*, 2764. k) Wang, X.; Buchwald, S. J. *Am. Chem. Soc.* **2011**, *133*, 19080.
3. a) Devon, T. J.; Phillips, G. W.; Puckette, T. A.; Stavinocha, J. L.; Vanderbilt, J. J. US Patent 4694109, **1987**. b) Herrmann, W. A.; Kohlpaintner, C. W.; Herdtweck, E.; Kiprof, P. *Inorg. Chem.* **1991**, *30*, 4271. c) Casey, C. P.; Whiteker, G. T.; Melville, M. G.; Lori, L. M.; Gavney, J. A. Jr.; Powell, D. R. *J. Am. Chem. Soc.* **1992**, *114*, 5535. d) Herrmann, W. A.; Schmid, R.; Kohlpaintner, C. W.; Priermeier, T. *Organometallics* **1995**, *14*, 1961. e) Casey, C. P.; Paulsen, E. L.; Beuttenmueller, E. W.; Proft, B. R.; Petrovich, L. M.; Matter, B. A.; Powell, D. R. *J. Am. Chem. Soc.* **1997**, *119*, 11817.
4. a) Kranenburg, M.; van der Burgt, Y. E. M.; Kamer, P. C. J.; van Leeuwen, P. W. N. M. *Organometallics* **1995**, *14*, 3081. b) Van der Veen, L. A.; Boele, M. D.; Bregman, F. R.; Paul, P. C.; Van Leeuwen, P. W. N. M.; Goubitz, K.; Fraanje, J.; Schenk, H.; Bo, C. J. *Am. Chem. Soc.* **1998**, *120*, 11616. c) Carbo, J. J.; Maseras, F.; Bo, C.; Van Leeuwen, P. W. N. M. *J. Am. Chem. Soc.* **2001**, *123*, 7630. d) van der Slot, S. C.; Duran, J.; Luten, J.; Kamer, P. C. J.; van Leeuwen, P. W. N. M. *Organometallics* **2002**, *21*, 3873.
5. Klein, H.; Jackstell, R.; Wiese, K.-D.; Borgmann, C.; Beller, M. *Angew. Chem., Int. Ed.* **2001**, *40*, 3408.
6. Billig, E.; Abatjoglou, A. G.; Bryant, D. R. (UCC) US Patent 4769498, **1988**.
7. Burke, P. M.; Garner, J. M.; Kreutzer, K. A.; Teunissen, A. J. J. M.; Snijder, C. S.; Hansen, C. B. (DSM/Du Pont) PCT Int. Patent WO 97/33854, **1997**.

8. a) Cobley, C. J.; Klosin, J.; Qin, C.; Whiteker, G. T. *Org. Lett.* **2004**, *6*, 3277. b) Cobley, C. J.; Gardner, K.; Klosin, J.; Praquin, C.; Hill, C.; Whiteker, G. T.; Zanotti-Gerosa, A. *J. Org. Chem.* **2006**, *69*, 4031. c) Clark, T. P.; Landis, C. R.; Freed, S. L.; Klosin, J.; Abboud, K. A. *J. Am. Chem. Soc.* **2005**, *127*, 5040. d) Axtell, A. T.; Cobley, C. J.; Klosin, J.; Whiteker, G. T.; Zanotti-Gerosa, A.; Abboud, K. A. *Angew. Chem. Int. Ed.* **2005**, *44*, 5834. e) Lambers-Verstappen, M. M. H.; de Vries, J. G. *Adv. Synth. Cat.* **2003**, *345*, 478.
9. a) Yan, Y.; Zhang, X.; Zhang, X. *J. Am. Chem. Soc.* **2006**, *128*, 16058. b) Yu, S.; Chie, Y.; Guan, Z.; Zhang, X. *Org. Lett.* **2008**, *10*, 3469. c) Yu, S.; Chie, Y.; Guan, Z.; Zou, Y.; Li, W.; Zhang, X. *Org. Lett.* **2009**, *11*, 241. d) Yu, S.; Chie, Y.; Zhang, X. *Adv. Synth. Cat.* **2009**, *351*, 537. e) Yu, S.; Chie, Y.; Zhang, X.; Dai, L.; Zhang, X. *Tetrahedron Lett.* **2009**, *50*, 5575.
10. Davis, T. L.; Walker, J. F. *J. Am. Chem. Soc.* **1930**, *52*, 358.
11. Eilbracht, P.; Schmidt, A. M. *Top. Organomet. Chem.* **2006**, *18*, 65.
12. Cuny, G. D.; Buchwald, S. J. *J. Am. Chem. Soc.* **1993**, *115*, 2066.
13. Patrick, G. L. *An Introduction to Medicinal Chemistry*, 3<sup>rd</sup> ed., Oxford University Press: New York, **2005**.
14. Chen, C.-Y. in *The Art of Process Chemistry*; Yasuda, N., Eds.; Wiley-VCH: Weinheim, German, 2011; pp 117-142.
15. a) Hansch, C.; Leo, A.; Taft, R. W. *Chem. Rev.* **1991**, *91*, 165. b) By a rigid definition,  $\sigma_p$  is not applicable to 2,4-difluoro in Ligand **9**; however, since the 2,4-difluoro groups are remote to the phosphorus coordination center, the value of ( $\sigma_p + \sigma_m$ ) was used to estimate the electron-withdrawing capacity of 2,4-difluoro groups even though this treatment is not accurate.
16. Connors, K. *Chemical Kinetics, the study of reaction rates in solution*, John Wiley & Sons, New York, **1990**.
17. Brown, C. K.; Wilkinson, G. *J. Chem. Soc. A* **1970**, 2753. b) Evans, D.; Osborn, J. A.; Wilkinson, G. *J. Chem. Soc. A* **1968**, 3133. c) Evans, D.; Yagupsky, G.; Wilkinson, G. *J. Chem. Soc. A* **1968**, 2660.
18. Cleij, M.; Archelas, A.; Furstoss, R. *J. Org. Chem.* **1999**, *64*, 5029.
19. Van Wagenen, B.C.; Moe, S.T.; Balandrin, M.F.; DelMar, E.G.; Nemeth, E. F. US Patent 6211244, **2001**.

## Chapter 3 Tetrakisphosphine Ligands for Highly Regioselective

### Hydroformylation of Terminal and Internal Olefins

#### 3.1 Introduction

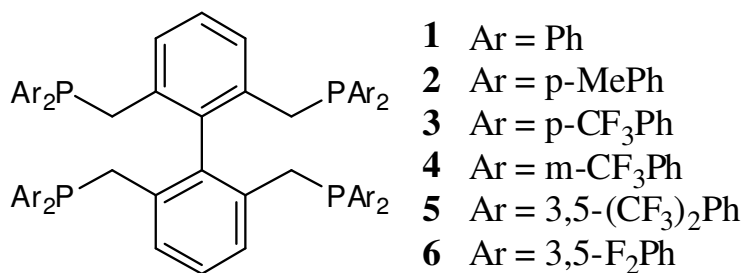
In Chapter 2, we have developed pyrrole based tetrakisphosphoramidite ligands for the regioselective hydroformylation of functionalized olefins, styrene and its derivatives, which showing an exceptionally high regioselectivity towards the formation of linear aldehydes. The structural features of tetrakisphosphoramidite ligands include 1) multiple coordination modes that are able to reduce the formation of unselective catalytic species in the catalytic cycle, 2) the large bite angle of the nine-member chelating complex is capable of forming equatorial-equatorial coordination at the rhodium center that can improve the regioselectivity,<sup>1</sup> and 3) the electron-withdrawing property of *N*-pyrrolylphosphorus moiety that makes the pyrrole based ligands good  $\pi$ -acceptors and thus in general leads to high regioselectivity.<sup>2</sup> These structural features contribute to the high linear selectivity of the olefin hydroformylation that we observed when the tetrakisphosphoramidite ligands were used. Furthermore, our studies on the ligand structural effects indicate that the steric effect is dominating over the electronic effect.

In this chapter, we will report our research on the development of tetrakisphosphine ligands as another efficient ligand systems for highly regioselective hydroformylation of terminal and internal olefins. Particularly, this type of ligand is effective for the hydroformylation at high operating temperatures. For example, the ligands reported in this



chapter afforded greater than 97% linear selectivity for the hydroformylation of 1-octene and 1-hexene at 140 °C. Since hydroformylation reaction at high temperature affords higher reaction rate, from the view of industrial applications, it is desirable to have a regioselective ligand for high temperature hydroformylation. Furthermore, a challenging but commercial important reaction is the hydroformylation of long chained olefins, which will produce aldehydes with high boiling points that require high temperature to distill them out during the production process. This requires the ligands have high stability at high operating temperatures.

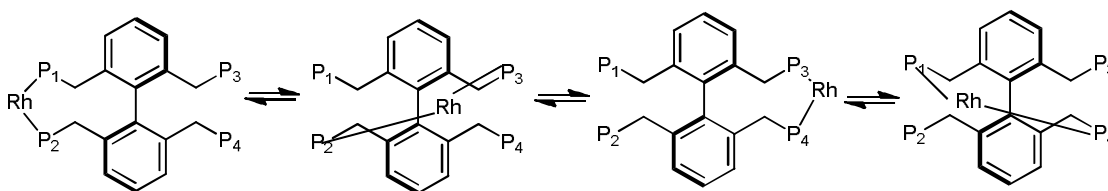
### 3.2 Design of Tetraphosphine Ligands



**Figure 3.1.** Tetraphosphine ligands.

The structures of our new tetraphosphine ligands are depicted in Figure 3.1. Like the tetraphosphoramidite ligands, these ligands are also based on a biphenyl backbone, and have four equivalent symmetric phosphorus groups. The tetraphosphine ligands are expected to work similarly to the tetraphosphoramidite ligands. As illustrated in Scheme 3.1, the tetraphosphine ligands are able to bind to Rh bidentately through a dynamic multiple chelating mode with each phosphine group coming from the different aromatic rings. In this bidentate Rh complex, the existing free phosphorus atoms can effectively increase the local phosphorus concentration around the metal center and hence enhance the

chelating ability. When a phosphine in the bidentate Rh complex dissociates from the metal, any one of the two equivalent phosphines from the same aromatic ring can coordinate to Rh and form the bidentate complex again. Such kind of multidentarity can stabilize the bidentate Rh complex and promote the catalyst longevity at elevated temperatures.<sup>3</sup>



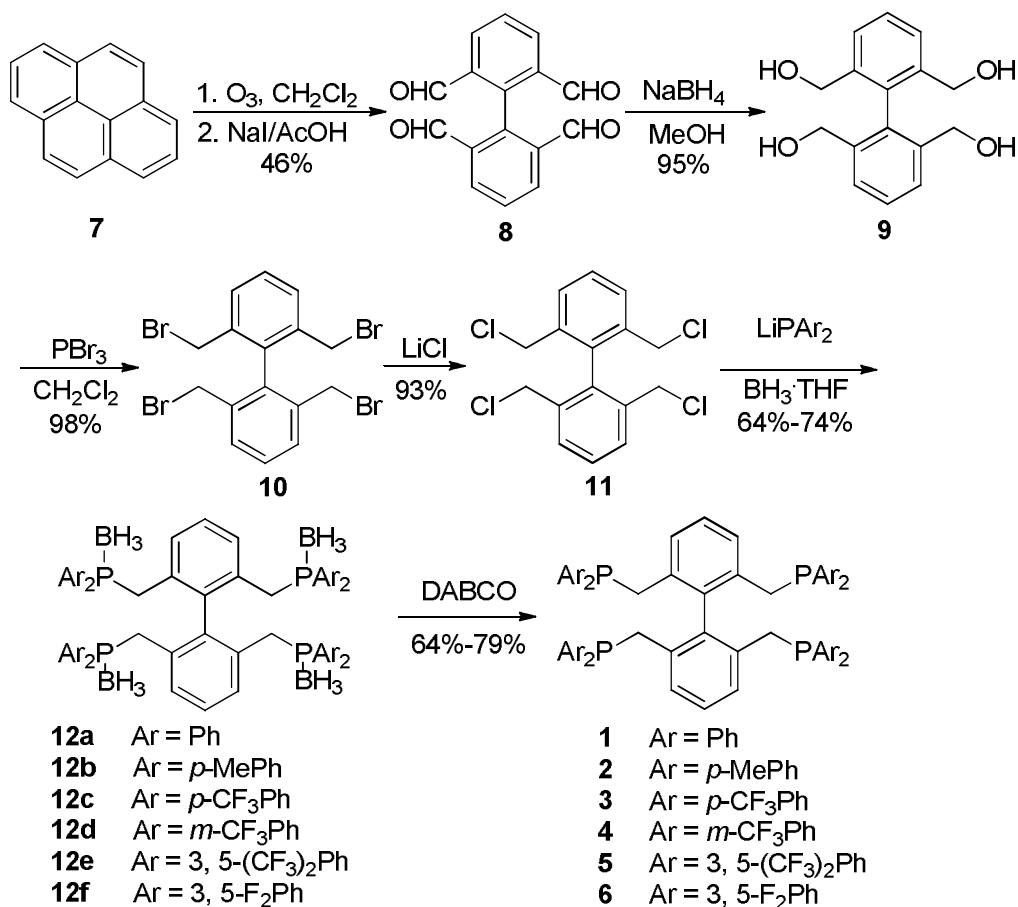
**Scheme 3.1.** Multiple chelating modes of tetraphosphine ligands due to enhanced local phosphorus concentration.

The idea to conceive tetraphosphine ligands in Figure 3.1 is based on the hydroformylation performance of the bisphosphine ligand Bisbi (section 1.1, Figure 1.1), which was developed by Devon and coworkers at Eastman Kodak. Bisbi provided exceptionally high regioselectivity for the hydroformylation of simple terminal olefins.<sup>4</sup> As we illustrated in Scheme 2.2 (Chapter 2, section 2.2), one of the reasons for the eroded regioselectivity in Rh-catalyzed hydroformylation at high temperature is the formation of unselective catalytic species, due to the dissociation of phosphorus ligands from the metal center. Carbonyl monoxide is a strong  $\pi$ -acid and competes to bind to the rhodium center with the phosphorus ligand. And at high temperature the exchange between the ligands also accelerated. To ensure the formation of the selective catalytic species, usually a large excess of monophosphorus ligands are used. The development of bisphosphorus ligands affords higher regioselectivity and less use of the ligand which may partly arising from the formation of the more bulky and robust selective catalytic species. Thus, we envision that

tetraphosphine ligand **1** should afford better regioselectivity at high temperature than its bisphosphine analogue Bisbi because the multiple chelating modes of a tetraphosphine ligand can better stabilize the selective catalytic species and hence enhance the concentration of the selective catalytic species.

### 3.3 Synthesis of Tetraphosphine Ligands

The synthesis of ligands **1** to **6** is shown in Scheme 3.2. Starting from the ozonolysis of pyrene **7**, reduction of biphenyl-2,2',6,6'-tetracarbaldehyde by sodium borohydride, and bromination of 2,2',6,6'-tetrakis(hydroxymethyl)biphenyl, tetrabromide **8** was prepared in high yields.<sup>5</sup> Whereas the literature reported the synthesis of Bisbi by reaction of lithium diphenylphosphine with 2,2'-bisbromomethyl-1,1'-biphenyl in high yield,<sup>4a</sup> the reaction of tetrabromide **10** with lithium diphenyl phosphine gave complex mixture of unidentified products as monitored by *in situ* <sup>31</sup>P NMR spectra. The reactivity of tetrabromide **10** thus showed was very different from its corresponding dibromide, 2,2'-bisbromomethyl-1,1'-biphenyl. To overcome this problem, we transferred tetrabromide **10** to less reactive tetrachloride **11** by the reaction of tetrabromide with LiCl in DMF at room temperature. The tetrachloride **11** was obtained in high yield (93%). We were then pleased to find that the reaction of tetrachloride **11** with lithium diarylphosphine cleanly afforded the desired tetraphosphine as indicated by a single peak in *in situ* <sup>31</sup>P NMR spectra.<sup>6</sup> Since tetraphosphines **1-6** are air-sensitive compounds, they were protected *in situ* with borane for purification. A simple deprotection of the borane with DABCO afforded the desired tetraphosphine ligands **1-6** in 64-79% yields.



**Scheme 3.2.** Synthesis of tetraphosphine ligands **1-6**.

### 3.4 Hydroformylation of Terminal Olefins

#### 3.4.1 Hydroformylation of 1-Hexene and 1-Octene

Hydroformylation of terminal olefins with the new tetraphosphine ligand **1** was then investigated. The hydroformylation reaction was conducted in toluene with 1-octene as the standard substrate and decane as internal standard. The rhodium catalyst was prepared *in situ* by mixing the tetraphosphine ligand **1** with Rh(acac)(CO)<sub>2</sub> in toluene. The substrate catalyst ratio was 2000 and the catalyst concentration was 1.0 mM. The reaction was terminated after 1 h.

The effects of ligand/metal ratio on hydroformylation of terminal olefins with the tetraphosphine ligand **1** were examined. As shown in Table 3.1 (entries 1-4), a slight decrease of both *l:b* ratio and isomerization were observed when the ligand/metal ratio increased from 1:1 to 6:1. The effects of reaction temperature on hydroformylation reaction were also investigated (Table 3.1, entries 3, 5-7). To our delight, only a slight decrease in *l:b* ratio was observed when the reaction temperature increased from 100 °C to 140 °C. As expected, hydroformylation at lower temperatures led to less olefin isomerization. Finally, the effects of CO/H<sub>2</sub> pressure were tested (Table 3.1, entries 3, 8-10). At high CO/H<sub>2</sub> pressure, the regioselectivities were low. The regioselectivities could be increased by lowering the CO/H<sub>2</sub> pressure. The highest regioselectivity (*l:b* ratio = 66.7) was obtained under a CO/H<sub>2</sub> pressure of 5/5 atm. However, high percentage of isomerization was observed under this pressure, indicating low CO/H<sub>2</sub> pressures facilitate the olefin isomerization.

**Table 3.1.** Optimization of Reaction Conditions for the Hydroformylation of 1-Octene.<sup>[a]</sup>

$$n\text{-C}_6\text{H}_{13}\text{CH=CH}_2 \xrightarrow[\text{CO/H}_2]{[\text{Rh}]/\text{ligand } \mathbf{1}} n\text{-C}_6\text{H}_{13}\text{CH}_2\text{CH}_2\text{CHO} + n\text{-C}_6\text{H}_{13}\text{CH=CHCHO}$$

Entry	L/Rh	T (°C)	CO/H <sub>2</sub>	<i>l:b</i> <sup>[b]</sup>	Linear <sup>[c]</sup>	Iso. <sup>[d]</sup>	TON <sup>[e]</sup>
			(atm)		(%)	(%)	
1	1:1	100	10/10	53.7	98.2	7.9	1.8 x10 <sup>3</sup>
2	2:1	100	10/10	53.4	98.2	7.3	1.8 x10 <sup>3</sup>
3	4:1	100	10/10	50.5	98.1	5.6	1.8 x10 <sup>3</sup>

4	6:1	100	10/10	48.9	98.0	5.6	1.8 x10 <sup>3</sup>
5	4:1	140	10/10	45.2	97.8	6.5	1.8 x10 <sup>3</sup>
6	4:1	120	10/10	49.8	98.0	5.8	1.8 x10 <sup>3</sup>
7	4:1	80	10/10	34.2	97.2	3.4	1.4 x10 <sup>3</sup>
8	4:1	100	30/30	16.5	94.3	2.9	1.2 x10 <sup>3</sup>
9	4:1	100	20/20	22.3	95.7	3.0	1.2 x10 <sup>3</sup>
10	4:1	100	5/5	66.7	98.5	17.3	1.6 x10 <sup>3</sup>

<sup>[a]</sup>S/C = 2000, [Rh] = 1.0 mM, reaction time = 1 h, toluene as solvent, decane as internal standard. <sup>[b]</sup>Linear/branched ratio, determined based on GC. <sup>[c]</sup>Percentage of linear aldehyde in all aldehydes. <sup>[d]</sup>Isomerization to internal olefins. <sup>[e]</sup>Turnover number, determined based on GC.

For comparison, bisphosphine ligand Bisbi was employed in the hydroformylation of terminal olefins under the same reaction conditions. The results are summarized in Table 3.2. It was clearly showed that tetraphosphine ligand **1** always afforded higher regioselectivity than bisphosphine ligand Bisbi under the same reaction conditions. It should be noted that, at high temperature, dramatic decrease of regioselectivity and high percentage of isomerization has been observed with bisphosphine ligand Bisbi (Table 3.2, entries 1-2, 7-8). For example, in the hydroformylation of 1-octene, the regioselectivity was significant low (*l:b* ratio = 2.4) and isomerization was significant high (24%) at 140 °C with Bisbi as ligand; whereas the regioselectivity remained high (*l:b* ratio = 45.2) and isomerization remained low (6.5%) using tetraphosphine ligand **1** at the same temperature.

**Table 3.2.** Comparison of Tetrphosphine and Bisphosphine Ligands.<sup>[a]</sup>

$$\text{R}-\text{CH}=\text{CH}_2 \xrightarrow[\text{CO/H}_2]{[\text{Rh}]/\text{ligand}} \text{R}-\text{CH}(\text{CH}_3)-\text{CHO} + \text{R}-\text{CH}_2-\text{CH}_2-\text{CHO}$$

Entry	substrate	T (°C)	Ligand	<i>l</i> : <i>b</i> <sup>[b]</sup>	Linear <sup>[c]</sup> (%)	Iso. <sup>[d]</sup> (%)	TON <sup>[e]</sup>	TOF <sup>[f]</sup> (h <sup>-1</sup> )
1	1-octene	140	<b>1</b>	45.2	97.8	6.5	1.8x10 <sup>3</sup>	9.3 x10 <sup>3</sup>
2	1-octene	140	Bisbi	2.4	70.6	24	1.5 x10 <sup>3</sup>	6.2 x10 <sup>3</sup>
3	1-octene	120	<b>1</b>	49.8	98.0	5.8	1.8 x10 <sup>3</sup>	7.3 x10 <sup>3</sup>
4	1-octene	120	Bisbi	29.5	96.7	8.7	1.8 x10 <sup>3</sup>	5.7 x10 <sup>3</sup>
5	1-octene	100	<b>1</b>	50.5	98.1	5.6	1.8 x10 <sup>3</sup>	2.5 x10 <sup>3</sup>
6	1-octene	100	Bisbi	45.2	97.8	6.7	1.6 x10 <sup>3</sup>	3.4 x10 <sup>3</sup>
7	1-hexene	140	<b>1</b>	43.8	97.8	7.7	1.8 x10 <sup>3</sup>	9.5 x10 <sup>3</sup>
8	1-hexene	140	Bisbi	4.9	83.1	20	1.6 x10 <sup>3</sup>	8.7 x10 <sup>3</sup>
9	1-hexene	120	<b>1</b>	48.5	98.0	7.1	1.8 x10 <sup>3</sup>	6.6 x10 <sup>3</sup>
10	1-hexene	120	Bisbi	35.8	97.3	9.1	1.8 x10 <sup>3</sup>	6.0 x10 <sup>3</sup>
11	1-hexene	100	<b>1</b>	48.6	98.0	6.6	1.8 x10 <sup>3</sup>	3.3 x10 <sup>3</sup>
12	1-hexene	100	Bisbi	43.2	97.7	9.4	1.7 x10 <sup>3</sup>	2.6 x10 <sup>3</sup>

<sup>[a]</sup> S/C = 2000, [Rh] = 1.0 mM, ligand/Rh ratio = 4:1, CO/H<sub>2</sub> = 10/10 atm, reaction time = 1 h, toluene as solvent, decane as internal standard. <sup>[b]</sup> Linear/branched ratio, determined based on GC. <sup>[c]</sup> Percentage of linear aldehyde in all aldehydes. <sup>[d]</sup> Isomerization to internal olefins. <sup>[e]</sup> Turnover number, determined based on GC. <sup>[f]</sup> Turnover frequency, determined based on GC, reaction time = 10 min.

At lower temperature (100 °C), both tetrphosphine **1** and bisphosphine Bisbi afford high regioselectivity and low isomerization with *l*:*b* ratios >40 and isomerization < 10 % (Table 3.2, entries 5-6, 11-12). The *similar* performances with both ligands at low

temperature and dramatic difference at high temperature suggest that the better performance at high temperature with ligand **1** is indeed due to the enhanced chelating ability of tetraphosphine ligands **1**. This result is also important from the practical point of view because highly regioselective hydroformylation can be carried out now at higher temperature to gain high reaction rate.

### 3.4.2 Ligands Effects on the Hydroformylation of 1-Hexene and 1-Octene

Ligands **2-6** were varied with the introduction of different substituents on the diphenyl moiety of ligand **1**. These ligands were subjected to the rhodium-catalyzed hydroformylation of 1-hexene and 1-octene under different temperatures, and the results are listed in Tables 3.3 and 3.4, respectively. It was found that the introduction of different substituents did affect the regioselectivity of the aldehydes and activity of the catalytic system. In both reactions, ligands **3-6** with electron-withdrawing substituents showed higher activity than ligand **2** with the electron-donating group. As for the regioselectivity, the trend for those ligands was not that obvious. While ligand **6** afforded the best linear to branch ratio at 140 °C for 1-hexene (87.9), ligand **5** was found somewhat better than **6** for 1-octene under similar reaction conditions (52.4 versus 47.4, Table 3.3, entry 1, and Table 3.4, entries 1 and 11). The position of the substituents may also exert some influence on the regioselectivity. Ligand **3** with a CF<sub>3</sub> substituent at *para* position of the diphenylphosphine moiety gave higher linear to branch ratio for the hydroformylation of the 1-hexene than the corresponding ligand **4** with a CF<sub>3</sub> substituent at the *meta* position (Table 3.3, entries 4 and 9). Apparently, ligand **4** has a larger steric effect compared with ligand **3**. This effect was reversed when 1-octene was examined (Table 3.4, entries 4 and 9). With one more CF<sub>3</sub> substituent at the *meta* position of the diphenylphosphine moiety, the increase of the



regioselectivity for 1-octene was continued whereas the value for 1-hexene decreased (Table 3.3, entry 11 and Table 3.4, entry 11). From those results, it clearly showed that the subtle changes in the chain length resulted in a new choice of suitable ligand.

**Table 3.3.** Hydroformylation of 1-hexene with tetraphosphine ligands **2-6**.<sup>[a]</sup>

$$n\text{-C}_4\text{H}_9\text{CH=CH}_2 \xrightarrow[\text{CO/H}_2]{[\text{Rh}]/\text{ligand}} n\text{-C}_4\text{H}_9\text{CH(CH}_3\text{)CHO} + n\text{-C}_4\text{H}_9\text{CH}_2\text{CH}_2\text{CHO}$$

Entry	Ligand	T (°C)	<i>l:b</i> <sup>[b]</sup>	Linear <sup>[c]</sup> (%)	Iso. <sup>[d]</sup> (%)	TON <sup>[e]</sup>	TOF <sup>[f]</sup> (h <sup>-1</sup> )
1	<b>6</b>	140	87.9	98.9	4.8	1.8 x 10 <sup>3</sup>	1.1 x 10 <sup>4</sup>
2	<b>6</b>	120	92.1	98.9	4.6	1.8 x 10 <sup>3</sup>	7.6 x 10 <sup>3</sup>
3	<b>6</b>	100	125.9	99.2	4.2	1.8 x 10 <sup>3</sup>	5.7 x 10 <sup>3</sup>
4	<b>3</b>	140	64.1	98.5	5.1	1.8 x 10 <sup>3</sup>	9.9 x 10 <sup>3</sup>
5	<b>3</b>	120	87.3	98.9	4.8	1.8 x 10 <sup>3</sup>	7.3 x 10 <sup>3</sup>
6	<b>3</b>	100	95.7	98.9	4.5	1.8 x 10 <sup>3</sup>	5.1 x 10 <sup>3</sup>
7	<b>2</b>	140	41.3	97.6	7.4	1.4 x 10 <sup>3</sup>	6.1 x 10 <sup>3</sup>
8	<b>2</b>	120	44.8	97.8	7.2	1.1 x 10 <sup>3</sup>	5.3 x 10 <sup>3</sup>
9	<b>4</b>	140	32.4	97.0	8.7	1.8 x 10 <sup>3</sup>	1.1 x 10 <sup>4</sup>
10	<b>4</b>	120	55.2	98.2	6.5	1.8 x 10 <sup>3</sup>	9.9 x 10 <sup>3</sup>
11	<b>5</b>	140	28.8	96.6	8.8	1.8 x 10 <sup>3</sup>	1.6 x 10 <sup>4</sup>
12	<b>5</b>	120	49.3	98.0	6.6	1.8 x 10 <sup>3</sup>	1.3 x 10 <sup>4</sup>

<sup>[a]</sup>S/C = 2000, [Rh] = 1.0 mM, reaction time = 1 h, toluene as solvent, decane as internal standard. <sup>[b]</sup>Linear/branched ratio, determined based on GC. <sup>[c]</sup>Percentage of linear aldehyde in all aldehydes. <sup>[d]</sup>Isomerization to internal olefins. <sup>[e]</sup>Turnover number, determined based on GC.

**Table 3.4.** Hydroformylation of 1-octene with tetraphosphine ligands **2-6**.<sup>[a]</sup>

$$n\text{-C}_6\text{H}_{13}\text{CH=CH}_2 \xrightarrow[\text{CO/H}_2]{[\text{Rh}]/\text{ligand}} n\text{-C}_6\text{H}_{13}\text{CH}_2\text{CH}_2\text{CHO} + n\text{-C}_6\text{H}_{13}\text{CH(CH}_3\text{)CHO}$$

Entry	Ligand	T (°C)	<i>l:b</i> <sup>[b]</sup>	Linear <sup>[c]</sup> (%)	Iso. <sup>[d]</sup> (%)	TON <sup>[e]</sup>	TOF <sup>[f]</sup> (h <sup>-1</sup> )
1	<b>6</b>	140	47.4	97.9	5.7	1.9 x 10 <sup>3</sup>	1.0 x 10 <sup>4</sup>
2	<b>6</b>	120	53.7	98.2	5.4	1.9 x 10 <sup>3</sup>	9.1 x 10 <sup>3</sup>
3	<b>6</b>	100	77.9	98.7	4.9	1.8 x 10 <sup>3</sup>	7.4 x 10 <sup>3</sup>
4	<b>3</b>	140	17.9	94.7	7.1	1.9 x 10 <sup>3</sup>	9.7 x 10 <sup>3</sup>
5	<b>3</b>	120	33.5	97.1	6.8	1.9 x 10 <sup>3</sup>	7.9 x 10 <sup>3</sup>
6	<b>3</b>	100	63.2	98.4	5.2	1.9 x 10 <sup>3</sup>	5.3 x 10 <sup>3</sup>
7	<b>2</b>	140	24.4	96.0	7.7	1.6 x 10 <sup>3</sup>	6.3 x 10 <sup>3</sup>
8	<b>2</b>	120	38.9	97.5	7.4	1.2 x 10 <sup>3</sup>	5.5 x 10 <sup>3</sup>
9	<b>4</b>	140	42.8	97.7	5.4	1.9 x 10 <sup>3</sup>	1.2 x 10 <sup>4</sup>
10	<b>4</b>	120	67.3	98.5	4.5	1.9 x 10 <sup>3</sup>	9.1 x 10 <sup>3</sup>
11	<b>5</b>	140	52.4	98.1	5.6	1.9 x 10 <sup>3</sup>	1.4 x 10 <sup>4</sup>
12	<b>5</b>	120	64.1	98.4	5.1	1.8 x 10 <sup>3</sup>	1.1 x 10 <sup>4</sup>

<sup>[a]</sup>S/C = 2000, [Rh] = 1.0 mM, reaction time = 1 h, toluene as solvent, decane as internal standard. <sup>[b]</sup>Linear/branched ratio, determined based on GC. <sup>[c]</sup>Percentage of linear aldehyde in all aldehydes. <sup>[d]</sup>Isomerization to internal olefins. <sup>[e]</sup>Turnover number, determined based on GC.

### 3.4.3 Summary

In summary, a series of various substituted tetraphosphine ligands **1-6**, have been designed, synthesized and applied in the Rhodium-catalyzed hydroformylation of terminal

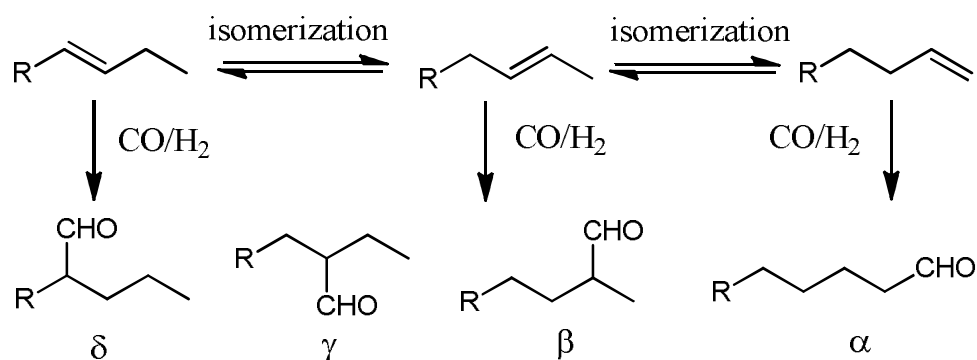
olefins. Compared with the commonly observed low regioselectivity at high temperature when other bisphosphine analogues were used, the high performance achieved by these tetraphosphine ligands is remarkable. The steric and electronic effects of substituents on diarylphosphine moiety have also been examined. The ligands with electron-withdrawing substituents showed better catalytic activity than the ligand with an electron-donating group. The electronic effect on the regioselectivity is not clear. The steric effect of ligand is also observed. The ligand with a substituent at the *meta* position afforded faster reaction rate than the ligand with the same substituent at the *para* position. However, the steric effect on the regioselectivity is depended on the terminal olefin studied.

### 3.5 Hydroformylation of Internal Olefins

Low-cost olefin feedstocks with mixtures of both internal and terminal alkenes are preferred starting materials in large scale hydroformylation process. For example, Raffinate II is an economical feedstock, which is one effluent from the steam cracking process and consists of ca. 11% 1-butene/isobutene and 42% *trans*- and *cis*-2-butene.<sup>7</sup> While it is a well established process for the hydroformylation of terminal olefins, the development of regioselective hydroformylation of internal olefins to form linear aldehydes in a commercially acceptable reaction rate is quite challenging. Over the last decade, only a few catalysts have been reported to show high regioselectivity with a decent reaction rate for the hydroformylation of internal olefins. These catalyst include van Leeuwen's Xantphos derivatives (linear to branch ratio (*l:b*) = 9.5 for 2-octene),<sup>8</sup> Beller's Naphos-type ligands (*l:b* = 10.1 for 2-octene and up to 99:1 with its sulfonated derivatives in a biphasic system),<sup>9</sup> Börner's acylphosphite ligands (*l:b* = 2.2 for a mixture of octene

isomers),<sup>10</sup> and bulky phosphite ligands of UCC<sup>11</sup> ( $l:b = 19$  and  $17$  for 2-hexene and 2-octene, respectively) and DuPont/DSM ( $l:b = 35$  for 2-hexene).<sup>12</sup>

The hydroformylation of an internal olefin is depicted in Scheme 3.3. The hydroformylation of an internal to olefin form a terminal aldehyde is complicated with the isomerization of the internal double bond. To obtain highly linear selective terminal aldehyde, the double bond of an internal olefin must migrate to the end. This sets two kinetic requirements: 1) the isomerization of an internal olefin must be faster than its hydroformylation, and 2) the hydroformylation of a terminal olefin must be faster than the corresponding internal olefins. Otherwise, branched aldehydes will be produced. Therefore, having catalysts that can differentiate these reaction rates are crucial for obtaining high turnover numbers of linear aldehydes from internal olefins. Such requirements make necessary a finely tuning of catalyst and reaction conditions to maximize the linear selectivity.



**Scheme 3.3.** Isomerization and hydroformylation of an internal olefin.

### 3.5.1 Optimization of Hydroformylation Conditions

In this section, the hydroformylation of internal olefins was studied using Rh/tetraphosphine complex as the catalyst. In our initial study, 2-hexene was used as the model substrate and ligand **6** was tested first. The catalyst complex was prepared *in situ* by mixing the ligand and Rh(acac)(CO)<sub>2</sub> in toluene. Even that we did not intend to fully optimize the reaction conditions at this stage, several important reaction parameters, such as ligand to Rh ratio (L/Rh), temperature and CO/H<sub>2</sub> pressure, were tested for their influences on the regioselectivity. Under the conditions listed in Table 3.5, as we expected, the catalyst smoothly converted 2-hexene to the corresponding aldehydes with the linear aldehyde as the main product. The pressure effect was significant (Table 3.5, entries 1-4). As CO/H<sub>2</sub> pressure increased from 2.5/2.5 to 20/20, the linear to branch ratio decreased from 36.5 to 8.6, and the turnover number (TON) slightly decreased from 330 to 280. The temperature effect was also compared (Table 3.5, entries 1, 5 and 7) under otherwise the same conditions. The highest linear selectivity was obtained at 100 °C with an *l:b* ratio of 76.2 and a TON of 230. Moreover, the catalyst was highly selective for the linear aldehyde formation even at 140 °C (Table 3.5, entry 1, *l:b* = 36.5). This is quite desirable since for a long chain olefin, it often requires high temperatures to isolate the product by distillation. The reaction at 120 °C (Table 3.5, entry 5) afforded an *l:b* ratio of 43.9 and a TON of 310, a slight improvement in linear selectivity and a slight decrease in TON compared to those at 140 °C (Table 3.5, entry 1). The effect of L/Rh ratio is also compared (Table 3.5, entries 5, 8 and 9). As L/Rh ratio increased from 2 to 4 to 6, the *l:b* ratio improved from 41.9 to 43.9 to 53.0, and the TON varied from 190 to 310 to 260, respectively. This indicates that sufficient amount of ligand is required to stabilize the catalyst, but an over presence of

ligand will compete the binding site with olefin and therefore slows down the reaction. A fairly good set of reaction conditions is using  $L/Rh = 4$ ,  $120\text{ }^{\circ}\text{C}$  and  $\text{CO}/\text{H}_2 = 2.5/2.5\text{ atm}$  (Table 3.5, entry 5). Under these conditions, the catalyst has good stability, and after 4 h, a total aldehyde yield of 89% (TON = 890) was obtained with an  $l:b$  ratio of 36.0 (Table 3.5, entry 6).

**Table 3.5.** Optimization of reaction conditions for the hydroformylation of 2-hexene with Ligand **6**.<sup>[a]</sup>

Entry	L/Rh	T ( $^{\circ}\text{C}$ )	CO/H <sub>2</sub> (atm)	t (h)	$l:b$ <sup>[b]</sup>	TON <sup>[c]</sup>
1	4	140	2.5/2.5	1	36.5	$3.3 \times 10^2$
2	4	140	5/5	1	26.1	$3.2 \times 10^2$
3	4	140	10/10	1	19.4	$3.1 \times 10^2$
4	4	140	20/20	1	8.6	$2.8 \times 10^2$
5	4	120	2.5/2.5	1	43.9	$3.1 \times 10^2$
6	4	120	2.5/2.5	4	36.0	$8.9 \times 10^2$
7	4	100	2.5/2.5	1	76.2	$2.3 \times 10^2$
8	2	120	2.5/2.5	1	41.9	$1.9 \times 10^2$
9	6	120	2.5/2.5	1	53.0	$2.6 \times 10^2$

<sup>[a]</sup> S/C = 1000,  $\text{Rh}(\text{acac})(\text{CO})_2 = 1.0\text{ mM}$ , toluene as solvent, decane as internal standard. Results determined by GC, average of 3 repeated runs. <sup>[b]</sup> Linear to branch ratio. <sup>[c]</sup> Turnover number.

### 3.5.2 Ligand Effects on the Hydroformylation of 2-Hexene and 2-Octene

After a good set of reaction conditions was identified, the ligands in Figure 3.1 that bearing various electron-donating or electron-withdrawing groups were screened for the hydroformylation of 2-hexene (Table 3.6). We are pleased to find that in all cases, the tetraphosphine ligands afforded >90% linear aldehyde. Ligand **1** is the tetraphosphine without any substituent on the phenyl group. With this ligand, a TON of 770 was obtained with an *l:b* ratio of 27.2 (Table 3.6, entry 1). The *l:b* ratio was dropped to 16.0 when an electron-donating group is attached to the phenyl (ligand **2**, Table 3.6, entry 2). The highest linear selectivity was obtained with ligand **3** that bearing a CF<sub>3</sub> group at the *para* position (*l:b* = 56.4, Table 3.6, entry 3). However, if the CF<sub>3</sub> group is attached at the *meta* positions, very small or no improvement was observed for the linear selectivity (Table 3.6, entries 4 and 5) compared to ligand **1**. Similarly, ligand **6** that bearing two strong electron-withdrawing fluoro groups at the *meta* positions afforded an *l:b* ratio of 36.0, a small improvement in the linear selectivity (Table 3.6, entry 6). Regarding to catalytic activity, all ligands that bearing electron-withdrawing groups (Table 3.6, entries 3-6) showed improved turnover numbers compared to ligand **1**. This observation is consistent with the findings reported by van Leeuwen et al. on the hydroformylation of 1-octene using electronically modified thixantphos ligands.<sup>8d</sup> It is generally reasoned that an electron-withdrawing phosphorus ligand can weaken the  $\pi$  back bonding of rhodium to the carbonyl group and therefore facilitates its dissociation from the rhodium center and enhances the alkene coordination, resulting in an increase in reaction rate. Conversely, a ligand attached with a more electron-donating group will lower the hydroformylation speed. Indeed, this was observed for ligand **2** (Table 3.6, entry 2), which has the lowest

turnover number (TON = 730) in this series of ligands. The highest TON was obtained with ligand **5**, which bearing two CF<sub>3</sub> group at the *meta* positions (Table 3.6, entry 5). For comparison, the bisphosphine ligand (Bisbi) was applied in the hydroformylation of 2-hexene under the same conditions (Table 3.6, entry 7). Clearly, the tetraphosphine ligands have better performance than Bisbi with respect to both catalyst activity and regioselectivity. Matsumoto and Tamura have reported that there is a synergistic effect by applying a mixture of mono and bisphosphine ligands in Rh-catalyzed hydroformylation of terminal olefins.<sup>13</sup> For this reason, benzyl diphenylphosphine (Ph<sub>2</sub>PBn) and a 1:2 mixture of Bisbi and Ph<sub>2</sub>PBn were also tested for the hydroformylation of 2-hexene as control reactions (Table 3.6, entries 8-9), which afforded *l:b* ratios of 0.2 and 0.3, respectively. Therefore, the high regioselectivity afforded by the tetraphosphorus ligands is indeed arising from the enhanced stabilization effect for the selective catalyst intermediate, not from a potential synergistic effect of monodentate and bidentate coordination modes.



**Table 3.6.** Hydroformylation of 2-hexene with ligands **1-6**.<sup>[a]</sup>

Entry	Ligand	<i>l:b</i> <sup>[b]</sup>	Linear <sup>[c]</sup>	TON <sup>[d]</sup>
1	<b>1</b>	27.2	96.5	7.7 x 10 <sup>2</sup>
2	<b>2</b>	16.0	94.1	7.3 x 10 <sup>2</sup>
3	<b>3</b>	56.4	98.3	8.9 x 10 <sup>2</sup>
4	<b>4</b>	27.5	96.5	8.5 x 10 <sup>2</sup>
5	<b>5</b>	25.3	96.2	9.4 x 10 <sup>2</sup>
6	<b>6</b>	36.0	97.3	8.9 x 10 <sup>2</sup>
7	Bisbi <sup>[e]</sup>	1.6	61.5	6.9 x 10 <sup>2</sup>
8	Ph <sub>2</sub> PBn <sup>[f]</sup>	0.2	16.7	6.8 x 10 <sup>2</sup>
9	Bisbi + Ph <sub>2</sub> PBn <sup>[g]</sup>	0.3	23.1	7.1 x 10 <sup>2</sup>

<sup>[a]</sup> S/C = 1000, Rh(acac)(CO)<sub>2</sub> = 1.0 mM, L/Rh = 4, 120 °C, CO/H<sub>2</sub> = 2.5/2.5 atm, time = 4 h, toluene as solvent, decane as internal standard. Results determined by GC, average of 3 repeated runs. <sup>[b]</sup> Linear to branch ratio. <sup>[c]</sup> Percentage of linear aldehyde in all aldehydes. <sup>[d]</sup> Turnover number. <sup>[e]</sup> 2,2'-bis-((diphenylphosphino)methyl)-1,1'-biphenyl. When Bisbi/Rh ratio is varied from 2 to 4 to 8, the *l:b* ratios are 1.4, 1.6 and 1.6, respectively. <sup>[f]</sup> Benzyl diphenylphosphine. <sup>[g]</sup> A 1:2 mixture of Bisbi and Ph<sub>2</sub>PBn.

The hydroformylation of 2-octene with ligands **1** to **6** was followed and the results are listed in Table 3.7. Similar to the results of 2-hexene, in all cases, the tetraphosphine ligands afforded >90% linear aldehyde. The ligand effects on the regioselectivity and catalytic activity are also similar to the trends observed for 2-hexene. All ligands that bearing electron-withdrawing groups (Table 3.7, entries 3-6) showed improved catalytic activity in terms of turnover numbers compared to ligand **1**. The highest linear selectivity was obtained with ligand **3** that bearing a CF<sub>3</sub> group at the *para* position (*l:b* = 46.1, Table 3.7, entry 3).

**Table 3.7.** Hydroformylation of 2-octene with ligands **1-6**.<sup>[a]</sup>

Entry	Ligand	<i>l:b</i> <sup>[b]</sup>	Linear <sup>[c]</sup>	TON <sup>[d]</sup>
1	<b>1</b>	15.5	93.9	6.7 x 10 <sup>2</sup>
2	<b>2</b>	12.4	92.5	5.2 x 10 <sup>2</sup>
3	<b>3</b>	46.1	97.9	9.2 x 10 <sup>2</sup>
4	<b>4</b>	25.1	96.2	9.1 x 10 <sup>2</sup>
5	<b>5</b>	22.8	95.8	9.5 x 10 <sup>2</sup>
6	<b>6</b>	45.9	97.9	8.7 x 10 <sup>2</sup>
7	Bisbi	10.6	91.4	6.3 x 10 <sup>2</sup>

<sup>[a]</sup> S/C = 1000, Rh(acac)(CO)<sub>2</sub> = 1.0 mM, L/Rh = 4, 120 °C, CO/H<sub>2</sub> = 2.5/2.5 atm, time = 4 h, toluene as solvent, decane as internal standard. Results determined by GC, average of 3 repeated runs. <sup>[b]</sup> Linear to branch ratio. <sup>[c]</sup> Percentage of linear aldehyde in all aldehydes. <sup>[d]</sup> Turnover number.

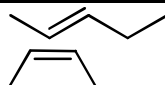

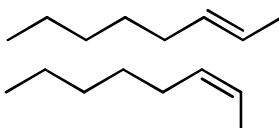
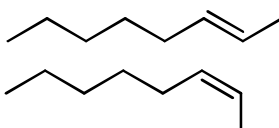
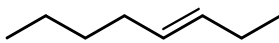
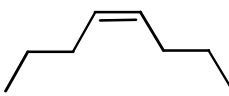

### 3.5.3 Hydroformylation of Other C<sub>5</sub> to C<sub>8</sub> Internal Olefins

Finally, ligand **3** was applied in the isomerization-hydroformylation of a series of olefins with varied chain lengths (Table 3.8). The reactions were screened under the following conditions: S/C = 1000, L/Rh = 4, 125 °C, CO/H<sub>2</sub> = 5/5 atm, toluene as solvent. In all cases, the isomerization and hydroformylation are two dominant reactions, and no or only very small quantities of hydrogenation products were observed. The results showed that ligand **3** is highly selective for the linear hydroformylation of C<sub>5</sub> to C<sub>8</sub> internal olefins with the double bonds at the β positions. For 2-pentene (Table 3.8, entry 1), after 2 h at 125 °C, >99% selectivity to the linear aldehyde was observed with 85% of starting materials converted to either aldehyde or 1-pentene (6%). For 2-octene (Table 3.8, entry 3), 98% selectivity to the linear aldehyde was obtained with 84% starting materials converted to

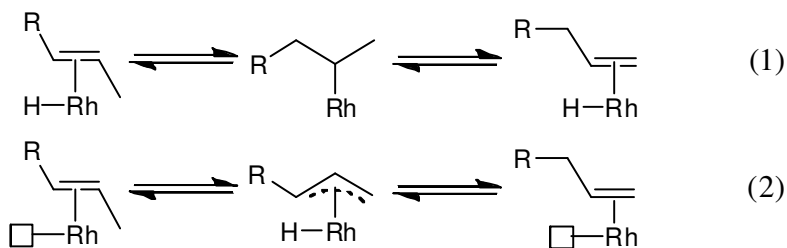
either aldehydes or isomers (16%). After a prolonged reaction time (12 h at 125 °C, Table 3.8, entry 4), the conversion was improved to 98% with 92% linear aldehyde, and the total branched aldehydes increased from 2% to 8%. Olefins with double bonds at the  $\gamma$  positions were also tested (Table 3.8, entries 2 and 5). For 3-hexene, the catalyst is linear selective, affording 88% linear aldehyde, 7%  $\beta$ -branched aldehyde and 5%  $\gamma$ -branched aldehyde (Table 3.8, entry 2). For 3-octene, a mixture of 40% linear, 33%  $\beta$ -branched and 27%  $\gamma$ - and  $\delta$ -branched aldehydes was observed (Table 3.8, entry 5). The hydroformylation of internal olefins with double bonds at the  $\delta$  positions was studied using 4-octene as the model substrate (Table 3.8, entries 6 and 7). The reaction of *trans*-4-octene showed better results than *cis*-4-octene. For *cis*-4-octene, a mixture of 47% linear, 29%  $\beta$ -branched and 24%  $\gamma$ - and  $\delta$ -branched aldehydes was observed; for *trans*-4-octene, a mixture of 66% linear, 18%  $\beta$ -branched and 16%  $\gamma$ - and  $\delta$ -branched aldehydes was observed. As listed in Table 3.8, from 2-pentene to 3-hexene to 4-octene, the increase of steric hindrance at the double bond resulted in a decrease of hydroformylation rate, an increase in the amount of branched aldehydes, and a large increase of olefin isomers. Interestingly, a much better conversion to the aldehydes and linear selectivity was obtained for *trans*-4-octene when it was compared to 3-octene (Table 3.8, entries 5 and 7). This appears surprising since the double bond of 4-octene is one more bond away from the terminal carbon than 3-octene. But considering the fact that the migration of the double bond in 3-octene can occur in both directions, the migration from the  $\gamma$  position to the  $\delta$  position is a thermodynamically favourable process, and the double bond migration toward the inside direction actually slows down the hydroformylation process. However, for 4-octene, the double bond can equally migrate in both directions from the middle position to the terminal positions;

therefore, 4-octene has twice the chance of isomerizing to 1-octene, resulting in higher yield of linear aldehyde.

**Table 3.8.** Isomerization-hydroformylation of C<sub>5</sub> to C<sub>8</sub> internal olefins using ligand **3**.<sup>[a]</sup>

Entry	Substrate	Aldehyde distribution (%) <sup>b)</sup>			Conv. (%) <sup>c)</sup>	Iso. (%) <sup>d)</sup>
		$\alpha$	$\beta$	$\gamma+\delta$		
1 <sup>e)</sup>		>99	<1	0	85	6
2		88	7	5	63	13
3 <sup>f)</sup>		98	2	0	84	16
4 <sup>g)</sup>		92	4	4	98	4
5		40	33	27	55	48
6		47	29	24	59	46
7		66	18	16	60	42

<sup>[a]</sup> S/C = 1000, Rh(acac)(CO)<sub>2</sub> = 1.0 mM, L/Rh = 4, reaction temperature 125°C, CO/H<sub>2</sub> = 5/5 atm, time = 2 h, toluene as solvent, decane as internal standard. Numbers are calculated from averages of 2 repeated runs. <sup>[b]</sup> Percent of  $\alpha$ ,  $\beta$ ,  $\gamma$  or  $\delta$  aldehyde of all aldehydes, determined by GC or proton NMR. <sup>[c]</sup> Conversion of substrate, determined by GC. The substrate was almost exclusively converted to aldehydes and isomers. <sup>[d]</sup> Percent of total isomers converted from substrate, determined by GC. <sup>[e]</sup> A mixture of 20% *cis*-2-pentene and 80% *trans*-2-pentene. <sup>[f, g]</sup> A mixture of 24% *cis*-2-octene and 76% *trans*-2-octene. <sup>[g]</sup> Reaction time = 12 h.



**Scheme 3.4.** Isomerization mechanisms of an internal olefin: 1) Rh-H addition and  $\beta$ -H elimination pathway, 2)  $\eta^3$ -allyl coordination and reductive elimination pathway. The open box represents a vacant coordination site of Rh.

For an internal olefin, there exist two common mechanisms for the double bond migration from an internal position to the terminal, either through a Rh-H addition and  $\beta$ -H elimination pathway or through reductive elimination of a  $\text{Rh}(\eta^3\text{-allyl})$  complex to shift the double bond to the end (Scheme 3.4).<sup>14</sup> Under our reaction conditions, both mechanisms appear possible. Compared to a terminal olefin, the double bond of an internal olefin needs to migrate one or more times in order to form the linear aldehyde. For example, it requires three consecutive double bond migrations for 4-octene to produce the linear aldehyde. During this consecutive isomerization process, each Rh/alkene intermediate complex has a chance to start its own hydroformylation catalytic cycle. As a result, branched aldehydes will be produced.<sup>15</sup> Our results indicate that for a  $\beta$  internal olefin (2-pentene, 2-hexene, or 2-octene), the hydroformylation rate of the branched Rh/alkene complex is slow enough compared to the rate of isomerization and the rate of terminal alkene hydroformylation so that linear aldehyde is formed as the main product. For a  $\gamma$  internal olefin (3-hexene or 3-octene), the outcome is affected by the steric hindrance of the substrate. For 3-hexene, the time of two consecutive isomerizations is still shorter than that of branched hydroformylation, resulting in the linear aldehyde as the main product; however, much

worse regioselectivity was observed for 3-octene, which has increased steric hindrance and less accessible double bond compared to 3-hexene. For a  $\delta$  internal olefin (*cis*- or *trans*-4-octene), our results indicate that the time spending on three consecutive isomerizations is not much shorter than that of branched hydroformylation, resulting in a lot of branched aldehydes and olefin isomers.

### 3.5.4 Summary

In summary, we have shown that by using our multiple chelating capable tetraphosphine ligands, the hydroformylation of some industrially important internal olefins can be achieved with high regioselectivity. The Rh/tetraphosphine catalyst system is highly effective for the isomerization- hydroformylation of 2-alkenes to form linear aldehydes. Greater than 95% linear selectivity and up to 94% yield of the total aldehydes were obtained for 2-pentene, 2-hexene and 2-octene. The catalyst system also showed high to moderate linear selectivity for the isomerization-hydroformylation of 3-hexene, 3-octene and 4-octene but with slow reaction rates.

We have already published the major results described in this chapter in the journals of *European Journal of Chemistry* and *Advanced Synthesis and Catalysis*.<sup>16</sup>

## Experimental Section

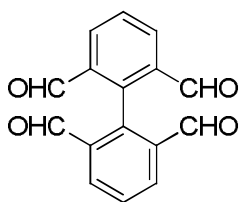
### General methods

All reactions and manipulations were performed in a nitrogen-filled glovebox or using standard Schlenk techniques, unless otherwise noted. All reagents and solvent were purchased from commercial vendors (Aldrich or TCI) unless otherwise noted. The reagents were used as is without further purification. Solvents were dried with standard procedures and degassed with N<sub>2</sub>. Column chromatography was performed using 200~400 mesh silica gel supplied by Natland International Corporation. Thin layer chromatography (TLC) was performed on 0.25 mm silica 60-F plates. <sup>1</sup>H NMR, <sup>13</sup>C NMR, <sup>19</sup>F NMR, and <sup>31</sup>P NMR spectra were recorded on Bruker Avance 400 MHz or 300 MHz NMR spectrometers. All chemical shifts are reported in ppm. GC analysis was carried on a Hewlett-Packard 6890 gas chromatograph using capillary columns.

### Experimental procedures and compound data

**General procedure for the hydroformylation of olefins:** To an 8 mL glass vial with a magnetic stirring bar was charged tetraphosphine ligand **1** (4 μmol) and Rh(acac)(CO)<sub>2</sub> (1 μmol in 100 μL toluene, charged as stock solution). The mixture was stirred for 5 minutes. Then 1-hexene (1 mmol) was added, followed by the addition of *n*-decane (100 μL) as internal standard. Additional toluene was added to bring the total reaction volume to 1 mL. The reaction mixture was transferred to an autoclave. The autoclave was sealed and purged with nitrogen for three times and subsequently charged with CO (5 atm) and H<sub>2</sub> (5 atm). The autoclave was then immersed in a preheated oil bath and was well stirred. After the

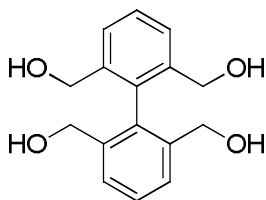
desired reaction time, the autoclave was taken out of the oil bath and cooled in ice water. The pressure was carefully released in a well ventilated hood. The reaction mixture was immediately analyzed by GC, and/or proton NMR to determine regioselectivity, conversion and turnover number. The reactions were repeated several times to ensure reproducibility.



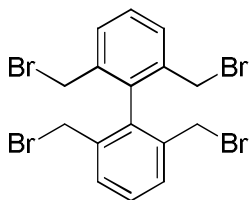
**Synthesis of 1,1'-biphenyl-2,2',6,6'-tetracarboxaldehyde (8):** To a 1-L three-neck flask equipped with a magnetic stirrer, a gas inlet tube, and a drying tube was charged pyrene **7** (10 g, 50 mmol) and dry  $\text{CH}_2\text{Cl}_2$  (350 mL). The resulting solution was cooled to  $-78^\circ\text{C}$  in a dry ice/acetone bath. Ozone was introduced to the stirred solution at  $-78^\circ\text{C}$  for 2.5 h, and the temperature of the reaction mixture was maintained at  $-78^\circ\text{C}$ . The excess ozone was removed by bubbling oxygen through the solution for 5 min at  $-78^\circ\text{C}$  and stirred for another 1 h. A solution of sodium iodide (68 g) in glacial acetic acid (500 mL) was added dropwise during 1 h to the reaction mixture at  $-78^\circ\text{C}$ . After stirring for 30 min at  $-78^\circ\text{C}$ , the reaction mixture was allowed to warm gradually to  $0^\circ\text{C}$ . The mixture was stored in a refrigerator ( $4^\circ\text{C}$ ) for 24 h. The reaction mixture was successively washed with aqueous  $\text{NaS}_2\text{O}_3$  (10 %, 800 mL), aqueous  $\text{NaHCO}_3$  (5%, 1.5 L), and water (500 mL) until the pH of aqueous layer equal to 7. The organic layer was then dried over  $\text{Na}_2\text{SO}_4$  and concentrated under reduced pressure. The crude product was dissolved in a minimum of  $\text{CH}_2\text{Cl}_2$  and chromatographed on a silica gel column using *n*-hexane and  $\text{CH}_2\text{Cl}_2$  as eluents. Pyrene was first eluted with *n*-hexane. It was followed by the tetraaldehyde which was eluted with



$\text{CH}_2\text{Cl}_2$ . The solvent was removed under reduced pressure. The crude product was recrystallized from toluene to give the title tetraaldehyde as a bright yellow solid (6.4 g, 50%).  $^1\text{H}$  NMR (300 MHz,  $\text{CDCl}_3$ )  $\delta$ : 9.69 (s, 4H), 8.25 (d,  $J = 7.72$  Hz, 4H), 7.84 (t,  $J = 7.66$  Hz, 2H);  $^{13}\text{C}$  NMR (75 MHz,  $\text{CDCl}_3$ )  $\delta$ : 189.72, 139.23, 135.83, 135.76, 129.94.

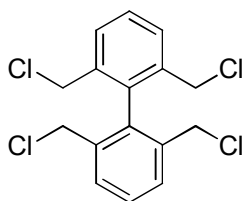


**Synthesis of 2,2',6,6'-tetrakis(hydroxymethyl)-1,1'-biphenyl (9):** To a solution of **8** (2.2 g, 4.2 mmol) in DMF (80 mL) was added LiCl (2.82 g, 67.2 mmol). The reaction mixture was stirred at room temperature for 6 h. The reaction mixture was cooled to 0 °C and 5% aqueous HCl solution (30 mL) was added carefully. After stirring for 5 min, the mixture was extracted with ether (4 x 40 mL) and washed with saturated aqueous NaCl solution (80 mL). The organic layer was separated, dried over  $\text{Na}_2\text{SO}_4$  and concentrated to dryness. Pure product was obtained by recrystallization from  $\text{CH}_2\text{Cl}_2$ /hexanes as a white solid (1.35 g, 93% yield).  $^1\text{H}$  NMR (300 MHz,  $\text{CD}_2\text{Cl}_2$ )  $\delta$ : 7.74-7.62 (m, 4H), 7.59-7.56 (m, 2H), 4.28 (s, 8H);  $^{13}\text{C}$  NMR (75MHz,  $\text{CD}_2\text{Cl}_2$ )  $\delta$ : 137.0, 135.8, 131.2, 130.2, 45.0; HRMS ( $\text{EI}^+$ ) calcd. for  $\text{C}_{16}\text{H}_{14}\text{Cl}_4$  [ $\text{M}^+$ ] 345.9853 , found 345.9850.



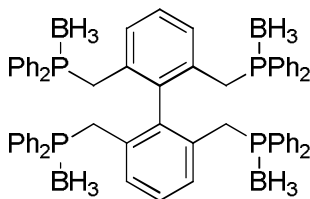
**Synthesis of 2,6,2',6'-Tetrakis(bromomethyl)-1,1'-biphenyl (10):** To a solution of 2,2',6,6'-tetrakis(hydroxymethyl) biphenyl **9** (5 g, 18.2 mmol) in  $\text{CH}_2\text{Cl}_2$  (80 mL) was

added dropwise, under anhydrous conditions at room temperature, a solution of phosphorus tribromide (30 mL, excess) in  $\text{CH}_2\text{Cl}_2$  (30 mL). After the addition was completed, the reaction mixture was heated to reflux (bath temperature  $50\text{ }^\circ\text{C}$ ) and stirred for 4 h. The reaction mixture was cooled to room temperature, and treated dropwise with water (80 mL). Caution: Hydrogen bromide was vigorously evolved during addition. After stirring for 5 min, the organic phase was separated, washed with water (3 x 30 mL) and dried over  $\text{Na}_2\text{SO}_4$ . The solvent was evaporated under reduced pressure. The residue was purified by recrystallization from hexane to afford the title tetrabromide as a white solid (6.9 g, 72 %).  $^1\text{H}$  NMR (300 MHz,  $\text{CD}_2\text{Cl}_2$ )  $\delta$ : 7.64-7.61 (m, 4H), 7.56-7.51 (m, 2H), 4.25 (s, 8H);  $^{13}\text{C}$  NMR (75MHz,  $\text{CD}_2\text{Cl}_2$ )  $\delta$ : 137.1, 135.6, 131.9, 130.4, 32.6.



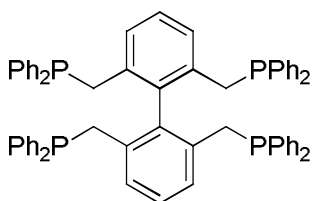
**Synthesis of 2,6,2',6'-Tetrakis(chloromethyl)-1,1'-biphenyl (11):** To a solution of 2,6,2',6'-tetrakis-bromomethyl-biphenyl **10** (2.2 g, 4.2 mmol) in DMF (80 mL) was added LiCl (2.82 g, 67.2 mmol). The reaction mixture was stirred at room temperature for 6 h. After the reaction was complete, the reaction mixture was cooled to  $0\text{ }^\circ\text{C}$ . To the cooled mixture was then added carefully 5% aqueous HCl solution (30 mL) (exothermic reaction). After stirring for 5 min, the mixture was extracted with ether (4 x 40mL) and washed with saturated aqueous NaCl solution (80 mL). The organic layer was separated, dried over  $\text{Na}_2\text{SO}_4$  and concentrated to dryness. Pure product was obtained by recrystallization from  $\text{CH}_2\text{Cl}_2$ /hexanes as a white solid (1.35 g, 93% yield).  $^1\text{H}$  NMR (300 MHz,  $\text{CD}_2\text{Cl}_2$ )  $\delta$ : 7.64-7.62 (m, 4H), 7.59-7.56 (m, 2H), 4.28 (s, 8H);  $^{13}\text{C}$  NMR (75MHz,  $\text{CD}_2\text{Cl}_2$ )  $\delta$ : 137.0,

135.8, 131.2, 130.2, 45.0; HRMS ( $\text{EI}^+$ ) calcd. for  $\text{C}_{16}\text{H}_{14}\text{Cl}_4$  [ $\text{M}^+$ ] 345.9853, found 345.9850.

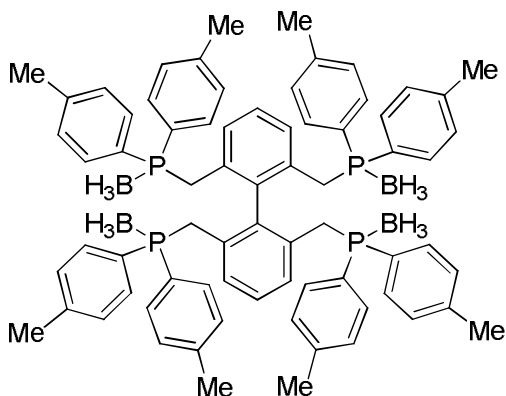


**General procedure for the synthesis of 2,2',6,6'-tetrakis((diphenylphosphino)methyl)-1,1'-biphenyl borane complex (12a):** To a cooled ( $-78\text{ }^{\circ}\text{C}$ ) solution of diphenylphosphine (2.32 mL, 13.2 mmol) in THF (10 mL) was added *n*-BuLi (5.28 mL, 2.5 M solution in hexane, 13.2 mmol) dropwise. After stirring for 10 min, the reaction mixture was allowed to warm to room temperature and stirred for 30 min. The reaction mixture was cooled to  $-78\text{ }^{\circ}\text{C}$  and **11** (1.05g, 3 mmol) in THF (10 mL) was added dropwise. After addition, the reaction mixture was allowed to warm to room temperature slowly and stirred overnight. The reaction mixture was cooled to  $0\text{ }^{\circ}\text{C}$  and a cold 1.0 M THF solution of  $\text{BH}_3$  (132 mL, 132 mmol) was added dropwise. The mixture was allowed to warm to room temperature and stirred for 4h. The reaction mixture was cooled to  $0\text{ }^{\circ}\text{C}$  and water was added carefully to quench the excess  $\text{BH}_3$ . The volatile was removed under vacuum. To the residue was added  $\text{CH}_2\text{Cl}_2$  (50 mL) and water (50 mL). The mixture was stirred for 10 min until all residues dissolved. The organic phase was separated. The aqueous phase was extracted with  $\text{CH}_2\text{Cl}_2$  (2 x 25 mL). The combined organic phase was washed with saturated aqueous NaCl solution (50 mL) and dried over  $\text{Na}_2\text{SO}_4$ . The solvent was removed under reduced pressure to obtain an off white solid. To the crude solid was added EtOAc (10 mL). The resulting suspension was stirred for 30 min and filtered. The residue was washed with cold EtOAc (2 x 5 mL) to give the pure borane protected title compound

**12a** (2.5 g, 73.8 %) as a colorless solid.  $^1\text{H}$  NMR (300 MHz,  $\text{CDCl}_3$ )  $\delta$ : 7.58-7.52 (m, 16 H), 7.45-.39 (m, 8 H), 7.36-7.31 (m, 16 H), 7.03-6.97 (m, 2 H), 6.87-6.84 (m, 4 H), 3.16 (d,  $J$  = 13.4 Hz, 8 H), 1.53-0.75 (bs, 12 H);  $^{13}\text{C}$  NMR (75 MHz,  $\text{CD}_2\text{Cl}_2$ )  $\delta$ : 133.1, 132.5 (d,  $J$  = 9.1 Hz), 131.5, 131.3, 130.6, 130.4, 129.2 (d,  $J$  = 9.9 Hz), 127.5, 30.2 (d,  $J$  = 30 Hz);  $^{31}\text{P}$  NMR (146 MHz,  $\text{CD}_2\text{Cl}_2$ )  $\delta$ : 15.2. HRMS ( $\text{ES}^+$ ) calcd. For  $\text{C}_{64}\text{H}_{66}\text{NaP}_4\text{B}_4$  [ $\text{M}+\text{Na}^+$ ] 1025.4385, found 1025.4431.

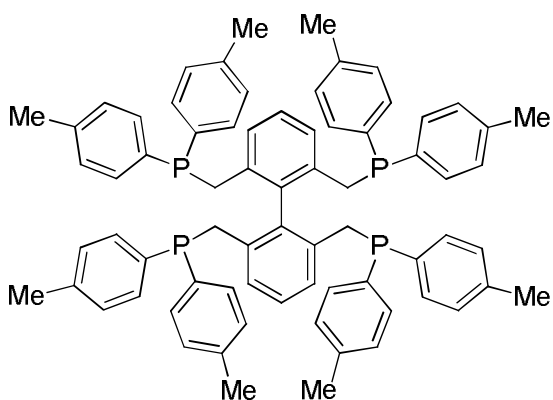


**General procedure for the synthesis of 2,2',6,6'-tetrakis((diphenylphosphino)methyl)-1,1'-biphenyl (1):** To a solution of DABCO (448 mg, 4 mmol) in toluene (10 mL) was added **5a** (501 mg, 0.5 mmol) in portions. The resulting suspension was stirred for 30 min at room temperature and slowly heated to 60 °C. The stirring was continued for 6 h at 60 °C. The reaction mixture was cooled to room temperature and additional toluene (10 mL) was added. The diluted solution was charged on a short silica gel column through cannula and eluted with toluene (40 mL). The solvent was removed under vacuum to give the desired ligand **1a** (376 mg, 79.4%) as a white solid.  $^1\text{H}$  NMR (300 MHz,  $\text{CDCl}_3$ )  $\delta$ : 7.32-7.22 (m, 40 H), 6.91-6.86 (m, 2 H), 6.76-6.74 (m, 4 H), 3.24 (s, 8 H);  $^{13}\text{C}$  NMR (75 MHz,  $\text{CD}_2\text{Cl}_2$ )  $\delta$ : 139.6, 139.3, 137.1, 137.0, 133.5, 133.3, 128.9, 128.7, 127.4, 35.0 (d,  $J$  = 25.8 Hz);  $^{31}\text{P}$  NMR (146 MHz,  $\text{CD}_2\text{Cl}_2$ )  $\delta$ : -15.3. HRMS ( $\text{ES}^+$ ) calcd. for  $\text{C}_{64}\text{H}_{55}\text{P}_4$  [ $\text{MH}^+$ ] 947.3254, found 947.3237.



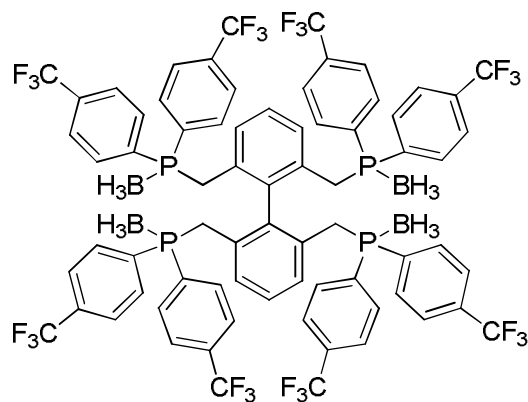
**2,2',6,6'-tetrakis(di(*p*-methylphenyl)phosphino)methyl]-1,1'-biphenyl borane**

**complex (12b):** Compound **12b** was prepared according to the general procedure using di(4-methylphenyl)phosphine (9.1 g, 42.8 mmol), *n*-butyl lithium (17.2 mL, 2.5M solution in hexane, 42.8 mmol), 2,2',6,6'-tetrakis(chloromethyl)biphenyl (3.4 g, 9.7 mmol) and BH<sub>3</sub> (200 mL, 1.0 M solution in THF, 200 mmol) in THF: yield: 7.6 g (71.2 %), white solid; <sup>1</sup>H NMR (400 MHz, CDCl<sub>3</sub>): δ = 7.48 (t, *J* = 9.2 Hz, 16 H), 7.13–7.08 (m, 16 H), 6.97 (t, *J* = 7.8 Hz, 2 H), 6.85 (d, *J* = 7.8 Hz, 4 H), 3.17 (d, *J* = 13.6 Hz, 8 H), 2.35 (s, 24 H), 1.15–0.85 (brs, 12 H); <sup>13</sup>C NMR (100 MHz, CDCl<sub>3</sub>): δ = 141.1 (d, *J* = 2.2 Hz), 138.8 (d, *J* = 7.7 Hz), 132.9, 132.0 (d, *J* = 9.4 Hz), 129.7 (d, *J* = 5.0 Hz), 127.9, 127.4, 127.1, 29.9 (d, *J* = 35 Hz), 21.3; <sup>31</sup>P NMR (161 MHz, CDCl<sub>3</sub>): δ = 13.3; HRMS (ESI): *m/z* = 1114.5739, calcd. for C<sub>72</sub>H<sub>82</sub>B<sub>4</sub>P<sub>4</sub> [M<sup>+</sup>]: 1114.5722.



**2,2',6,6'-tetrakis(di(*p*-methylphenyl)phosphino)methyl]-1,1'-biphenyl (2):**

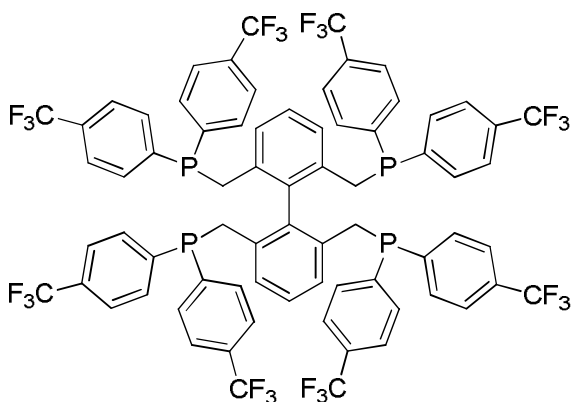
Compound **2** was prepared according to the general procedure using 2,2',6,6'-tetra(di(*p*-methylphenyl)phosphino)methyl]-1,1'-biphenyl borane complex **12b** (1.10 g, 1.0 mmol) and DABCO (0.896 g, 8.0 mmol); yield: 825 mg (78.0 %); white solid;  $^1\text{H}$  NMR (400 MHz,  $\text{CDCl}_3$ ):  $\delta$  = 7.16 (t,  $J$  = 7.2 Hz, 16 H), 7.04 (d,  $J$  = 7.2 Hz, 16 H), 6.90 (t,  $J$  = 7.6 Hz, 2 H), 6.78 (d,  $J$  = 7.6 Hz, 4 H), 3.16 (s, 8 H), 2.33 (s, 24 H);  $^{13}\text{C}$  NMR (100 MHz,  $\text{CDCl}_3$ ):  $\delta$  = 138.1, 136.8 (d,  $J$  = 11.4 Hz), 135.9 (d,  $J$  = 14.5 Hz), 133.0 (d,  $J$  = 20.1 Hz), 129.4 (d,  $J$  = 10.1 Hz), 129.0 (d,  $J$  = 6.8 Hz), 128.0 (d,  $J$  = 5.1 Hz), 126.9, 34.7 (d,  $J$  = 14.1 Hz), 21.3;  $^{31}\text{P}$  NMR (146 MHz,  $\text{CDCl}_3$ ):  $\delta$  = -16.4; HRMS (ESI):  $m/z$  = 1059.4522, calcd. for  $\text{C}_{72}\text{H}_{71}\text{P}_4$   $[\text{M}+\text{H}^+]$ : 1059.4501.



**2,2',6,6'-tetrakis(di(*p*-trifluoromethylphenyl)phosphino)methyl]-1,1'-biphenyl**

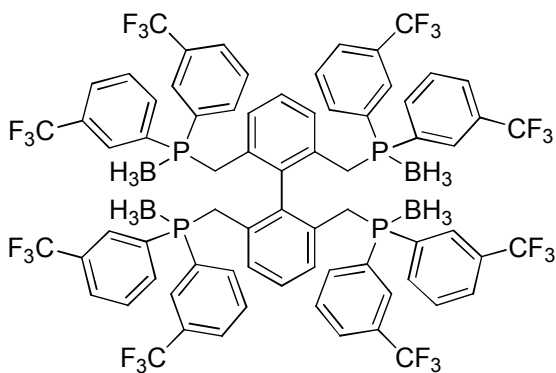
**borane complex 12c:** Compound **12c** was prepared according to the general procedure using di(*p*-trifluoromethylphenyl)phosphine (6.5 g, 20.3 mmol), *n*-butyl lithium (8.1 mL, 2.5M solution in hexane, 20.3 mmol), 2,2',6,6'-tetrakis(chloromethyl)biphenyl **11** (1.6 g, 4.6 mmol) and  $\text{BH}_3$  (200 mL, 1.0 M solution in THF, 200 mmol): yield: 4.9 g (68.9 %), white solid;  $^1\text{H}$  NMR (400 MHz,  $\text{CDCl}_3$ ):  $\delta$  = 7.84 (t,  $J$  = 6.4 Hz, 16 H), 7.66 (d,  $J$  = 6.4 Hz, 16 H), 6.99 (t,  $J$  = 7.6 Hz, 2 H), 6.63 (d,  $J$  = 7.6 Hz, 4 H), 3.52 (d,  $J$  = 13.6 Hz, 8 H),

1.40–0.60 (brs, 12 H);  $^{13}\text{C}$  NMR (100 MHz,  $\text{CDCl}_3$ ):  $\delta$  = 138.6 (t,  $J$  = 7.7 Hz) , 134.3 (d,  $J$  = 52.3 Hz), 133.3 (qd,  $J_1$  = 33.6 Hz,  $J_2$  = 2.3 Hz), 132.5 (d,  $J$  = 9.5 Hz), 129.7 (d,  $J$  = 1.5 Hz), 128.5, 126.0 (dd,  $J_1$  = 9.8 Hz,  $J_2$  = 3.8 Hz), 123.3 (q,  $J$  = 270.1 Hz), 29.6 (d,  $J$  = 33.7 Hz);  $^{19}\text{F}$  NMR (376 MHz,  $\text{CDCl}_3$ ):  $\delta$  = -63.4;  $^{31}\text{P}$  NMR (161 MHz,  $\text{CDCl}_3$ ):  $\delta$  = 16.2; HRMS (ESI):  $m/z$  = 1546.3466, calcd. for  $\text{C}_{72}\text{H}_{58}\text{B}_4\text{F}_{24}\text{P}_4$  [ $\text{M}^+$ ]: 1546.3478.



**2,2',6,6'-tetra(di(*p*-trifluoromethylphenyl)phosphino)methyl]-1,1'-biphenyl (3):**

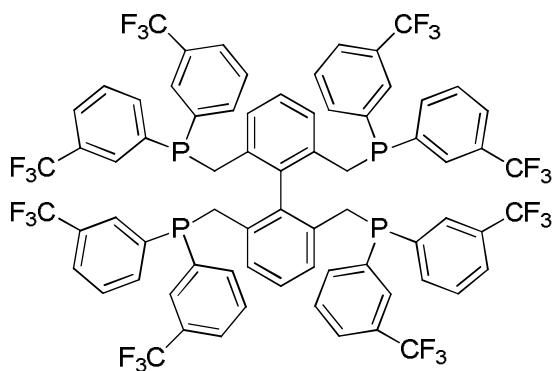
Compound **3** was prepared according to the general procedure using 2,2',6,6'-tetra(di(*p*-trifluoromethylphenyl)phosphino)methyl]-1,1'-biphenyl borane complex **12c** (773 mg, 0.5 mmol) and DABCO (0.448 g, 4.0 mmol); yield: 559 mg (75.0 %); white solid;  $^1\text{H}$  NMR (400 MHz,  $\text{CDCl}_3$ ):  $\delta$  = 7.42 (d,  $J$  = 7.6 Hz, 16 H), 7.21 (t,  $J$  = 18.2 Hz, 16 H), 6.97 (t,  $J$  = 7.6 Hz, 2 H), 6.70 (d,  $J$  = 7.6 Hz, 4 H), 3.20 (s, 8 H);  $^{13}\text{C}$  NMR (100 MHz,  $\text{CDCl}_3$ ):  $\delta$  = 142.7 (t,  $J$  = 26.4 Hz), 138.6, 136.2 (d,  $J$  = 10.8 Hz), 133.2 (d,  $J$  = 30.0 Hz), 131.4 (q,  $J$  = 33.5 Hz), 128.7 (d,  $J$  = 4.5 Hz), 128.2, 125.4 (t,  $J$  = 3.1 Hz), 123.8 (q,  $J$  = 270.2 Hz), 34.9 (dd,  $J_1$  = 10.2 Hz,  $J_2$  = 5.4 Hz);  $^{19}\text{F}$  NMR (376 MHz,  $\text{CDCl}_3$ ):  $\delta$  = -62.9;  $^{31}\text{P}$  NMR (161 MHz,  $\text{CDCl}_3$ ):  $\delta$  = -14.1; HRMS (ESI):  $m/z$  = 1491.2237, calcd. for  $\text{C}_{72}\text{H}_{47}\text{F}_{24}\text{P}_4$  [ $\text{M}+\text{H}^+$ ]: 1491.2245.



**2,2',6,6'-tetrakis(di(*m*-trifluoromethylphenyl)phosphino)methyl]-1,1'-biphenyl**

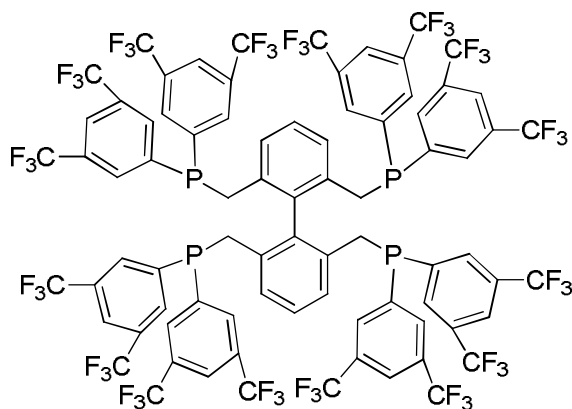
**borane complex (12d):** Compound **12d** was prepared according to the general procedure using di(*m*-trifluoromethylphenyl)phosphine (8.3 g, 25.7 mmol), *n*-butyl lithium (10.3 mL, 2.5M solution in hexane, 25.7 mmol), 2,2',6,6'-tetrakis(chloromethyl)biphenyl (2.0 g, 5.8 mmol) and BH<sub>3</sub> (250 mL, 1.0 M solution in THF, 250 mmol): yield: 6.0 g (67.1 %), white solid; <sup>1</sup>H NMR (400 MHz, CD<sub>2</sub>Cl<sub>2</sub>): δ = 7.98 (d, *J* = 10.8 Hz, 8 H), 7.88 (t, *J* = 8.8 Hz, 8 H), 7.75 (t, *J* = 8.8 Hz, 8 H), 7.57 (td, *J*<sub>1</sub> = 7.6 Hz, *J*<sub>2</sub> = 2.0 Hz, 8 H), 6.96 (t, *J* = 8.0 Hz, 2 H), 6.62 (d, *J* = 8.0 Hz, 4 H), 3.47 (d, *J* = 13.2 Hz, 8 H), 1.51–0.60 (brs, 12 H); <sup>13</sup>C NMR (100 MHz, CD<sub>2</sub>Cl<sub>2</sub>): δ = 139.3 (t, *J* = 7.8 Hz), 135.9 (d, *J* = 7.8 Hz), 132.5 (d, *J* = 66.2 Hz), 132.2 (qd, *J*<sub>1</sub> = 32.7 Hz, *J*<sub>2</sub> = 10.9 Hz), 130.6, 130.4 (d, *J* = 9.3 Hz), 130.3 (dd, *J*<sub>1</sub> = 6.0 Hz, *J*<sub>2</sub> = 1.0 Hz), 129.4 (dt, *J*<sub>1</sub> = 11.9 Hz, *J*<sub>2</sub> = 3.6 Hz), 129.2 (t, *J* = 4.3 Hz), 128.8, 121.4 (qd, *J*<sub>1</sub> = 270.2 Hz, *J*<sub>2</sub> = 1.7 Hz), 30.6 (d, *J* = 33.8 Hz); <sup>19</sup>F NMR (376 MHz, CD<sub>2</sub>Cl<sub>2</sub>): δ = -63.2; <sup>31</sup>P NMR (161 MHz, CD<sub>2</sub>Cl<sub>2</sub>): δ = 17.0; HRMS (ESI): *m/z* = 1546.3463, calcd. for C<sub>72</sub>H<sub>58</sub>B<sub>4</sub>F<sub>24</sub>P<sub>4</sub> [M<sup>+</sup>]: 1546.3478.





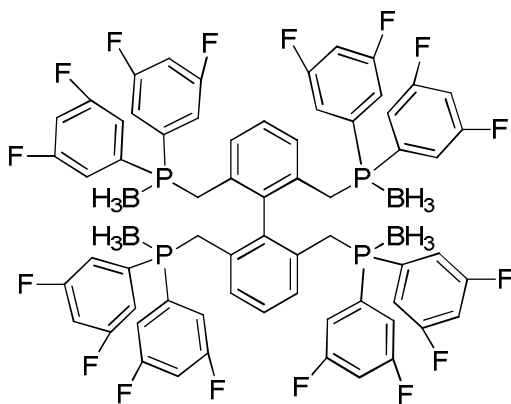
**2,2',6,6'-tetrakis(di(*m*-trifluoromethylphenyl)phosphino)methyl]-1,1'-biphenyl (4):**

Compound **4** was prepared according to the general procedure using 2,2',6,6'-tetra(di(*m*-trifluoromethylphenyl)phosphino)methyl]-1,1'-biphenyl borane complex **12d** (1.5 g, 1.0 mmol) and DABCO (0.896 g, 8.0 mmol); yield: 954 mg (64.0 %); white solid;  $^1\text{H}$  NMR (400 MHz,  $\text{CDCl}_3$ ):  $\delta$  = 7.58 (t,  $J$  = 6.4 Hz, 8 H), 7.48 (d,  $J$  = 3.2 Hz, 8 H), 7.42-7.33 (m, 16 H), 6.98 (t,  $J$  = 7.6 Hz, 2 H), 6.64 (d,  $J$  = 7.6 Hz, 4 H), 3.28 (s, 8 H);  $^{13}\text{C}$  NMR (100 MHz,  $\text{CDCl}_3$ ):  $\delta$  = 150.6, 139.4 (d,  $J$  = 8.0 Hz), 138.4, 136.0 (d,  $J$  = 74.4 Hz), 134.1, 131.0 (q,  $J$  = 32.7 Hz), 129.5 (d,  $J$  = 20.8 Hz), 129.0, 128.6, 128.1, 127.9, 125.8 (d,  $J$  = 3.7 Hz), 121.4 (q,  $J$  = 397.7 Hz), 35.4 (dd,  $J_1$  = 33.8 Hz,  $J_2$  = 5.1 Hz);  $^{19}\text{F}$  NMR (376 MHz,  $\text{CDCl}_3$ ):  $\delta$  = -62.8;  $^{31}\text{P}$  NMR (161 MHz,  $\text{CDCl}_3$ ):  $\delta$  = -13.1; HRMS (ESI):  $m/z$  = 1491.2233, calcd. for  $\text{C}_{72}\text{H}_{47}\text{F}_{24}\text{P}_4$  [ $\text{M}+\text{H}^+$ ]: 1491.2245.



**2,2',6,6'-tetrakis(di(3,5-trifluoromethylphenyl)phosphino)methyl)-1,1'-biphenyl (5):**

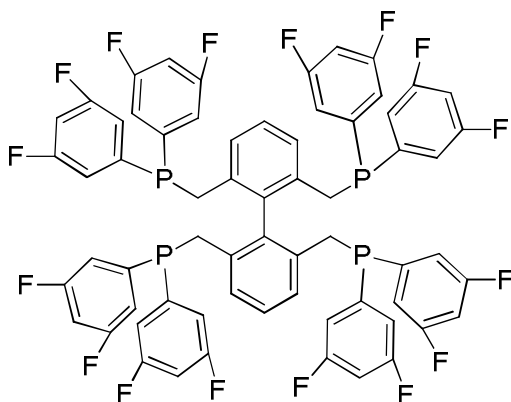
The corresponding borane complex has a poor solubility in toluene and other commonly used solvent. Thus, this ligand was synthesized directly without the protection of borane. Compound **5** was prepared according to the general procedure using di(3,5-ditrifluoromethylphenyl)phosphine (3.7 g, 8.0 mmol), *n*-butyl lithium (3.2 mL, 2.5M solution in hexane, 8.0 mmol), 2,2',6,6'-tetrakis(chloromethyl)biphenyl (635.0 mg, 1.8 mmol); yield: 3.0 g (81.7 %); white solid;  $^1\text{H}$  NMR (400 MHz,  $\text{C}_4\text{D}_8\text{O}$ ):  $\delta$  = 8.10 (s, 8 H), 7.77 (s, 16 H), 7.21 (t,  $J$  = 7.2 Hz, 2 H), 6.88 (d,  $J$  = 7.2 Hz, 4 H), 3.61 (s, 8 H);  $^{13}\text{C}$  NMR (100 MHz,  $\text{C}_4\text{D}_8\text{O}$ ):  $\delta$  = 141.8 (d,  $J$  = 12.4 Hz), 139.4, 137.4, 134.0, 133.3 (q,  $J$  = 35.1 Hz), 130.2 (d,  $J$  = 19.1 Hz), 124.8, 124.3 (q,  $J$  = 271 Hz), 36.3 (d,  $J$  = 24.1 Hz);  $^{19}\text{F}$  NMR (376 MHz,  $\text{C}_4\text{D}_8\text{O}$ ):  $\delta$  = -64.3;  $^{31}\text{P}$  NMR (161 MHz,  $\text{C}_4\text{D}_8\text{O}$ ):  $\delta$  = -10.0; HRMS (ESI):  $m/z$  = 2035.1231, calcd. for  $\text{C}_{80}\text{H}_{39}\text{F}_{48}\text{P}_4$   $[\text{M}+\text{H}^+]$ : 2035.1236.



**2,2',6,6'-tetrakis((di(3,5-difluorophenyl)phosphino)methyl)-1,1'-biphenyl borane**

**complex (12f):** Compound **12f** was prepared according to the general procedure using di(3,5-difluorophenyl)phosphine (7.9 g, 30.6 mmol), *n*-butyl lithium (12.3 mL, 2.5 M solution in hexane, 30.6 mmol), 2,2',6,6'-tetrakis(chloromethyl)biphenyl (2.4 g, 6.9 mmol) and  $\text{BH}_3$  (300 mL, 1.0 M solution in THF, 300 mmol): yield: 5.1 g (64.1 %), white solid;  $^1\text{H}$

NMR (400 MHz,  $\text{CDCl}_3$ ):  $\delta$  = 7.25-7.14 (m, 16 H), 7.12 (t,  $J$  = 8.0 Hz, 2 H), 6.99-6.92 (m, 16 H), 6.74 (d,  $J$  = 8.0 Hz, 4 H), 3.34 (d,  $J$  = 13.6 Hz, 8 H), 1.45–0.52 (brs, 12 H);  $^{13}\text{C}$  NMR (100 MHz,  $\text{CDCl}_3$ ):  $\delta$  = 163.1 (ddd,  $J_1$  = 254.2 Hz,  $J_2$  = 16.1 Hz,  $J_3$  = 11.8 Hz), 138.1, 133.5 (dt,  $J_1$  = 52.3 Hz,  $J_2$  = 8.0 Hz), 132.1, 129.9 (dd,  $J_1$  = 4.6 Hz,  $J_2$  = 1.5 Hz), 128.8, 115.1 (ddd,  $J_1$  = 18.5 Hz,  $J_2$  = 10.5 Hz,  $J_3$  = 8.6 Hz), 107.8 (t,  $J$  = 24.9 Hz), 29.8 (d,  $J$  = 33.6 Hz);  $^{19}\text{F}$  NMR (376 MHz,  $\text{CDCl}_3$ ):  $\delta$  = -105.2;  $^{31}\text{P}$  NMR (161 MHz,  $\text{CDCl}_3$ ):  $\delta$  = 19.0; HRMS (ESI):  $m/z$  = 1290.296, calcd. for  $\text{C}_{64}\text{H}_{50}\text{B}_4\text{F}_{16}\text{P}_4$  [ $\text{M}^+$ ]: 1290.298.



**2,2',6,6'-tetrakis((di(3,5-difluorophenyl)phosphino)methyl)-1,1'-biphenyl (6):**

Compound **6** was prepared according to the general procedure using 2,2',6,6'-tetra[[di(3,5-difluorophenyl)phosphino]methyl]-1,1'-biphenyl borane complex **12f** (1.3 g, 1.0 mmol) and DABCO (0.896 g, 8.0 mmol); yield: 901 mg (73.0 %); white solid;  $^1\text{H}$  NMR (400 MHz,  $\text{CDCl}_3$ ):  $\delta$  = 7.10 (t,  $J$  = 7.6 Hz, 2 H), 6.85-6.72 (m, 28 H), 3.21 (s, 8 H);  $^{13}\text{C}$  NMR (100 MHz,  $\text{CDCl}_3$ ):  $\delta$  = 141.8, 138.3 (d,  $J$  = 24 Hz), 135.6 (dd,  $J_1$  = 5.5 Hz,  $J_2$  = 3.2 Hz), 130.9, 129.1, 128.9 (q,  $J$  = 2.8 Hz), 128.5, 128.2, 125.3, 115.4 (td,  $J_1$  = 14 Hz,  $J_2$  = 7.3 Hz), 105.0 (t,  $J$  = 24.8), 35.0 (q,  $J$  = 5.8 Hz);  $^{19}\text{F}$  NMR (376 MHz,  $\text{CDCl}_3$ ):  $\delta$  = -108.1;  $^{31}\text{P}$  NMR (161 MHz,  $\text{CDCl}_3$ ):  $\delta$  = -11.1; HRMS (ESI):  $m/z$  = 1235.8623, calcd. for  $\text{C}_{64}\text{H}_{39}\text{F}_{16}\text{P}_4$  [ $\text{M}+\text{H}^+$ ]: 1235.8634.

## References

1. a) Casey, C. P.; Whiteker, G. T.; Melville, M. G.; Lori, L. M.; Gavney, J. A. Jr.; Powell, D. R. *J. Am. Chem. Soc.* **1992**, *114*, 5535. b) Casey, C. P.; Paulsen, E. L.; Beuttenmueller, E. W.; Proft, B. R.; Petrovich, L. M.; Matter, B. A.; Powell, D. R. *J. Am. Chem. Soc.* **1997**, *119*, 11817.
2. a) Trzeciak, A. M.; Ziółkowski, J. J. *Coord. Chem. Rev.* **1999**, *190-192*, 883. b) Trzeciak, A. M.; Glowiak, T.; Grzybek, R.; Ziółkowski, J. J. *J. Chem. Soc. Dalton Trans.* **1997**, 1831.
3. a) Evrard, D.; Lucas, D.; Mugnier, Y.; Meunier, P.; Hierso, J.-C. *Organometallics* **2008**, *27*, 2643-2653. b) Hierso, J.-C.; Beaupérin, M.; Meunier, P. *Eur. J. Inorg. Chem.* **2007**, 3767-3780. c) Hierso, J.-C.; Smaliy, R. V.; Amardeil, R.; Meunier, P. *Chem. Soc. Rev.* **2007**, *36*, 1754-1769. d) Hierso, J.-C.; Amardeil, R.; Bentabet, E.; Broussier, R.; Gautheron, B.; Meunier, P.; Kalck, P. *Coord. Chem. Rev.* **2003**, *236*, 143-206.
4. a) Devon, T. J.; Phillips, G. W.; Puckette, T. A.; Stavinocha, J. L.; Vanderbilt, J. J. US Patent 4694109, **1987**. b) Herrmann, W. A.; Kohlpaintner, C. W.; Herdtweck, E.; Kiprof, P. *Inorg. Chem.* **1991**, *30*, 4271. c) Herrmann, W. A.; Schmid, R.; Kohlpaintner, C. W.; Priermeier, T. *Organometallics* **1995**, *14*, 1961.
5. Agranat, I.; Rabinovitz, M.; Shaw, W. *J. Org. Chem.* **1979**, *44*, 1936.
6. The lithium diarylphosphine used was prepared in situ by the dropwise addition of the butyl lithium/hexane solution to the related diarylphosphines, which were prepared according to Busacca's protocol: Busacca, C. A.; Lorenz, J. C.; Grinberg, N.; Haddad, N.; Hrapchak, M.; Latli, B.; Lee, H.; Sabila, P.; Saha, A.; Sarvestani, M.; Shen, S.; Varsolona, R.; Wei, X.; Senanayake, C. H. *Org. Lett.* **2005**, *7*, 4277-4280
7. Kumar, P.; Vermeiren, W.; Dath, J.-P.; Hoelderich, W. F. *Energy & Fuel* **2006**, *20*, 481.
8. a) van der Veen, L. A.; Kamer, P. C. J.; van Leeuwen, P. W. N. M. *Angew. Chem. Int. Ed.*, **1999**, *38*, 336. b) van der Veen, L. A.; Kamer, P. C. J.; van Leeuwen, P. W. N. M. *Organometallics*, **1999**, *18*, 4765. c) van der Slot, S. C.; Duran, J.; Luten, J.; Kamer, P. C. J.; van Leeuwen, P. W. N. M. *Organometallics* **2002**, *21*, 3873; d) van der Veen, L. A.; Boele, M. D. K.; Bregman, F. R.; Kamer, P. C. J.; van Leeuwen, P. W. N. M.; Goubitz, K.; Fraanje, J.; Schenk, H.; Bo, C. *J. Am. Chem. Soc.* **1998**, *120*, 11616.
9. a) Klein, H.; Jackstell, R.; Wiese, K.-D.; Borgmann, C.; Beller, M. *Angew. Chem. Int. Ed.*, **2001**, *40*, 3408. b) Klein, H.; Jackstell, R.; Beller, M. *Chem. Commun.*, **2005**, 2283. c) Jackstell, R.; Klein, H.; Beller, M.; Wiese, K.-D.; Röttger, D. *Eur. J. Org. Chem.* **2001**, 3871.

10. Selent, D.; Hess, D.; Wiese, K.-D.; Kunze, C.; Börner, A. *Angew. Chem. Int. Ed.* **2001**, *40*, 1696.
11. Billig, E.; Abatjoglou, A. G.; Bryant, D. R. (UCC) US Patent 4769498, **1988**.
12. Burke, P. M.; Garner, J. M.; Kreutzer, K. A.; Teunissen, A. J. J. M.; Snijder, C. S.; Hansen, C. B. (DSM/Du Pont) PCT Int. Patent WO 97/33854, **1997**.
13. a) Matsumoto, M.; Tamura, M. *J. Mol. Catal.* **1982**, *16*, 209; b) Matsumoto, M.; Tamura, M. *J. Mol. Catal.* **1982**, *16*, 195.
14. Arthurs, M.; Sloan, M.; Drew, M. G. B.; Nelson, S. M. *J. Chem. Soc., Dalton Trans.* **1975**, 1794.
15. a) Brown, C. K.; Wilkinson, G. *J. Chem. Soc. A* **1970**, 2753. b) Evans, D.; Osborn, J. A.; Wilkinson, G. *J. Chem. Soc. A* **1968**, 3133. c) Evans, D.; Yagupsky, G.; Wilkinson, G. *J. Chem. Soc. A* **1968**, 2660.
16. a) Yu, S.; Zhang, X.; Yan, Y.; Cai, C.; Dai, L.; Zhang, X. *Chem. Eur. J.* 2010, *16*, 4938. b) Cai, C.; Yu, S.; Liu, G.; Zhang, X.; Zhang, X. *Adv. Synth. Cat.* 2011, *353*, 2665.

## Curriculum Vita

Chaoxian Cai

### EDUCATION

Ph.D., Medicinal Chemistry, Rutgers University, New Brunswick, NJ, 2012

M.S., Computer Science, University of Kentucky, Lexington, KY, 2000

M.S., Chemistry, University of Kentucky, Lexington, KY, 1998

B.S., Chemistry, Peking University, Beijing, China, 1990

### PUBLICATION

1. C. Cai, J. K. Lumpp, *J. Mater. Res.* **2001**, *16*, 670.
2. J. Y. L. Chung, C. Cai, J. C. McWilliams, R. A. Reamer, P. G. Dormer, R. J. Cvetovich, *J. Org. Chem.* **2005**, *70*, 10342.
3. C. Cai, N. R. Rivera, J. Balsells, R. Sidler, J. C. McWilliams, C. S. Shultz, Y. Sun, *Org. Lett.* **2006**, *8*, 5161.
4. C. Cai, J. Y. L. Chung, J. C. McWilliams, Y. Sun, C. S. Shultz, M. Palucki, *Org. Proc. Res. Dev.* **2007**, 328.
5. S. Yu, X. Zhang, Y. Yan, C. Cai, L. Dai, X. Zhang, *Chem. Eur. J.* **2010**, *16*, 4938.
6. C. Cai, S. Yu, G. Liu, X. Zhang, X. Zhang, *Adv. Synth. Cat.* **2011**, *353*, 2665.
7. G. Liu, K. Huang, C. Cai, B. Cao, M. Chang, W. Wu, X. Zhang, *Chem. Eur. J.* **2011**, *17*, 14559.